CROWD EVACUATION IN HIGH - DENSITY SCENARIOS

Ines Cilenti

Crowd Evacuation in high-density scenarios

Ines Cilenti

Abstract
Nowadays, is becoming increasingly frequent holding events in outdoor environments, involving a large number of people, even though these spaces were not designed from a safe prospective, in the way that safety is defined today. In such events, high density conditions is a very critical aspect, and the evacuation becomes very complex due to the space design and the interaction among pedestrians. Modelling tools can be used to identify optimal evacuation and crowd management strategies but their use for high and extreme density scenarios, still needs to be evaluated.

This thesis presents a possible approach to investigate the simulations of high density scenarios based on the field observation of a real event (video analysis).

The observation of the real case study allowed to get important data, e.g., speed, density and flow, in a complex high density scenario. It has been found that high local (dynamic) densities can be reached in critical points, i.e., bottleneck, despite the controlled (static) densities in the area. A set of tests (simulations), using first the default input parameters and then introducing the output from the field observation, were run in a continuous evacuation model (Pathfinder) to investigate how such type of evacuation models should be calibrated in high density scenarios. Earlier, before this it has been investigated the geometrical limit of the tool, i.e., body size of the agents and comfort distance parameters. The objective was to reproduce the local density and the flow recorded during the real event. The results indicated that it has been possible to achieve reasonable values for both, by prescribing the speed, the agent's body size, the comfort distance and the initial density. This conclusion is important due to more reliable models can be used for crowd management in outdoor high density scenarios, and to identify solutions/critical conditions ahead of the events.

Furthermore, the high density issue is tightly connected to the pressure increase among pedestrians, which represents one of the major factor leading to fatalities in crush events. For this reason a simple model to forecast the force among pedestrian has been introduced. This model is based on the combination of existing models borrowed from other scientific fields, e.g., "leaning crowd model", frictional forces and the drained discontinuous assembly of particles under load, which is very similar to the high density packing scenario. The pressure values obtained with the novel modelling approach and the data from the literature are comparable.

Lund University

Faculty of Engineering

Department of Fire Safety Engineering

Academic Year 2017-2019

Crowd evacuation in high-density scenarios

Ines Cilenti

Promoters:

Enrico Ronchi, Lund University

Giuseppe G. Amaro, GAE ENGINEERING s.r.l. Italy

Michele Fronterrè, CANTENE s.r.l. Italy

Master thesis submitted in the Erasmus Mundus Study Programme

International Master of Science in Fire Safety Engineering

Disclaimer

This thesis is submitted in partial fulfilment of the requirements for the degree of *The International Master of Science in Fire Safety Engineering (IMFSE)*. This thesis has never been submitted for any degree or examination to any other University/programme. The author(s) declare(s) that this thesis is original work except where stated. This declaration constitutes an assertion that full and accurate references and citations have been included for all material, directly included and indirectly contributing to the thesis. The author(s) gives (give) permission to make this master thesis available for consultation and to copy parts of this master thesis for personal use. In the case of any other use, the limitations of the copyright have to be respected, in particular with regard to the obligation to state expressly the source when quoting results from this master thesis. The thesis supervisor must be informed when data or results are used.

Read and approved,

Ines Cilenti

30/04/2019

Summary/Abstract

Nowadays, is becoming increasingly frequent holding events in outdoor environments, involving a large number of people, even though these spaces were not designed from a safe prospective, in the way that safety is defined today. In such events, high density conditions is an ongoing issue, as the evacuation becomes very complex, due to the space design and the interaction among the pedestrians.

It becomes, therefore, essential to understand the crowd dynamics in high density conditions in order to design crowd management safely. In this context, modelling tools can be used to identify optimal evacuation and crowd management strategies. Such tools are mainly designed for low to middle density scenarios and, as a result, their use for high (intended here as 2-6 persons/m^2) and extreme (>6 persons/m^2) density scenarios needs to be evaluated.

This thesis presents a possible approach to investigate the simulations of high density scenarios based on the field observation of a real event and by applying the findings to a real case study. The crowd dynamics were taken into account as the combination of three hierarchical components, i.e., theory, data and application, which influence each other and cannot be investigated separately. The theoretical background is presented through the state of the art literature review. Data, which is a very sensitive parameter, required an idea about what to collect (theory) and their interpretation. They were collected performing a video analysis and then were used in the application, i.e., to calibrate the simulation models.

The observation of the real case study allowed to get important data, e.g., speed, density and flow, in a complex, high density scenario, due to field data available in literature to this topic are scarce. It has been found that high local (dynamic) densities can be reached in critical points, i.e., bottleneck, despite the controlled (static) densities in the area. A set of tests (simulations), using first the default input parameters and then introducing the output from the field observation, were run in a continuous evacuation model (Pathfinder) to investigate how such type of evacuation models should be calibrated in high density scenarios. Earlier, before this it has been investigated the geometrical limit of the tool, i.e., body size of the agents and comfort distance parameters. The objective was to reproduce the local density and the flow recorded during the real event. The results indicated that it has been possible to achieve reasonable values for both, by prescribing the speed, the agent's body size, the comfort distance and the initial density. This conclusion is important due to more reliable models can be used for crowd management and to identify solutions/critical conditions ahead of the events.

Finally, the high density issue is tightly connected to the pressure increase among pedestrians, which represents one of the major factor leading to fatalities in crush events. For this reason a simple model to forecast the force among pedestrian has been introduced. This model is based on the combination of "leaning crowd model", frictional forces and the drained discontinuous assembly of particles under load, which is a very similar to the high density

packing scenario. The pressure values obtained with the novel modelling approach and the data from the literature are comparable.

Sommario/Estratto

Oggi sono sempre più frequenti manifestazioni che coinvolgono un gran numero di persone in ambienti esterni che, tuttavia, non sono stati progettati da un punto di vista della sicurezza, come intesa oggi. In questi eventi l'esodo diventa molto complesso a causa della configurazione del sito e dell'interazione tra pedoni dovuti alle alte densità. In questo scenario, la problematica relativa all'alta densità della folla è una tematica in via di sviluppo.

Diventa, quindi, essenziale comprendere la dinamica della folla ad alte densità per poter definire un relativo piano di gestione in sicurezza. Programmi di modellazione possono essere utilizzati, in questo contesto, per identificare un piano di esodo ed una gestione ottimali. Questi programmi sono principalmente progettati per basse e medie densità, di conseguenza, è necessario valutare il loro uso per alte (qui intese come 2-6 persone/m^2) ed estreme (>6 persone/m^2) densità.

In questa tesi è stato presentato un possibile approccio per indagare le simulazioni di scenari ad alte densità basato sull'osservazione di un evento reale e applicando i dati ottenuti ad un caso di studio reale. La dinamica della folla è stata analizzata considerando tre aspetti in modo gerarchico: teoria, dati e applicazione, che si influenzano reciprocamente. La contestualizzazione teorica è stata presentata attraverso la revisione dello stato dell'arte. I dati, che rappresentano un parametro molto sensibile, richiedono, in primis, un'idea su cosa indagare (teoria) e, successivamente, la loro interpretazione. Sono stati ottenuti eseguendo una video analisi e, successivamente, sono stati utilizzati in modo applicativo per calibrare i modelli di simulazione.

L'osservazione del caso di studio reale ha permesso di ottenere dati importanti, ad esempio la velocità, la densità e il flusso, in uno scenario complesso e ad alta densità, poiché i dati da campo disponibili in letteratura, in riferimento a questa tematica, sono scarsi. È stato riscontrato che densità locali (dinamiche) elevate possono essere raggiunte in punti critici, come ad esempio colli di bottiglia, nonostante le densità (statiche) controllate nell'area. Una serie di test (simulazioni) sono stati effettuati, utilizzando un modello di esodo continuo (Pathfinder), per capire come calibrare questi tipi di modelli di evacuazione in presenza di alte densità. Sono stati utilizzati prima i parametri di input predefiniti e successivamente introdotti gli output da osservazione su campo con l'obiettivo riprodurre densità locali e flusso registrati durante lo svolgimento dell'evento. Ancora prima è stato studiato il limite geometrico del programma, dimensione corporea degli agent e la comfort distance. È stato possibile ottenere valori plausibili sia per la densità locale che per il flusso impostando la velocità, la dimensione degli agent, la comfort distance e la densità iniziale dell'area. Questa conclusione è importante perché modelli più affidabili possono essere utilizzati per la gestione della folla e per identificare soluzioni/condizioni critiche prima degli eventi.

Infine, l'elevata densità è strettamente collegata all'aumento della pressione tra i pedoni, che rappresenta uno dei maggiori fattori che causano mortalità in eventi di massa,

schiacciamento. Per questo motivo è stato introdotto un modello semplice per fare una stima della forza agente su un pedone all'interno della folla. Questo modello si basa sulla combinazione di diversi modelli: "modello di pendenza della folla", forza di attrito e arrangiamento discontinuo di particelle sotto carico; quest'ultimo presenta una configurazione molto simile a quella della folla ad alta densità. I valori di pressione ottenuti con il modello sembrano essere comparabili con quelli ottenuti da letteratura.

Acknowledgements

Table of contents

List of figures

List of tables

1. Introduction & Objective

Designing an effective evacuation strategy for places of public assembly may present several challenges. Every building or public area is unique and operational efficiency during emergency egress cannot be fully tested until a real crisis occurs. Therefore, the challenge is anticipating the scenarios that may occur during an emergency, especially when they involve the complexity of human behaviour [1]. How can this be done?

Pedestrian movement has been empirically investigated for more than four decades [2][3][4]. Initially, these studies were performed based on direct observation and the main goal was to develop a Level-of-Service concept [5][6]. The use of modelling tools has been introduced relatively recently, and they have been used more extensively within performance based design since the middle of the 1990s [7]. Those tools may take into account the self-organization effect of the pedestrian crowd, which is the result of non-linear interactions between many objects or subjects without the intervention of external influences, causing different kinds of spatial-temporal patterns of motion [8]. A phenomenological approach to define crowd states that: it is a group of people sharing the same space and focus and where, typical phenomena like lane formation or speed reduction, due to high densities, are observed [9].
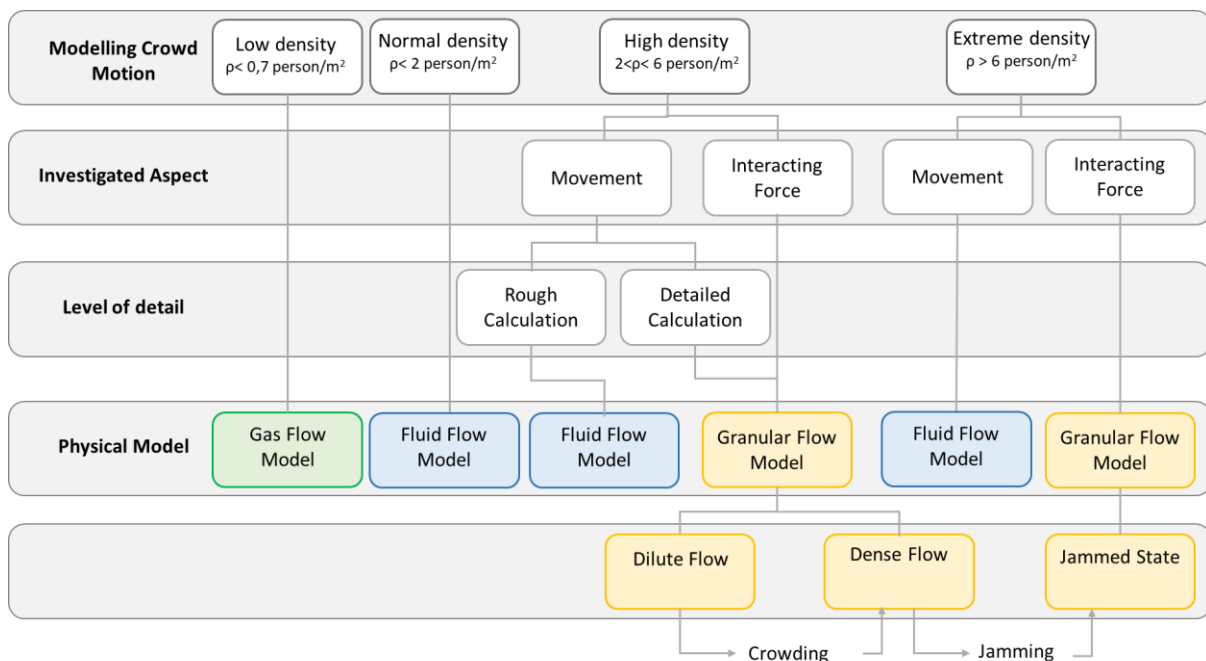
Figure 1. Approaches for modelling crowd motion. The scheme shows a summary of the possible physical model to use performing and investigating the crowd motion according with the density level and the investigated aspect. It has been developed referring to the literature review.

There are two distinct approaches for modelling crowd motion [10]. The first one treat pedestrians as discrete individuals, which are modelled by using a granular material. The second approach, applicable only in large crowds, treats the crowd as a whole, using a fluid behaviour assumption. A schematic summary concerning the following discussion about this

topic is provided in Figure 1, which shows the possible combinations among physical model, density crowd motion and investigated aspect. Many assumptions are necessary to develop a scientific approach to study the pedestrian and crowd movement. From this prospective, it is not surprising the attempt to establish similarity among pedestrian behaviour and classic physics fields [11]. Previously pedestrian crowds were considered behaving like a gas, when density is low and people can freely move [5], or a fluid, at medium and high density when the motion of pedestrians shows analogies with the fluid motion [5][10]. In fact, observing footprints in snow they look similar to streamlines of fluids [12]. At borderlines between opposite directions of walking one can observe "viscous fingering" [13]. The emergence of pedestrian streams through standing crowds [14] appears analogous to the formation of river beds [15]. However, this approximation is valid only in some instances, due to the interaction of the particles, i.e. avoidance and deceleration manoeuvres, and this assumption seems not to be valid at very high-density level [5]. In fact, similarities with driven granular flow can be observed at very high densities, when pedestrians tend to frequently change their speed and direction resulting in complex interaction among each other [16]. It can be stated that fluid dynamic analogies is reasonably valid in "normal" situations, on the contrary granular aspects dominate at extreme densities [17]. It seems to be reasonable to apply the fluid similarity for high density, due to the strong interaction among particles, which makes the pedestrian move as a *unicum* [18], like in wave front formation. However, the issue of investigating the impact of contact forces among pedestrians is still a problem. The validity of physics models seems to be strictly related to what we are looking for. For rough calculations, which are fast and easy to handle, flow similarity is well suited [9]. If detailed results are required, such as the sequence of an evacuation and spatial and temporal distribution of congestion, hydraulic modelling may not be sufficient in most cases [9]. In this circumstance influences like populations characteristics are decisive. These can be represented in sufficient detail in microscopic models only [9]. The evacuation process can be modelled on many different levels of details, ranging from hydro dynamic models to artificial intelligence and multi-agent model [19][20]. The increased diffusion of the artificial intelligence has made possible to come up at a realistic human motion models combining the Helbing's social force model [20][21] with Laumond's human locomotion model, which may reproduce the pedestrian motions both in free space and highly crowd environment. This is called Headed Social Force Model and it is still at a preliminary stage [22]. The dynamics must be described and understood on different levels from the physical, physiological, psychological and social. For this reason the scientific investigation of evacuation dynamics involves many research areas and disciplines [7].

Research has analysed first the laminar flow, where the motion is fast and smooth, stop and go flow, and finally the turbulent flow in the presence of extreme density, where backward phenomena can occur [23]. Helbing at al. investigated the behaviour of pedestrian crowd under extreme conditions, which is decisive for the safety of crowds during the access to or

egress from mass events, as well as for situations of emergency evacuation [23]. There is still a lack of empirical studies of extreme crowding [23].

Advances in the understanding of this processes have only begun recently, after the physics of granular materials have been under intense investigations [24]. It is now believed that the diverse phenomena of traffic flow, pedestrian flow and floating ice are related to the non-linear behaviour of granular materials, which can exhibit both solid-like and fluid-like behaviour. These peculiar properties give rise at least at three important "states" in granular flow, namely the dilute flow, the dense flow and the jammed state [24]. The phenomenon of crowding can be understood as a transition from dilute to dense flows, and that of jamming is a transition from dense flow to a jammed phase [24]. The nature and the properties of the transition are governed by the interactions among the granular particles in the flow. In principle, these transitions and states can be well characterised when these interactions are known such as in the cases of equilibrium system.

Nevertheless, the model of a crowd is still under debate, based on the human behaviour literature the pedestrians are often modelled as simple "particles" that interact with each other. However, other studies point out that, when crowd density equals the plan area of the human body, individual control is lost, as one becomes an involuntary part of the mass [25]. The force among people is the crucial factor that results in casualties, and it has been formed only when the density is higher than certain threshold value [25]. As Fruin has reported: At occupancies of about 7person/m^2 the crowd becomes almost a fluid mass [1]. Shock waves can be propagated through the mass, sufficient to propel them distances of 3 meters or more [26].

The awareness that the pedestrian streams are one of the most important factors to ensure the safety of people can be tracked back to more than 100 years ago [7]. The starting point for studying the influences of the emergency exits and the dynamics of the pedestrian streams was the disaster at the Troquois Theatre in Chicago with more than 500 fatalities, where only the decoration of the building burned, demonstrating the need for more effective evacuation planning [27]. In recent years there have been several major evacuation incidents which gained the global attention. For example, the terrorist attacks of 9/11 (2.749 casualties) [28][29] and the capsizing of the Baltic Sea Ferry MV Estonia in 1994(852 casualties) [30]. Other example, which have been affecting the public opinion on the topic are the Hillsborough stadium disaster in Sheffield in 1989 (96 casualties) [28] and the crowd crush in Baghdad in 2005 (1.011 casualties) [31]. Furthermore, recent terrorist attacks are getting more frequent all around Europe [32] such as Nice 2017, Barcelona 2017 and others [6]. Crowd incidents occur also due to other reasons, such as the case of Torino 2017 [33] in which a rapid evacuation was allegedly initiated by a pepper-spray attack and more than 1.500 soccer fans were injured. The same initiating event has led to a crowd crash in a nightclub in Corinaldo 2018 (Italy) [34][35], in this case 6 casualties and 120 injuries were recorded. The initiating event in all above mentioned cases are very different, from external human

antagonistic scenarios (e.g., terrorism or looting), to external physical dangers (fire) and even false alarms associated with absence of any actual threat [7]. A common factor is the collective phenomena. High people density is known as a critical factor in crowd management, which is becoming a relevant aspect in large event organization. Actual examples, such as the Love Parade in Duisburg [36] pointed out how the combination of high density of people, evacuation planning issues and operational errors can be enough to trigger a tragedy. The analysis of the critical flow conditions, local densities and velocities can help to make decisions concerning the measures to adopt in case of crowd events. A trustworthy *"performance analysis"* allowed a good prevision and in this way an anticipative crowd control became possible increasing the level of safety during mass events.

To clarify this concept, during the safety management plan for an event, a pre-determined design density is generally accounted for in order to satisfy a prescriptive code. Nevertheless, it may occur that, even though the regulation seems to be fulfilled in terms of *static-density*, in certain locations, where we have a *dynamic-density*, the local density that may occur can be much higher than the one previously estimated. It represents a serious safety issue, which may occur in a variety of scenarios. Nowadays, this is often related to the complexity of the building egress design due to the concept of "liquid architecture", and in the outdoor urban context due to the physical barriers/elements in place, e.g., the street-branches surrounding a square. Marcus Novak [37] proposed in 1993 the term "*Liquid Architecture*" in relation to virtual reality, in the telematics information era and Zygmunt Bauman applied the concept of liquidity in 2000 in the sociological sphere probing the relationship between architecture and landscape [38][39][40]. This definition underlines the complexity, mutability and continuity of space and pathways from both a planning and building prospective.

Events and festival may take place outdoor involving thousands of people. A particularly challenging situation is the case of religious or traditional events, in which the most relevant feature is that they may not occur in areas designed for large scale events, as arenas or stadium. Furthermore, these events usually include different sub-events, as music party in squares, parades, ritual ceremonies [41]. All of these presents a set of challenges from the perspective of evacuation safety, some of which are the same identified for music festivals [42].

Pedestrian dynamics is a complex subject, which needs to be investigated taking into consideration different density conditions. Data-sets investigate low density conditions; by contrast the very high end regime of densities (i.e., above 6 person/m^2 [43]) are rarely investigated. This is reasonable, since it is difficult and sometimes dangerous to set up experiments or perform field observations in this regime. Nonetheless, these high density scenarios may occur, and often lead to critical conditions for both design and operation [44].

Numerical simulations can be used to test evacuation plans or reproduce the ordinary movement of a crowd inside a specific area. Obtaining qualitative and quantitative information on evacuation times, space usage and high local densities in critical points, e.g.,

the merging flow, should therefore be considered a key aspect to consider in such type of analyses.

1.1 Purpose and Aim

The phenomena of crowding or jamming are common in our daily lives related to the frequency of crowd or large concentrations of people events happen in the modern society. The objective of this thesis project is to investigate crowd dynamics in case of high-density scenarios. More precisely, the overall aim is to investigate the macroscopic parameters, i.e., density, speed and flow, relating them to a real case study considering high-crowd density scenarios. Furthermore, the intention is to look at both the analyses of the observed data from video and the simulation issues connected with high density scenarios. It has been observed that these large gatherings of people generally occur without serious problems, although occasionally the combination of inadequate facilities and deficient crowd management results in injury and death, often related to the increase in pressure among pedestrians [26]. In light of that, further objective is to give a simple model to evaluate the local pressure.

The *eidos* is to point out the issues from the specific case study under consideration in order to give possible suggestions applicable to other cases.

Firstly, the main core of this work has focused on the merging-diverging flow, also called T-junctions. They represent one of the most common configurations in public infrastructures that may lead to a critical hazardous situations. Studies [45] showed that there have been numerous fatalities and injuries due to crowded situations in the bottleneck areas. Nevertheless, empirical data required for model calibration and validation are limited in the literature, as mentioned before, as well as the investigation of the flow directions on the performance of pedestrian flows [46]. Recent studies [47] showed that the major shortcoming of the existing models is the lack of appropriate validation with empirical data especially concerning complex crowd movement patterns [45][48]. Relevant crowd dynamic parameters have been extracted and analysed from a case study in light of these considerations. The investigated scenarios is the *"Festa di San Giovanni"*, an outdoor event located in Torino (Italy). These type of events are common in Italy and worldwide, and generally include very crowded scenarios, due to the complexity of the site and the heterogeneity of people. People movement data-sets are the starting point to understand pedestrian crowd dynamics in a real event.

The movement of large number of pedestrians in complex built environment, such as open-air events is important from a safety point of view. Understanding the pedestrian crowd dynamics is crucial, in order to develop design solutions to minimise the negative consequences.

In order to develop a design solution to prevent or minimise damaging consequences of crowd disasters, it is necessary to develop reliable models. Those should be able to perform

and predict with accuracy the critical aspects that might arise in a certain context, such as high density scenarios. This is an ongoing hotspot concerning the evaluation and the ability to predict high local densities. In the context of this work the Pathfinder [49][42] evacuation model has been tested in local high density scenarios. The accuracy of the model prediction has been evaluated by comparing field observations and model results based on a range of input configurations.

Secondly, the accident-causing theory has been used to investigate overcrowded pedestrian scenarios and possible crowd disasters [50]. A simple method to evaluate the physical forces among pedestrians in high density scenarios has been developed.

Finally, a short overview has been made on the impact of crowd management strategies on congestion levels and densities. The large scale events has been referred and a crowd management strategies for large-scale evacuation has been identified.

1.2 Limitations and delimitations

In the context of this thesis, the boundaries within the work have been name *delimitations*. The constraints which have been faced during the work performed are named *limitations*.

All the *assumptions* made in order to analyse the video recordings represent a delimitation of the analysed scenario, which have been listed in the section 3.2.1. Briefly, pedestrian speed has been evaluated considering only the straight movement. Children carried on the back have not been considered in the counting to evaluate the density and strollers have been counted as a person. In addition, the area outside the bottlenecks has been analysed in a qualitative way from the video and in a quantitative way from the simulation tests. Only the results linked with the high-density scenarios have been presented here.

Data collection, software and *physical model in use* are associated with a set of limitations. Data accuracy is limited by measurement uncertainties, e.g., the location and the quality of the camera recordings. Furthermore, the analysed data come from normal movement but the intention is to extrapolate them to emergency scenarios.

Software limitations are related to the program itself, e.g., limitations in the obtained results. These limitations are affected also by the absence of a wide data set available in the literature and a lack of experiments and field observations in high density scenarios.

Concerning the *physical model in use,* the fluid dynamics analogy may be reasonably valid in middle density ranges; on the contrary, granular aspects may dominate the flows at extreme densities. Nonetheless, this has been considered a reasonable approximation when looking at the macroscopic parameters, such as density, speed and flow. The analysis has been developed considering the crowd as a fluid. A short time interval has been considered between each measurement, i.e., 1s. This has been done to have a more precise data to perform the analysis, and later assess noise related to the post processing of the data. The evacuation model Pathfinder use a set of assumptions to reproduce the variability in human

behaviour during the evacuation, e.g., delay time distributions, etc. For this reason, it is necessary to perform a number of repeated runs to evaluate a convergence in the results [42][51][52]. To address this issue, the post processing of the data from the simulations was performed considering moving averages, so that the convergence is intrinsically solved within a given simulation.

1.3 Pedestrian and Crowd Dynamics

Crowd Dynamics can be defined as the study of how and where the crowds form and move. At high density there is the potential for overcrowding and personal injury. It is therefore important to understand the dynamics of crowds, how crowds understand and interpret information systems, how management systems affect crowd behaviour. This field of science has been called crowd dynamics [1].

How can high density be defined? What can be considered as high density is not unequivocal. The occurrence of high density is related to the body size distribution, which has a dramatic influence on the speed-density relationship and the fundamental diagram [53][54]. For example, it has been observed that the average diameter of Maccah pilgrims is smaller than the European or American citizens [23]. This difference causes discrepancies in the collected and analysed data when comparing them to different studies. In fact, it would be desirable if measurement from different countries could be mathematically transformed to a universal curve [23]. This may be possible only giving an unequivocal definition of the density. *Predtechenskii and Milinskii* in 1978 gave a density definition based on the project body area, which also had limitations due to the fact that not all video recording are taken perpendicularly, which is very rarely performed in field observations. Furthermore, the cultural setting affects not only the body size, but also the walking speed and the comfort distance. For example, the fastest average walking speed to walk down 60ft (18,288m) of the Singaporean population (10,55 s which correspond to 1,73 m/s) is three times higher than the slowest Malawian one (31,60s which correspond to 0,58 m/s) [55], see Figure 2.
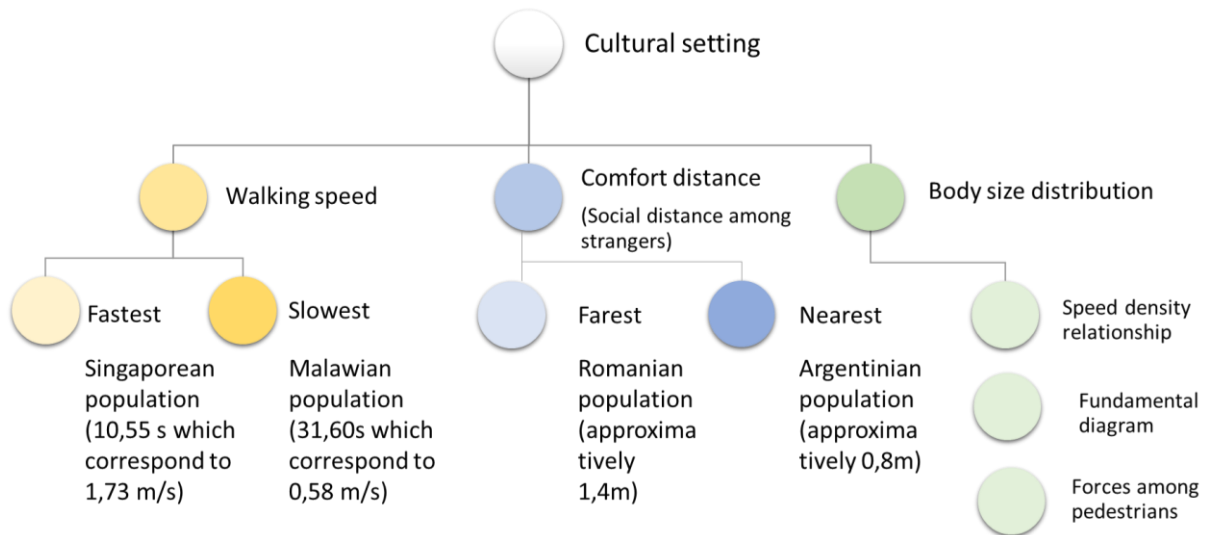
Figure 2. The cultural setting has effect on the walking speed, comfort distance and body size distribution, which combined together define the occurrence of high density condition.

Understanding crowd dynamics is essential to design crowd safety [1]. This section has been developed giving an overview of the complex problem related to the "laws" of crowd motion in light of this principle.

Complex movement patterns are frequently observed in major public infrastructures, ranging from uni-directional to multi-directional flows, which may result in increased number of conflicts, resulting in delay and congestion [56]. Conflict refers here to uncomfortable and undesired interactions among pedestrians, due to multidirectional movements. Duives at al. [57] proposed a classification of crowd motion cases based on the flow patterns. These consists in two main categories, unidirectional flow, i.e., straight flow, rounding a corner, entering and exiting, and multidirectional flow, i.e., bidirectional flow, two strips crossing flow, more than two strips crossing flow and random crossing flow without focal point. The combination of these cases could be able to cover the entire range of complex scenarios [57]. They stated that the simplest pedestrian motion is walking straight in one direction at uniform speed, unidirectional and uniform movement. Nevertheless, the speed and direction changes leading to more complex interactions among pedestrians. When the speed changes, internal conflicts are generated within the crowd [16]. These multidirectional movement types trigger most of the crowd disasters. In presence of high-density situations, the body movement is restricted by the interaction with the surrounding pedestrians. A further increase of flow compression waves may cause accidents [58][59].

The complex movements represent the combination of individual and crowd motions. Considering similarities with the world of physics, especially with the fluid flow, people have a choice in their direction, have no conservation of momentum and can stop and start. These factors make people different from a fluid [1]. Physical movement variable, i.e., speed, density and flow, might be more easily calculated if the behavioural variable, i.e., desired walking

manner due to the competition of space and time, were not taken into consideration. Nevertheless, those variables cannot be neglected. The interaction among behavioural and physical movement variable become more and more complex at high densities, which makes the prediction of the movement much more difficult [60].

In order to classify these movements, during the last two decades, research has been carried out to investigate pedestrian traffic system [16]. The first form to collect physical movement data concerning crowds was employed by researchers such as Hankin and Wright [61] in 1958 and Predtechinskii and Milinskii [43] in 1969. This method consisted of one scientist walking within a crowd of moving people, and timing his transition from one test point to the next in order to estimate the average speed of the group that he was walking with. Another scientist was counting the number of people passing through a previously located 'test line', over a specific period of time, to calculate crowd flow rates. Recently the data collecting form used is the analysis of time lapse photographs [60].

Phenomenological description of collective effects

Shi at al. [16] classified the complex movement in two general categories, the *Externally Governed Movement (EGM) and* the *Internally Driven Movement (IDM)* based on the governing factors of the motion patterns. The *EGM is* dominated by the interaction between pedestrians and external factors such as infrastructure constraints, e.g., T-Junctions [45]. The *IDM,* which consists in spontaneous configurations due to interpersonal interactions driven by the willingness of pedestrians to behave in their own manner or following the need for affiliation, e.g. Lane Formation [62]. The macroscopic effects reflect the individuals' microscopic interactions, thus give important information for any modelling approach [7].

Figure 4 [16] shows the combination of External and Internal movements. In the graph, the dotted line represent the interface between *EGM and IDM* pointing out that may could be overlapping between these two movements, e.g., merging flow may display 'lane formation' or 'faster is slower effect'. Furthermore, it can be seen in the graph that as soon as the complexity of the movement increase also the crowd dynamics become more complex. Over more, the crowd dynamics is affected simultaneously by both *EGM and IDM,* which are not absolutely independent among each other.

In Figure 3 is represented the purposed categorization by Duives at al. [57], extended at other complex movement introduced by Shi at al. [16], i.e., turning, weaving, merging and diverging. These movements have been investigating theoretically or empirically in literature [16]. The main point was the investigation of unidirectional flow (straight flow, rounding a corner, entering and exit) and multidirectional flow (bidirectional flow, two strips crossing flow and random crossing flow). Starting from a unidirectional movement, the pedestrian motion can get complex moving in counter flow, merging, diverging, and waving or in presence of random flow [16]. The more complex become the moving the more uncertain become the prediction of walking directions and potential conflicts. As can be seen, the hierarchy of the complex

movement is well defined and it has been possible decompose the EGM in seven main motion based patterns: straight line, turning, egress (stripping) and ingress (stuffing), opposing, weaving, merging, diverging and random flow.
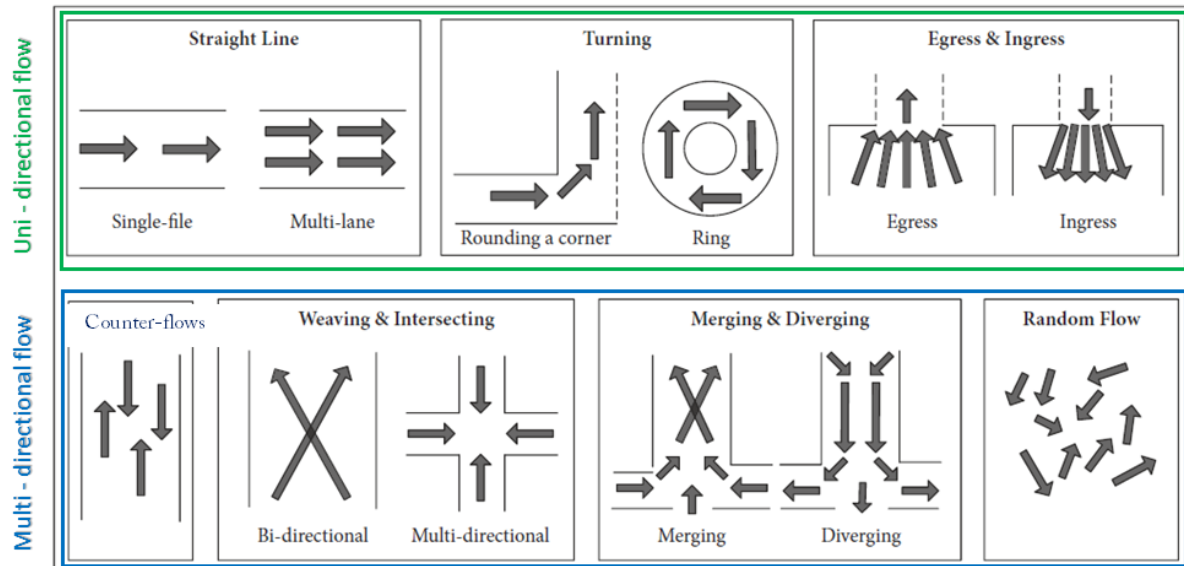
Figure 3. Diagram of external governed complex movement in two dimensions (2D). It represent the complex movements that have been investigated theoretically or empirically in literature [16]. *In case of 3D spaces, e.g., staircases, the movement may get more complex.*

The *EGM* generate observable flow patterns, which generally occurs at fixed locations. As shown in Figure 3 these movements can be classified in two subcategories (uni -directional and multi – directional flow).

The *IDM* represent more complex patterns due to the possibility to be observed only in peculiar condition, such as location and flow status. These represent the major causes in the dynamic of crowd disaster as arises from empirical study [46], where the sudden transitions from laminar to stop and go and turbulent flow was responsible of a fast and sudden rate of pressure release comparable with earthquakes.

The graph made by Shi at al., Figure 4, highlight the complexity of the way to classify pedestrian behaviour and the similarity with physical models. In it are shown the self-motivated individual and crowd motion behaviour (overtaking [63], evading [64], following [65], self-slowing [66], queuing [67] and grouping [68]) and the self-organization phenomena (herding[69], bubble effect [1], lane formation[62], stripe formation [1], zipper effect [70], oscillatory flow [71], faster is slower [21], freezing by heating [72], stop go waves [73] and turbulent flow [74]). Some of these concepts have been largely debated in the pedestrian dynamics community.
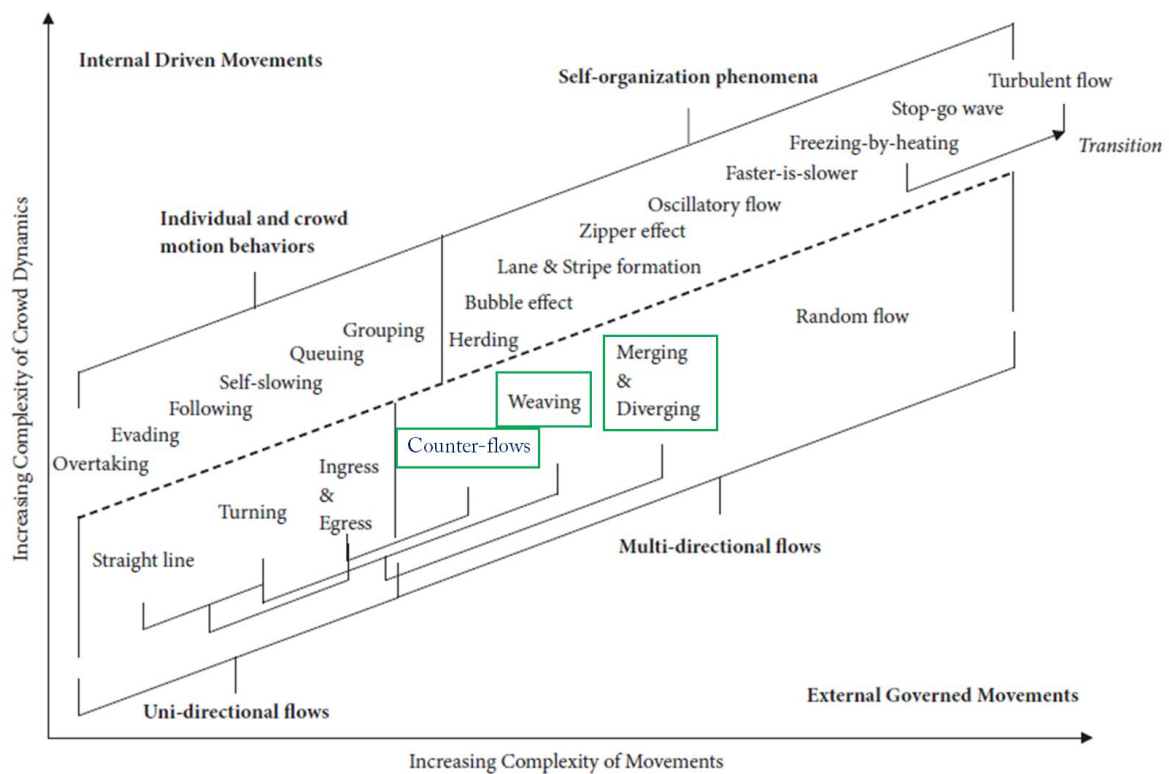
Figure 4. Classification of a complex movement, taken from Duives et al [16]. In the green box have been highlighted the multidirectional flow observed in the analysis.

The overview of the complexity of motions, which may be present in a field analysis scenario, it has been considered essential in this work in order to easily and better understanding the choice behind the developed analysis and the understanding of the results.

1.4 The relations among macroscopic parameters in crowd dynamics

Macroscopic parameters of pedestrian crows include density, speed and flow and their relationship represent the so called "fundamental diagram". This diagram is used in engineering field in order to assess the performance of pedestrian facilities [75][43][76]. It helps establishing the relationship between volume, speed and comfort at different pedestrian concentrations [6]. In the results section various "fundamental diagrams" used in planning guidelines and measurements of two selected empirical studies represent the overall range of the data. This terminology is not broadly accepted by the research community, since the comparison among these curves reveals substantial differences [7]. These differences are still under debt and they may depend on several factors, e.g., cultural and population differences [46], differences among uni and multi-directional flow [77], influence of psychological factors given by the incentive of the movement and on the type of traffic [78]. By contrast, Fruin [76] states that the fundamental diagrams of multidirectional and unidirectional flow differ only slightly. The only agreement among the different studies is that the speed decreases with increasing density [7].

The first study concerning the impact of these variables has been developed in 1970 by Fruin [6]. He defined the Level of Service concept, where the density and speed relationship have been stated as guidelines for comfort and safety. He has observed/formulated six levels of service, from A to F, which provide a qualitative method of designing new or evaluating existing pedestrian environments [79]. LOS describes the "conditions" in which agents/pedestrian move, e.g., speed, movement time, freedom of movement, comfort and density. This correlation is highlighted through the LOS scale that goes from level A, where agents/pedestrians are free to move without altering their travel speed up to F level, where the speed of movement is severely restricted [80]. It is important to note that Fruin made his measurements in a pedestrian street environment. Crowd behaviour on a city street with its many distractions, and in a normal conditions, is quite different from an egress behaviour in public space or a high density open-air scenarios, and very different from emergency egress behaviour [79]. On the basis of the Fruin's definition of LOS, the crowd exhibits marked speed reduction when space around a person is lower than $1 m^2$. This is true of a random, non-directional crowd, such as one would find in a shopping mall or busy city street. Nevertheless, there are phenomena of high density crowds which fall outside his reported observations [1]. Clearly there is a margin for increased density and flow in a safe and non-threatening environment.

More recent research [80] highlights the concept behind the definition of Level of Service and the relation with the Interactive Behaviours, in order to easily visualise the problem. Pedestrians are influenced by others during their movement, some of these interactions are helpful to get their targets, e.g., follow effect, while some others may be an impediment, e.g., rejections effect. During the process of moving in clusters, common interactive behaviours will inevitably happen, e.g., over tracking behaviour and evasive behaviour. The characteristics of this behaviour at different densities are one key element that affect the pedestrian flow and the ability for pedestrian to evacuate safely. These characteristics are decisive indicators to evaluate the *Leve of Service* (LOS) of pedestrian flow. Previous studies have been mostly focussed on distances necessary for overtaking, evasive and weaving behaviours to occur at a microscopic level, and on frequencies at a specific density on a macroscopic level [81].

A review study, concerning the Level of Service based on characteristic of Pedestrian Interactive Behaviours (PIBs) and developed in 2015, pointed out that available space for PIBs is the main factor contributing to the intensity features [80]. The intensity of PIBs initially increases in a moderate density scenario, while decreases in high density condition, due to reduction in space. In LOS E and F almost no one of the pedestrian interactive behaviours can occur, due to the high restricted space. Pedestrians can only follow the others. When the density increases, intensity of PBIs increases to the maximum value at a certain density, 0,5-0,6person/m^2, LOS D. The increasing trend of intensity reflects the increasing interactive effect among pedestrians and the demand for taking PBI is also rising. For high density the restriction for taking behaviour becomes stronger and stronger, at a such point that from LOS

D it turned into LOS F, where the pedestrian flow condition changes from interference with each other to restraint among pedestrians [80].In Figure 5 it has been shown a schematic summary of the reviewed LOS related to the PIBs.
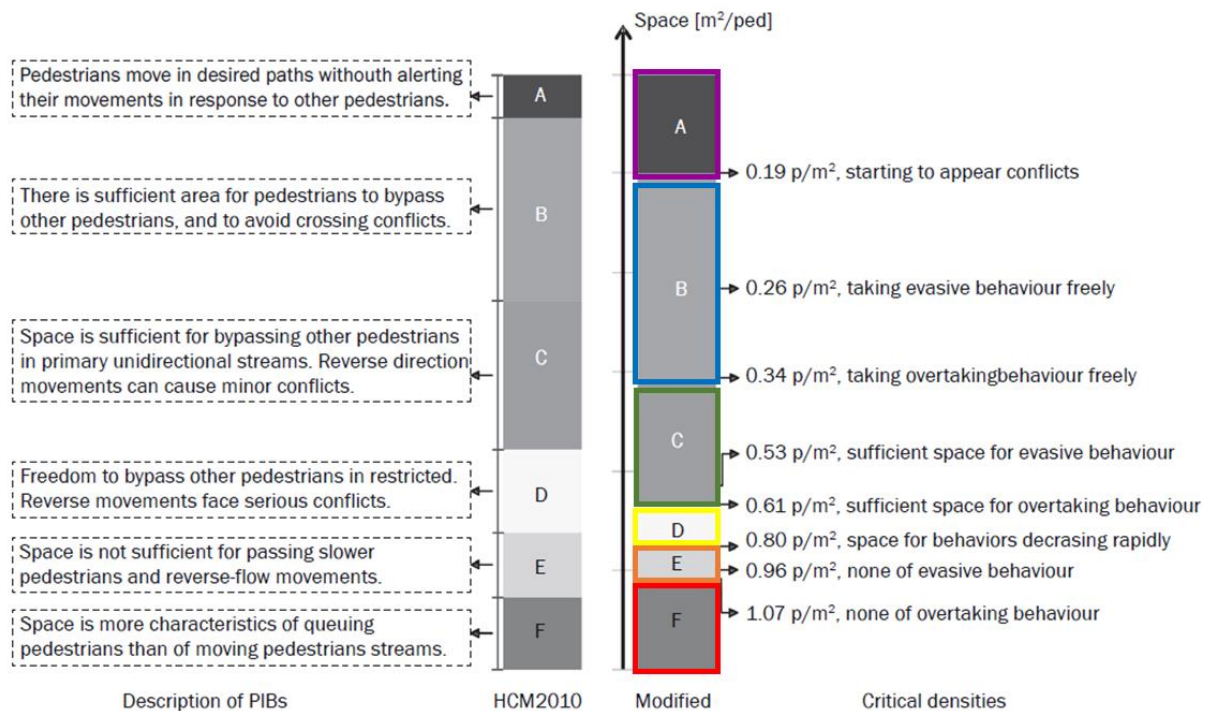
Figure 5. Description of Pedestrian Interactive Behaviour (PBIs) and the revised LOS based on Fruin [80]

The LOS standards, as a design criteria, is clearly an ideal guideline to achieve. But flow does not cease at the Fruin LOS-F. The Fruin Level of Service is a good guideline to be used as a general rule of thumb. Fruin also states his concerns clearly [1].

2. Methodology

The workflow of the thesis is presented in Figure 6. The first step of this work was to create a knowledge background to work on, looking into the state of the art. The literature study has looked at existing research regarding pedestrian and crowd dynamics. The main methods for measuring pedestrian density, flow and speed in real observational studies have been reviewed.
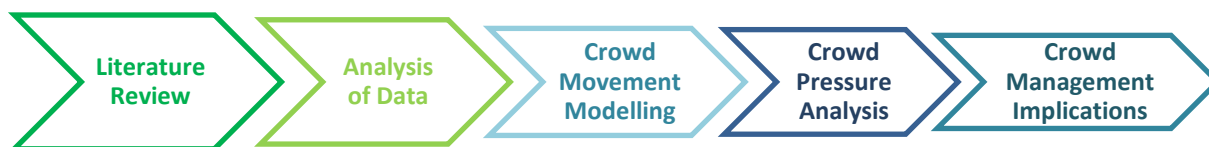
Figure 6. Thesis workflow. It represents the steps and aspects taken into consideration in representing high-density crowd evacuation scenarios.

Secondly, video observation analysis was performed in high density scenarios. This choice was made noting that in the literature the available data in this topic are mostly related to low up to middle densities scenarios [43], i.e., 0,1 to 2 persons/m², since to get data in high density conditions is a very complex problem, due to ethical issues, relative to setting up laboratory experiment and practical problems to perform field study as well. In this way, the macroscopic parameters of pedestrian crowd, i.e., density, speed and flow, using the hydraulic model and for a specific case have been found.

The following study has been performed to compare the output obtained from the video analysis with the output get from the simulations. The objective is to test the program in high density scenarios setting a model, which can simulate the scenario analysed in the reality, i.e., showing the same critical aspects found in observation field, e.g., the local high density. In this case the investigation has been performed in a bottleneck area. In 2014 an experimental study on pedestrian flow through wide bottleneck has been made [82]. The statement of this study was that the density and speed inside the bottleneck do not depend on the *bottleneck* width and a linear relation has been found between flow and bottleneck width, up to 5 m. However, this linear relation does not exist anymore if data from steady state are used in the analysis [82]. It has been pointed out that the density decreases in the bottleneck if compared with the recorded density in the front of the bottleneck [82]. The data obtained in the simulations task mostly agreed with the literature statement. Further details have been referred in the section 3.4.

Before running a simulation, a model should be selected. Evacuation can be represented in computer models in different ways, each having its own advantages and limitations according to the geometry and evacuees representation [83]. There are two fundamentally different ways of representing people in evacuation models, i.e., macroscopic and microscopic models

[84]. The microscopic approach is today the most common way of representing evacuees [83], who are represented by an autonomous agent with certain properties, e.g., pre-movement time, travel and speed. This approach is more similar to the reality rather than macroscopic representation, because the crowd movement is the result of individual movement of people in large group. Concerning the geometry, it should be mentioned three basic ways of representing the space, i.e., course network, fine network and continuous models. The most sophisticated method is the continuous models, where the geometry is represented by a continuous space containing agents. They have coordinates describing their location and they are not restricted by a grid or network, they can move instead around freely in the continuous space. This model allow for the closest representation of actual people movement. For a more comprehensive classification system and an evaluation of the pros and cons the reader may refer to [85][83].

The method used in this study was the application of evacuation modelling technique [42], to simulate large scale evacuation scenarios with high level of sophistication adopting a multi agent based model with continuous modelling approach.

To test the accuracy of the model, a series of 42 tests have been performed. The results have been summarised in Appendix B - Main results obtained in the Tests' Task.

. This may bring out the problem of the *Circle Validation Issue* due to the fact that the model has been set based on a single experimental data set. However, this is not the case since it is not a proper validation, but a test and in this specific part of the work the main focus have been the investigation of the parameters, which most affect the local high density in a continuous model.

Direct consequence of the high density is the increase in interacting pressures among pedestrians. This topic have been introduced in chapter 4, where prediction of human crowd pressure will be investigated, but it is not the main topic of this work, and more study is necessary to better understanding this issues.

To sum up, possibilities concerning how these issues can be managed were introduced in the discussion part, and possible crowd management strategy for safe evacuation purposes were discussed.

Uncertainties present in this work

Most of the evacuation models use a probabilistic approach, which means that it is necessary to take into account the uncertainties related to the variability of human behaviour [86]. During the modelling work, four different types of uncertainties have been considered [87].

Measurement uncertainties, which are directly linked with the data collecting or pedestrian tracking techniques employed. Video analysis has been made in a crowded outdoor scenario, and the observation of pedestrian with a camera pointed out several factors affecting the

accuracy of these values, e.g., the distortion angle, image resolution affected by the camera and also by the day time of the video recording and especially by the level of the density reached during the video tracking. In video analysis study, is given as a general rule the location of the camera perpendicular to the observed area, to reduce the shadow effect that generally taller people have on shorter people. In this case it has not been possible. The quality of the video has been found clear during the daylight and with low-density flow, as can be seen in Figure 10, although has been found extremely poor in the darkness and in presence of a high-density flow, as already saw in Figure 11. These uncertainties have mostly been affected the counting of the people during the stripping phase, when the combination of the angle of the camera, the darkness, the high-density and the dominance of dark clothing made the counting more difficult.

 Model input uncertainties are associated with the post production of the data recorded during the *measurement* phase and that has been used as model input. Several assumptions have been made in order to simulate the observed local density in the real scenario, e.g., the *body size* of the agents, the *walking speed* and the *comfort coefficient*.

Intrinsic uncertainties associated with the model used for the simulations. Properly, these uncertainties depend on the physical and mathematical assumptions behind the model. In this context a continuous model, Pathfinder, has been used [84].

Behaviour uncertainties [88][84]*,* which are linked with the stochastic nature of the human behaviour .

*"*In this work behavioural uncertainty has been treated considering the average of the density, speed and flow with a time interval of 1s. Due to the moving average approach for both the data processing of the video analysis and the final simulations tests performed, the same test has not been run several times. It was not necessary to verify the convergence, since they are moving averaged values, for this reason intrinsically convergence. The moving average is a method for smoothing time series by averaging a fixed number of consecutive terms. Generally, the longer the interval of the average, smoother is the resulting series [89]. In this context a time interval of 5 seconds has been used due to the time analysis of the video, since the moving average is not defined for the first and the last time series values. In order to compute the moving average for those values, the series must be back casted and forecasted.

3. Low Density vs High Density: comparison of two opposite situations observed in the same study case

The values of density, speed and flow for a wide bottleneck had been investigated here in free flow movement and congested flow. More specifically, an outdoor situation has been investigated focussing on a public event, *"Festa di San Giovanni"* on 24th of June 2018 in Torino, Italy. In that day the following analysed data had been collected.

3.1 Setup and geometry of the investigated area

The observed case study is a traditional outdoor event in the city involving a large number of people (around 35.000 people).

The event has taken place in Torino city centre, particularly in the areas of *Piazzetta Reale, Piazza Castello, Piazza S. Carlo* and the surrounding zones as shown in the Figure 7. An inspection to the area where the event has been carried out had been made, in order to locate the camera location and to become familiar with the walkways in the area.

Figure 7. Framework of the monitored area. The image, taken from Google maps, show the location of the event, Piazza Castello, and the Analysed Gate, which connect the square to Via Garibaldi. This gate was used to leave the event place.

More specifically, the focus is the *Gate* where Piazza Castello merges with Via Garibaldi, which represent one of the major way out from the square with its 11,2m wide. The monitoring and the follow-up have taken place through one camera placed on the balcony of the first floor in a hotel building located in Via Garibaldi, with the view direct to Piazza Castello as shown in Figure 9. The camera was a Sony HDR-30 Full HD 1920*1080 50p and it has been placed by the GAe Engineering srl, which took permission from the municipality to place the camera.
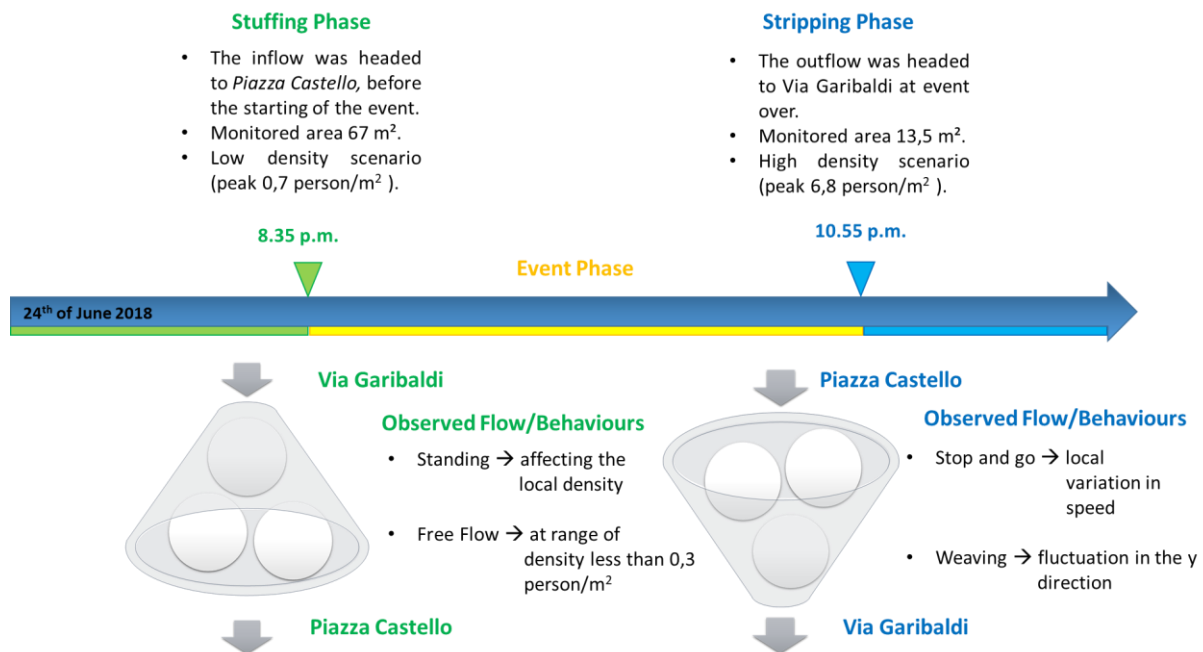
Figure 8. Time line of Stuffing and Stripping Phases. The observed times have been the "Stuffing phase" at 08:35pm, when the inflow was headed to Piazza Castello, before the starting of the event, and the "Stripping phase" at 10:55pm, when the outflow was headed in the opposite direction at event over. The monitored area during the "Stuffing phase" has been measured 11,2m*6m instead during the "Stripping phase" is around 11,2m*1,2m. The difference in covered area is due to the change in angle of the camera during the recording time.

The two time frames analysed have been selected due to the two extreme opposite situations, which can be summed up in *free flow* concerning the "*Stuffing phase*" and *congested flow* in the case of *"Stripping phase", see* Figure 8*.*

In this walkway two exits merge in the studied area, as we can see in Figure 9, people coming out from/going in other exit increase/decrease the number of the people present in the control area, which affect the recorded local density.
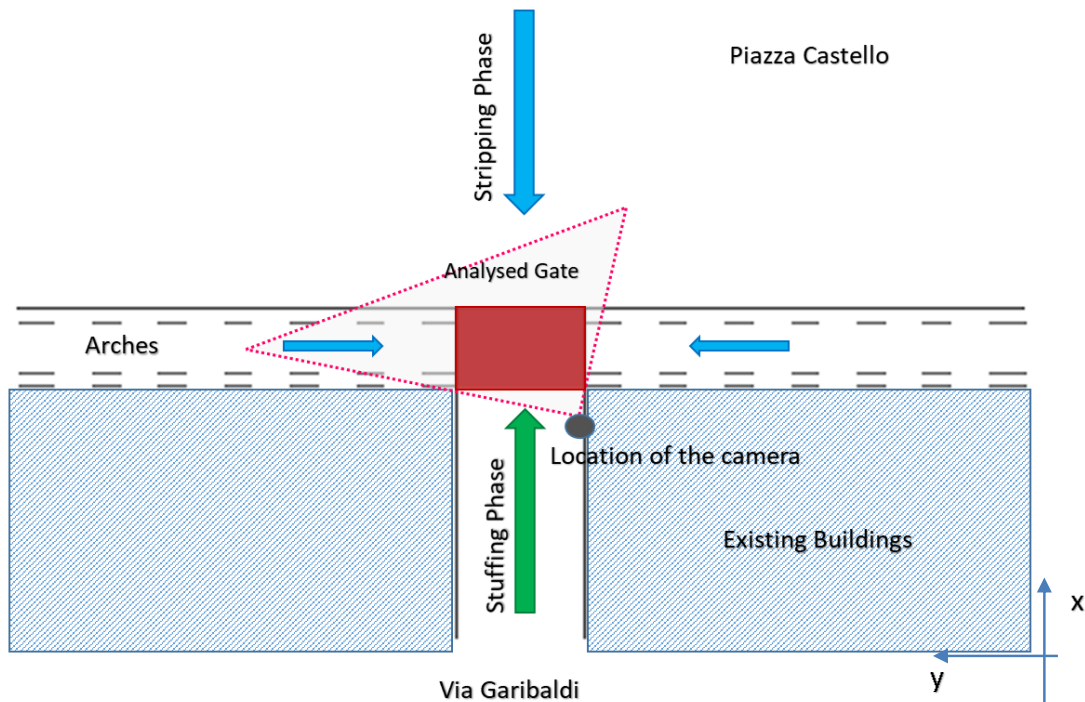
Figure 9. Schemes of the analysed area and the flow directions in the two different phases. In the image, in red is shown the analysed Gate (Bottleneck) and with the dots line the view camera.

Expecting high number of people, a crowd management approach was used during the event, which included the presence of stewards placed along the back roads jointed to the main walkway. The stewarding task was to monitor and limit an additional influx, which could have caused an increase in density, and consequently in pressure. This control was put into practice thought a hand counting conducted in each gate and communicated at a central system, head quartier, which was monitoring all the gates in order to control the number of people present in the square at the time of the event.

Four behaviour/flows have been observed in this event, which in some case coexist in the control area due to the extension of the same:

1. Standing, which is considered when the people do not move inside the control area but they will affect the local density;

2. Free flow, that is defined as the flow which occur at range of density less than $0,3 person/m^2$ [80], in a more intuitive way, when people move freely in the control area and overtaking behaviour can be observed;

3. Stop and go flow, the pedestrian slow down the speed until they stop and then they start again; in this case the local variation in speed becomes important to decide between starting and stopping [90];

4. Weaving behaviour, the pedestrian motion is extremely slowed down. Considering a Cartesian system, the motion of pedestrian is a fluctuation in the y direction without evident progression in the x direction.

The first two, i.e., standing and free flow, have been observed in the stuffing phase, which is characterised by low density. The second two i.e., stop and go and waiving, characterise the stripping phase which is typified by high density.

3.2 Data collection and processing

The geometric layout configuration was measured manually before the event; CAD drawings have been compared with them and, furthermore compared to the google earth measurement.

A video player for sport analysis, Kinovea™ version 0.8.15, was used to analyse the data. The possibility to insert a prospective grid into the video helped to visualise the control area during the video footage. The arches converged in via Garibaldi and the vanishing line of the floor have been used to draw the prospective grid and to define the height of the elevation from the ground. The control volume has been defined geometrically, according to the rules of the descriptive geometry as we can see in Figure 10.

Figure 10. Definition of the control volume using a prospective grid during the stuffing phase. The dots white line in the image is the prospective grid used to easily visualise people in the area. The green solid lines have been used to build the control volume, to draw them the vanishing line of the floor have been used. The red solid line has been used to measure the flow. The red cross has been used to count the people inside the control volume.
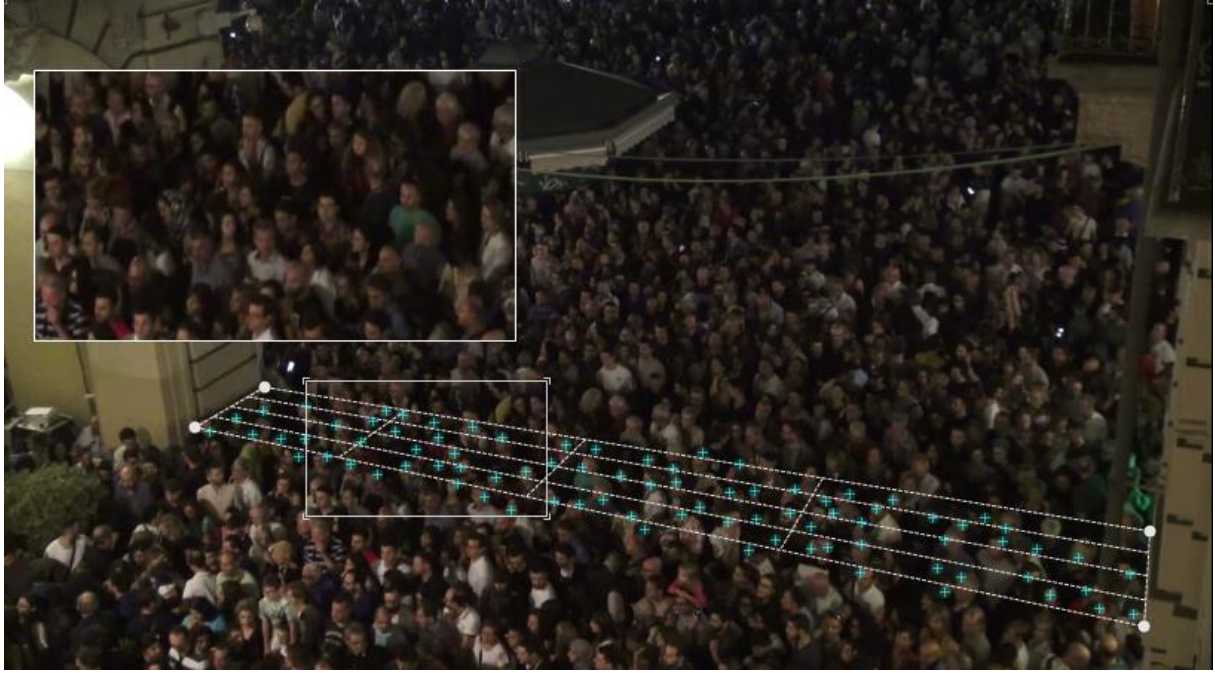
Figure 11. Location of the prospective grid used for the counting of people during the stripping phase. These values have been used to calculate the raw data for the video analysis. The same procedure has been applied to each data point in a time interval of 1second. The blue cross in the image correspond to a head in the control area.

The local density has been determined by taking screenshots, for each second in a timeframe of 60 seconds, counting people inside the control area at that specific moment and dividing it over the area. The decision of performing a manual counting has been taken due to the inefficiency to analyse the frame filtering the colour, because of the quality of the camera and the homogeneous pattern. This limit was relevant in high density scenario, where the environmental conditions were not favourable, i.e., night, crowd and dark clothes, as can be seen in Figure 11.

The density in the area has been estimated ΔN_p number of people inside the control area divided over the area A.

$$\rho = \frac{\Delta N_p}{A}; \tag{3.1}$$

In order to record the number of people leaving the control area, in the same way, a manual counts has been made. These values were compared with the one calculated using the flow equation from fluid dynamics. The results have been shown the values measured from manual counting, due to the greater relevance being observed values and not theoretical values.

$$Q = \rho * v = \frac{N_p}{A} * v = \frac{N_p}{L*t}; \tag{3.2}$$

Pedestrian entering and exiting the control area were recorded, and from these data the local average speed during the transit across the area was computed.

$$v = \frac{L}{t};$$ (3.3)

The obtained values have been used to draw the *"fundamental diagram"*.

Once the values of density, speed, and flow for each of the data points were found locally, the post processing of this data using a moving average approach has been performed.

3.2.1 Assumptions to analyse the video

The control volume analysed is the *Gate*, area which connect "Piazza Castello" trough "Via Garibaldi", red area in Figure 9.

Due to the aim of the event, the kind of people attended is wide and mixed, namely elderly, adults, youth, person with different disabilities. Observing the videos, this distinction does not affect the difference in motion, i.e., *"free flow"* and *"congested flow"*, since they are two extremes situations. Concerning the first motion, people move independently of the density present in the area. Their movement is mostly affected by behavioural variable, increasing and slowing down the speed according to the action of other people, with whom they are walking. Here, the highest speed is recorded for induvial. In the second case, almost a single fluid motion can be seen, due to the high local density recorded in the area.

In order to perform the analysis some assumption have been made:

1. To evaluate the pedestrian speed during the *stuffing phase*, the investigated flow is unidirectional, from the Garibaldi street, to the Castello square;

2. To evaluate the pedestrian speed during the *stripping phase*, the investigated flow is unidirectional, from the Piazza Castello square, to the Garibaldi street;

3. The presence of strollers has been considered as a further person inside the control volume, due to the similarity, in terms of projected area, with a person body size (averaged dimensions 60cm*50cm);

4. The presence of a child carried on the shoulders of an adult has been counted as one person (adult + child);

5. The area taken into consideration during the *stuffing phase* is a surface of 67 m^2, according to the view of the camera, location and rake angle;

6. The area taken into consideration during the *stripping phase* is a surface of 13,92 m^2, according to the view of the camera, location and rake angle;

The error has been estimated performing a second independent counting, i.e., made by a second researcher, on a random 10s included in the 60s. This time was previously analysed two times.

In Figure 12 and Figure 13 schemes of the grids that have been used to analyse the pedestrian movement in both situations have been represented.
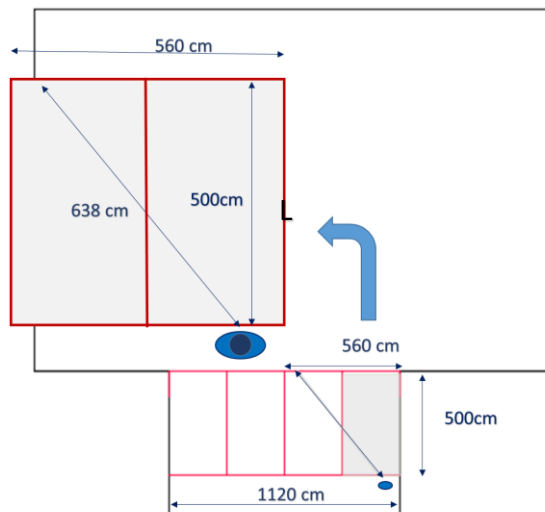
Figure 12. Scheme of the estimation of the error in transit length – Stuffing Phase (Low Density). The red grid have been used to analyse the pedestrian movement and to help the counting of the pedestrians present in the area in a specific time.
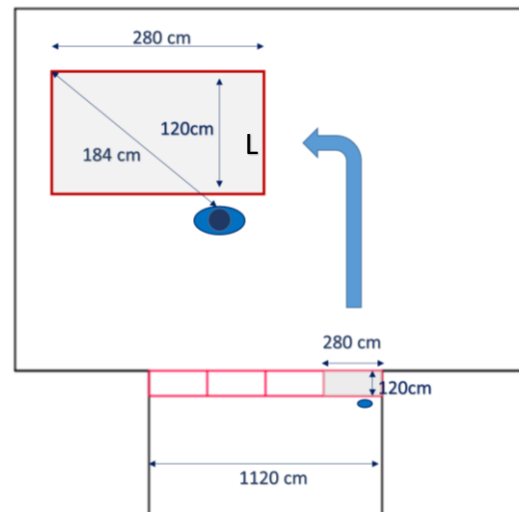
Figure 13. Scheme of the estimation of the error in transit length – Stripping Phase (High Density). The red grid have been used to analyse the pedestrian movement and to help the counting of the pedestrians present in the area in a specific time. In this case the length of the grid is shorter due to the view angle of the camera.

The errors have been found for both high and low density. The resulting values have been shown in the Appendix A (Tables 1-4).

The error are in the order of: density, which are the more reliable, $\varepsilon_{\rho(av)_{(\%)}}$ = 7,44 in case of low density and $\varepsilon_{\rho(av)_{(\%)}}$ = 13,28 in case of high density. In the transient time and the speed have been recorded higher values $\varepsilon_{t(av)_{(\%)}} = \varepsilon_{v(av)_{(\%)}}$ = 21,19 for low density and almost doubled for high density $\varepsilon_{t(av)_{(\%)}} = \varepsilon_{v(av)_{(\%)}}$= 40,33.

3.2.2 Schemes of the flows

The trajectories have been analysed by visual inspection and mostly focused, not on the individual movement, but on the whole flow.

The grid used to subdivide the *Gate* helped to develop the counting process as well as to identify the flow trend. In the analysed time interval, which has been the time frame 1:10:98 m.s.mms from the starting of the video recording at 03:29:12 m.s.mms, three relevant frames have been extracted, at 10s, 30s and 50s accordingly.   They are respectively shown in Figure

14, Figure 15 and Figure 16, schematically, to point out schematically the complexity of the flow in this bottleneck.

The sinusoidal shape of the arrows represents an uneven movement, i.e., weaving and stop and go movements. Due to the high density, pedestrians tend to move as a wave front, thus they present the same travel time. This behaviour is pointed out in the Figure 14 where, in the bottleneck area, it has been noted a complex but organised flow.

In the Figure 15 due to the superposition of several multi-directional flows, i.e., *opposing* in the first grid, *weaving, intersecting* and *merging* in the other cells, the movement becomes more and more complex. This complexity increases the local density in the central area, which then becomes a *congested area,* where the crowd remain completely still. The presence of still people in the area affects the density, for all the analysed time frame. In the frame Figure 16 at time 70s, the configuration is almost unchanged compared with the previous one at 50s.

It is interesting to point out that it has been noted an even flow inside the control area, which lasts longer in case of the high density rather than in case of the free flow at low density.
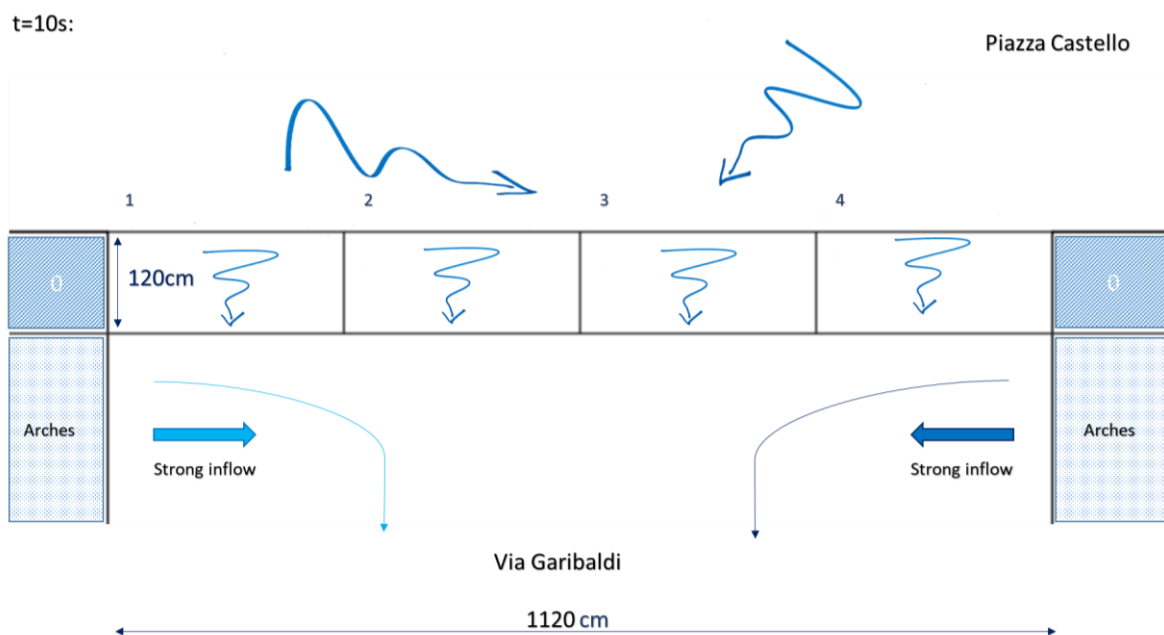
Figure 14. Flows scheme of the gate referred to the Stripping Phase at the 10s of the time frames observed. The shape of the arrows represents an uneven movement, i.e., weaving and stop and go movements. In the front of the bottleneck the two arrows indicate the intersecting movement of the crowds. The two straight lines in the opposite side indicate the lateral inflow and the shape of the thin arrows indicate the merging flow among the crowds.
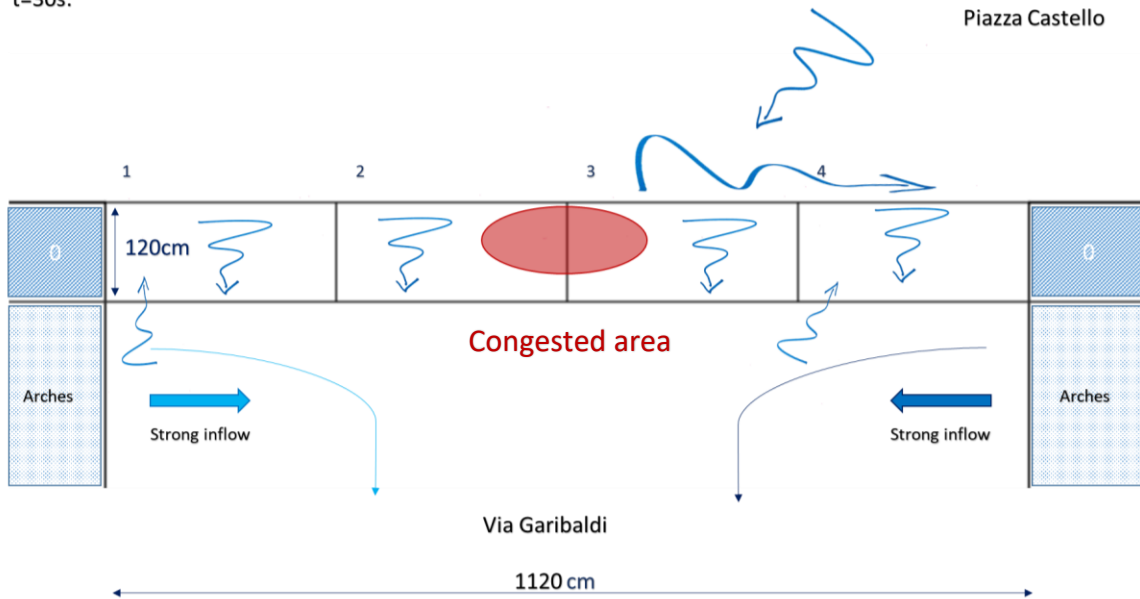
Figure 15. Flows scheme of the gate referred to the Stripping Phase at the 30s of the time frames observed. The shape of the arrows represents an uneven movement, i.e., weaving and stop and go movements. In the front of the bottleneck the two arrows indicate the intersecting movement of the crowds. The two straight lines in the opposite side indicate the lateral inflow and the shape of the thin arrows indicate the merging flow among the crowds. In the centre of the bottleneck in red oval is shown the congested area due to the combination of the multidirectional flows, i.e., merging, intersecting, in several point of the bottleneck region and both in the front and after it.
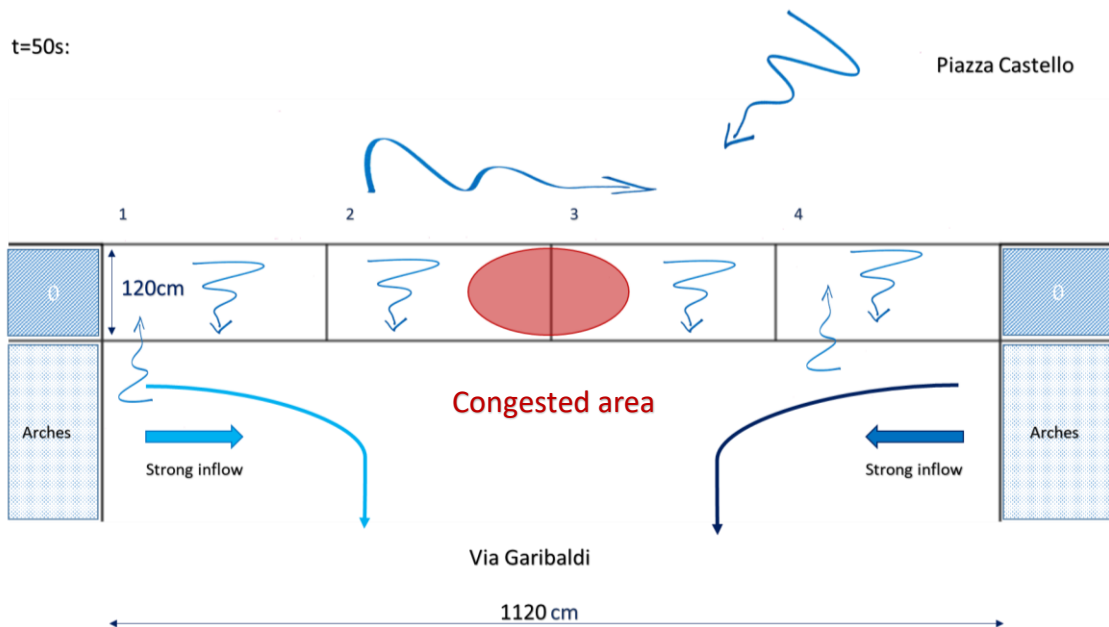
Figure 16. Flows scheme of the gate referred to the Stripping Phase at the 30s of the time frames observed. The shape of the arrows represents an uneven movement, i.e., weaving and stop and go movements. In the front of the bottleneck the two arrows indicate the intersecting movement of the crowds. The two straight lines in the opposite side indicate the lateral inflow and the shape of the thin arrows indicate the merging flow among the crowds. In the centre of the bottleneck in red oval is shown the congested area due to the combination of the multidirectional flows, i.e., merging, intersecting, in several point of the bottleneck region and both in the front and after it.

29

It has been observed that pedestrians try to exhibit self-organised behaviour by avoiding conflicts among each other. Despite their desire to stay in their current path, local interactions occurred at the merging point, which is demonstrated by the mix of trajectories [45]. The interactions slow down the speed at the merging points. The still crowd between the merging points highlights that the direction of the inflows may have an influence on the speed and on the outflow of pedestrians. The presence of a still crowd is probably due to the slowdown in speed, related with the mixing of trajectory.

3.3 Simulation work
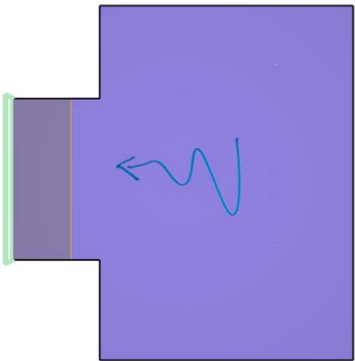
The simulation work is made in order to evaluate the performance of a typical continuous agent-based evacuation model in high density scenarios. Results obtained from the analysis have been used to set up the models. The goal is to reproduce the local density and the flow recorded during the real event.

Considering this, two different approaches have been followed using the output from the video analysis, as an inputs in the simulation analysis:

1. By setting the *body size* of the agents to achieve certain density in the area and using as input the *averaged flow* observed in the video analysis. To evaluate the possibility to reach the high *local density* previously observed in the video analysis phase, a series of tests have been performed.

2. By setting the *body size* of the agents to achieve certain density in the area and using as input the *averaged speed* observed in the video analysis. Also, in this case a series of tests have been performed to evaluate the possibility to reach the *averaged flow* shown in the video analysis section.

3.3.1 Assumptions and Sensitivity Analysis to set up the model

The sets of simulations has been performed using Pathfinder [91]. In the following Table 1 and Table 2 have been shown respectively the scenarios and the main assumptions that have been used to run the tests.

SCENARIOS		
TYPE	**Schemes**	**Description**
1		From test T1 up to T30 the geometry used to run the simulations was a **simple T-junction**. **Uni-directional flow**.

30
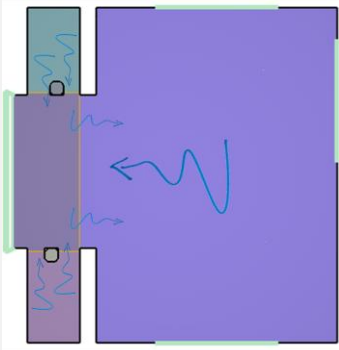
2		From test T31 up to T38 the geometry used to run the simulations was a **T-junction** combined with the **inflow from both sides**. **Multi-directional flow**.
3		Test T39 geometry used to run the simulations was a **T-junction** combined with the **inflow from both sides.** **Multi-directional flow**. The **holding area** has been **doubled**.
4		Test T40 and T41 geometry used to run the simulations was a **T-junction** combined with the **inflow from both sides**. **Multi-directional flow.** The **holding area** has been **tripled**.

Table 1. Scenarios run in the simulation task. The lateral inflows have been simulated using the Occupant source. The movement group template has been set 90% Movement Group and 10% Ungrouped. The maximum distance allowed, due to the case, has been set 0,3 m with slowdown time of 2s. The number of the group members is in the range of 2 up to 10 agents.

The first set of the simulation run, from T1 up T18 in Table 2, had as input the parameters calibrated, using uniform distribution, in order to cover a wide range of the sets parameter. This had the effect of making the evacuation scenario as realistic as possible, considering also the presence of locomotion disability giving the range of velocities of 0,4 m/s up to 1,2 m/s.

These threshold values closely approximate the minimum and the maximum value of the interquartile range of the speed found by Boyce [92], on horizontal by presence of locomotion disability. In the safety plan, on the square were forecast 20.000 agents, which correspond to an initial density of the area ρ=1,79 persons/m². This density value has been used as a starting point of the simulations set and it was increased up to 6 persons/m². Concerning the body size, it has been first used the default constant value, 45,58cm.

In the second set of simulations, from T19 up to T24 in Table 7, the uniform distribution has been used also to set up the body size of pedestrian in the range of 33 cm up to 35,34 cm, due to the limit in representing high local densities, as shown in details in Figure 17.

In the third set, from T25 up to T41 in Table 7, as input values they have been used the output values from the video analysis, combined with the uniform distribution of the body size, i.e., 33,00 -35,34 cm. Using experimental data rather than only default settings had the effect to make the evacuation scenarios as realistic as possible, while limiting the user effect [93], i.e., results affected by the choices of modellers during the process of input calibration [42]. All the process behind the development of the tests has been shown in the flow chart Figure 18.

More details concerning the tests have been presented in Appendix B - Main results obtained in the Tests' Task.

MAIN ASSUMPTIONS

SCENARIO	N°	Geometry Gate (m)	Shoulder Width (cm)	Averaged Density in the Area (person/m²)	Comfort Distance (m)	Imposed Flow (person/ m*s)	Imposed Speed (m/s)
1	[T1-T6P]	6,2*6	45,58	1,79	0,080 and 0,347	x	unif. 0,4-1,2
1	[T7-T12]	7*6 up to 11,2*6	45,58	1,79	0,347	x	unif. 0,4-1,2
1	[T13-T18]	11,2*6	45,58	1,79 up to 6,00	0,001 up to 0,164	x	unif. 0,4-1,2
1	[T19-T24]	11,2*6	33,00 - 35,34	1,79 up to 6,00	0,08 and unif.0,05 27-0,076	x	unif. 0,4-1,2
1	[T25-T26]	11,2*6	33,00 - 35,34	4,00 and 5,00	unif.0,05 27-0,076	x	const. 0,07
1	[T27-T30]	11,2*6	33,00 - 35,34	3,00 up to 5,00	unif.0,05 27-0,076	0,2137	const. 0,07
2	[T31-T35]	11,2*6	33,00 - 35,34	3,00 up to 5,00	unif.0,05 27-0,076	x	const.0,07 unif.0,05-0,08

							const. 0,045
2	[T36-T38]	11,2*6	33,00 - 35,34	4,00	unif.0,05 27-0,076	x	const.0,08 const.0,05 5 const.0,07
3	T39	11,2*6	33,00 - 35,34	4,00	unif.0,05 27-0,076	x	const.0,07
4	T40	11,2*6	33,00 - 35,34	4,00	unif.0,05 27-0,076	x	const.0,07
4	T41	11,2*6	33,00 - 35,34	4,00	unif.0,05 27-0,076	x	const.0,07

Table 2. Main assumptions to set up the tests. The green box in table highlight the main assumption related to series of tests, in which the recorded local high density in the bottleneck was almost the same get from video analysis. In the light blue box have been underlined the input related to the tests where the measured averaged flow found was in the range of the one found in the observation task. Finally, the lilac box points out the set, which allow to get both local high density and averaged flow. For details see Appendix B - Main results obtained in the Tests' Task.

The investigated aspect with this set of simulations was mainly the local density and the flow. Due to the cylindrical shape of occupants used in Pathfinder, the diameter of this cylinder represents the occupant and the value, which affects the number of people that can be added in a *Room* without overlapping [94]. This assumption makes a well representation of the reality in case of low density, but did not allow to represent real condition in case of high density, as shown in the simulation results. It has been observed that, the characteristic density cannot be reached with the default body size, setting properly the *Comfort Distance,* as shown in detail below.

The subsequent approach has been to change the size of the cylinder in a uniform distribution, 33 ÷ 35,34 cm, so that to reach the specific local density.

A raw analysis was performed from a geometrical approach. According to the averaged density $\rho = 6,43 \frac{Persons}{m^2}$, which was found, the disks with a uniform distribution of 33 cm $<$ $d <$ 35,34 cm have been fitted in a square metre of surface, as shown in Figure 17.
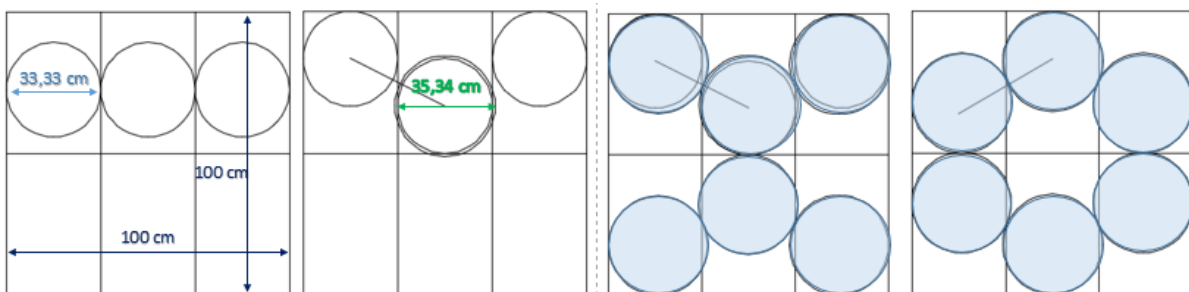
Figure 17. Setting of the cylinder's size. It represent the raw analysis made from a geometrical prospective to verify the reasonable body size of the agents in the model.

More specifically, in order to simulate the high density, found in the video analysis, it has been observed in the Pathfinder that is essential to set up:

The *Comfort Distance,* which is a parameter that specify the desired distance one agent will try to maintain in time with others, when he is within the range of them, enabled these occupants to be close enough when they are queued. This parameter was found, starting from an occupant area or an occupant density, based on a sphere packing, according to the equation below:

$$c = \frac{2}{\sqrt[4]{12}} \sqrt{a} - d; \qquad\qquad (3.4)$$

Where c is the comfort distance, a is the occupant area, and d is the occupant's shoulder width. In the specific case, it was assumed as a starting point the maximum occupant density and $a = \frac{1}{\rho}$ where ρ is the occupant density [94].

First, a simplified model has been tested by keeping unchanged the default parameter of pathfinder constant $d = 45{,}58\ cm$, which is in line with the average shoulder width of an adult [95]. Concerning the density, it has been used as an upper limit value $\rho = 7\frac{Persons}{m^2}$, which correspond to the maximum local density found by analysing the video. Here, they have been referred here only the parameters, which affect this analysis.

It is interesting also to note that this formula relates the allowed density in a certain area with the dimension of the agent in the area. Critical values have been found. These critical values have been observed as a transitional point between a positive value and a negative value, which makes the correlation to tell us that a pedestrian with a specific size cannot fit inside an area with that density. This is due to the way the program models the agents, as a stiff cylinder, without allowing deformation of the body. Over more, keeping d unchanged, the maximum density was allowed in that area by defending the default body size as 5,55person/m². On the other hand, unchanging ρ, the maximum occupant's shoulder dimension is $d = 40\ cm$.

According to the analysis above, and further considerations given below, a total amount of 42 tests, reported in Appendix B - Main results obtained in the Tests' Task, have been run in order to achieve the enhanced levels of approximation to the real case, being able to simulate the level of local density and flow.

It is given below a detailed scheme concerning the approach and the considerations behind this process:

Objectives	Assumptions in the model	Observations

1 — *Definition* of a simple *Initial Geometry* layout using all the Pathfinder default parameters

Pathfinder default parameters

2 — *Investigation* of the *Comfort Distance* parameter effect on the simulation density results

Set up the *Comfort Distance (CD)* according to the formula shown in the user guide

The *(CD)* parameter *affects the density* also keeping unchanged the body size and the initial density of the area

3 — *Comparisons* of the resulting flow according to the location of the door and the location of this in relation to the *Measurement Region*

Door's location following the *Measurement Region*

Door's location before the *Measurement Region*

The location of the door slightly affects the density in the *Measurement Region*

4 — *Investigation* of the *Width (W) effect* of the bottleneck on flow and density in the area. A series of tests have been run changing the W parameter.

The *width increased* (one metre a time) up to the *real dimension*

The *flow increases not exactly linearly*. The *following tests* were run with *real dimension of the bottleneck*

5 — *Increasing* the *initial density* of the *Holding Area*

Increasing the *Number of agents in the Holding Area*

Increasing the *initial density* and *setting up* the *CD* parameter, according to the maximum desired density, *the target has not been reached*.

To reach the desired local density in the bottleneck, according to the data from the video analysis, the *body size* of the agents has been *changed*. In the program, to simulate very high density scenarios, *it is necessary to find a balance among the agent's body size and the Comfort Distance parameter.*

| 6 | A series of tests have been run changing the **Body size, Comfort Distance** and **initial density** of the Holding area | **Set up of the body size** | Changing the **CD parameter** and reducing the **body size do not guarantee the "desired" local density** in the bottleneck |

| 7 | Introduction of a **waiting time** in the **exit door**, to increase the density | The **exit door** set with a **waiting time** | The **waiting time** (time In which the door is close) **do not affect the density** in the measured area |

To reach the desired local density in the Bottleneck, according to the data from the video analysis, a series of tests set with those parameters, i.e., averaged velocity and the averaged flow, have been run

| 8 | Setting the model with the **found parameter**, a series of tests have been run to investigate how the **initial density** of the **Holding area** affect the **local density** in the **Bottleneck** | Input parameters from video analysis (**v=0,07m/s; Q=0,2137P/m*s**) | Imposing the flow the initial density slightly affect the local density in the area, which was reached in all tests |

Changing the agent's body size, the comfort distance and introducing the output from video analysis (**v=0,07m/s; Q=0,2137P/m*s**) the program has been able to reproduce the local density found in the Bottleneck analysing the video.

| 9 | It has been introduced the **lateral inflow** from the arches and the **averaged velocity** found from video analysis, **no imposed flow** has been considered | The flow was not used as input parameters | |

| 10 | A series of tests have been run changing the **initial density**, the **averaged velocity** and the **comfort distance** | Changing the initial density in the holding area and the bottleneck | The **initial density**, as expectation, **affect the flow**. The desired flow has been reached only for a certain density, i.e., 4 person/m^2 |

| 11 | | Changing the averaged velocity / Changing the comfort distance | The **averaged velocity** and the *CD slightly affect the flow* and the *local density* measured in the *Measurement Region* |

| 12 | **Changing the geometry**, the **holding area (HA)** due to the bottleneck already had the real dimensions | First test the **HA doubled** / Second test the **HA tripled** | Increasing the HA, the **local density** in the Bottleneck has been **increased** reaching the desired value. However, the **total averaged flow** was respectively **doubled** or **tripled** |

Setting the body size, the initial density and the averaged velocity according with the output from video analysis the program has been able to reproduce the flow observed in the Bottleneck.

Both flow and local density related to high density scenario can be simulated by the program. According to the physic, increasing the density for a fixed averaged velocity, also the flow will increase. It has been possible to reach, from a single simulation, both flow and local density imposing the velocity, the agent's body size, the comfort distance and the initial density.
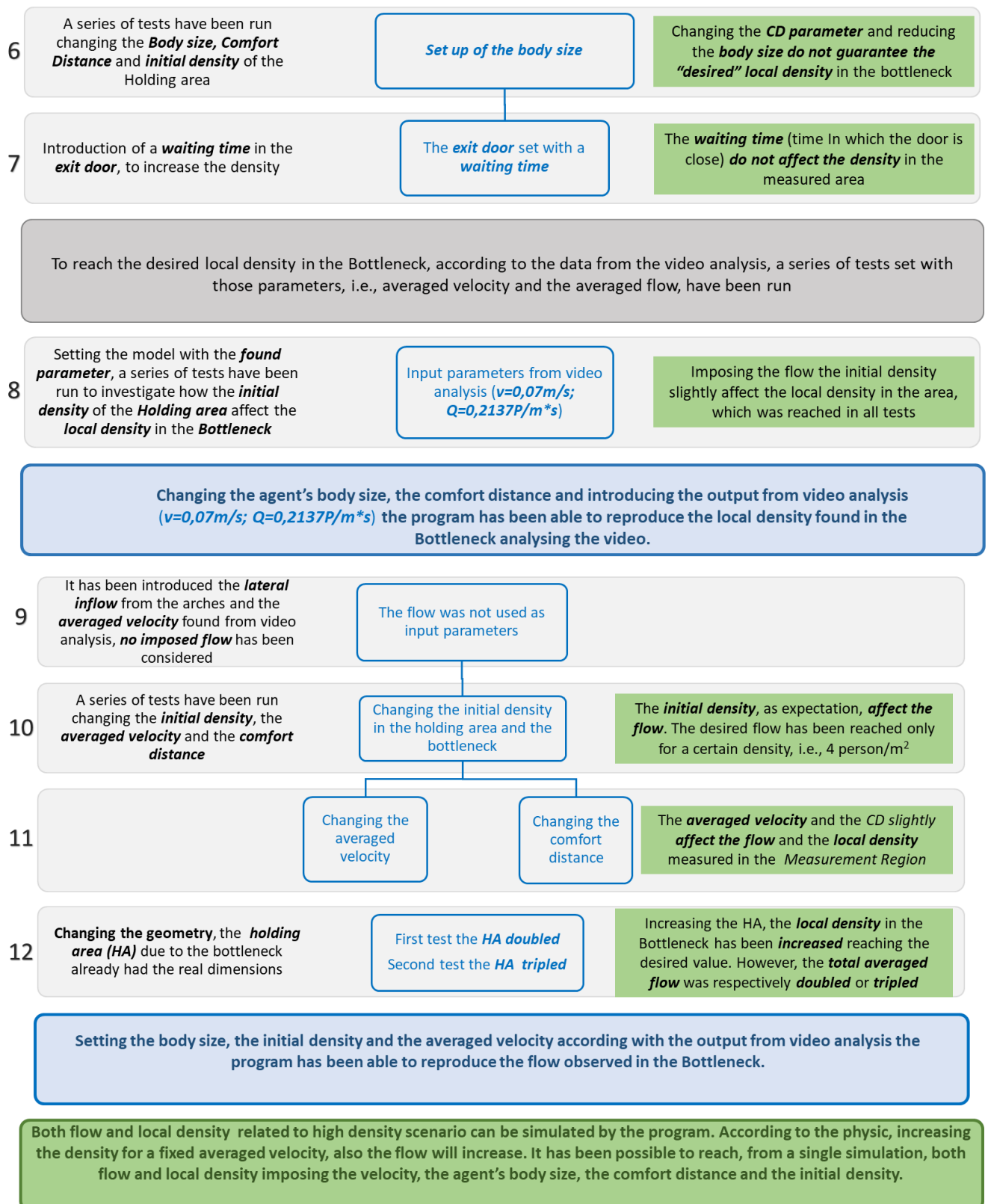
Figure 18. Flow chart related to the developed tests. It shows the steps followed to investigate the better setting of the simulation model to run in order to achieve, at the same time, flows and local densities found in the monitoring task (video analysis).

A further analysis has been made in order to evaluate the different densities observed in the area of the gate and the vicinity of this one. These values have been measured using a set of small *Measurement Region,* in order to get more reliable results. The partitions is due to the concept behind the *MR,* which is based on the integration over the interested area, for this reason and due to the extension of the interested area, more accurate results can be obtained.

Results and further details have been provided in the following paragraph 3.4.

3.4 Results and critical points (Hotspot)

In this section both results concerning the video analysis and the simulations test have been presented.

The statistical analysis of the data has been performed by using moving averages.

3.4.1 Video analysis results

Due to the high-density condition the pedestrians assume a waiving behaviour, which causes trajectories to oscillate along the centre of mass movement of the body. As observed in the video, this effect become stronger and stronger, as soon as the speed has been reduced, reaching the maximum when pedestrians are waiting in the same spot and the only movement allowed is the *leg swings*. This motion has been interrupted, in some areas, by the collective phenomenon of the lane formations during the analysed time, as it has been set out in the paragraph 3.2.2. It is a self-organised phenomenon, due to the extension of the examined control area.

As expected from the analysis, it is evident that in the *Stuffing phase,* with the density ranging between $0,4 < \rho < 0,7$ persons/m^2, the speed is higher, $0,3 < v < 1,2$ m/s, compared to the *Stripping phase*, which has a density range of $6,1 < \rho < 6,8$ persons/m^2 (see Figure 22), and the speed is lower, $0,02 < v < 0,08$ m/s (see Figure 23). By contrast, it is interesting to point out that in both cases the flow, Q, does not differ substantially. In the first case was found $0,09 <$ Q $< 0,25$ persons/m*s with an averaged flow value of $0,16$ person/m*s or $9,58$ persons/m*min. In the second case $0,08 < Q < 0,27$ persons/m*s (see Figure 21 and for the flow Figure 19 and *Figure* 20) with an averaged flow value of $0,21$ persons/m*s or $12,85$ persons/m*min.

The results are shown in the following graphs.

Specific Flow and Flow Rate
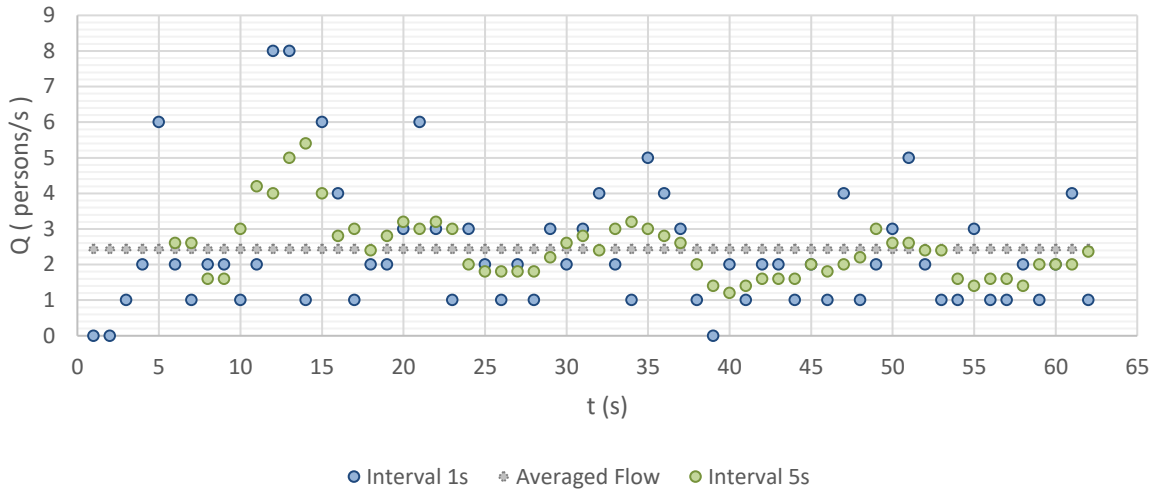
Figure 19. Flow-Rate diagram at high density scenario from the video analysis, time interval 5s
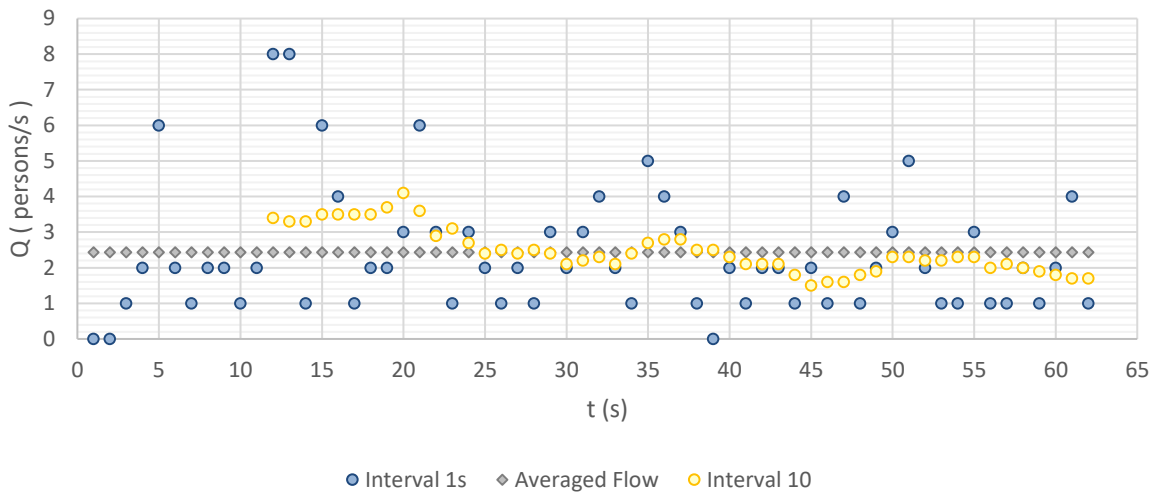
Figure 20. Flow-Rate diagram at high density scenario from the video analysis, time interval 10s
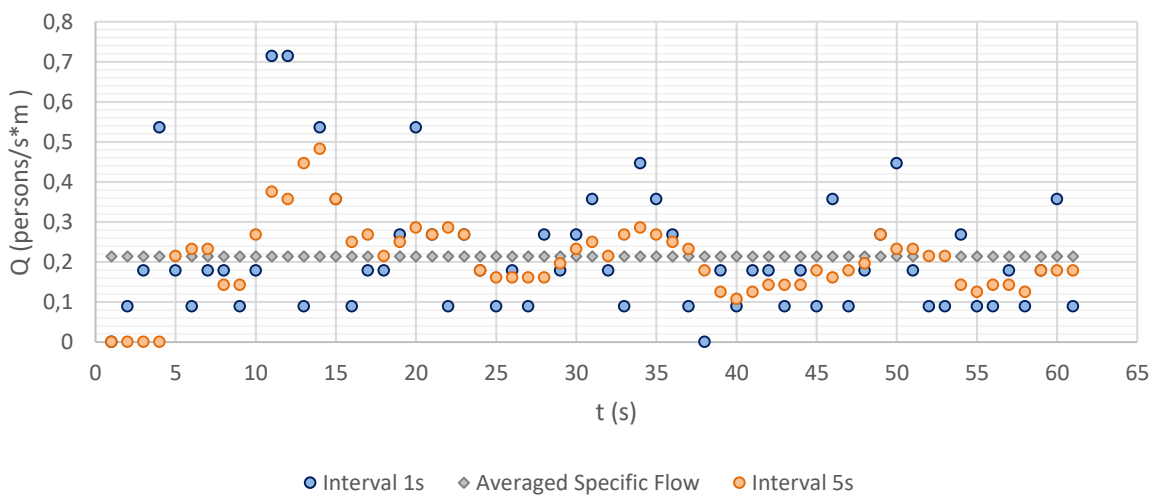
Figure 21. Specific Flow diagram at high density scenario from the video analysis

Density
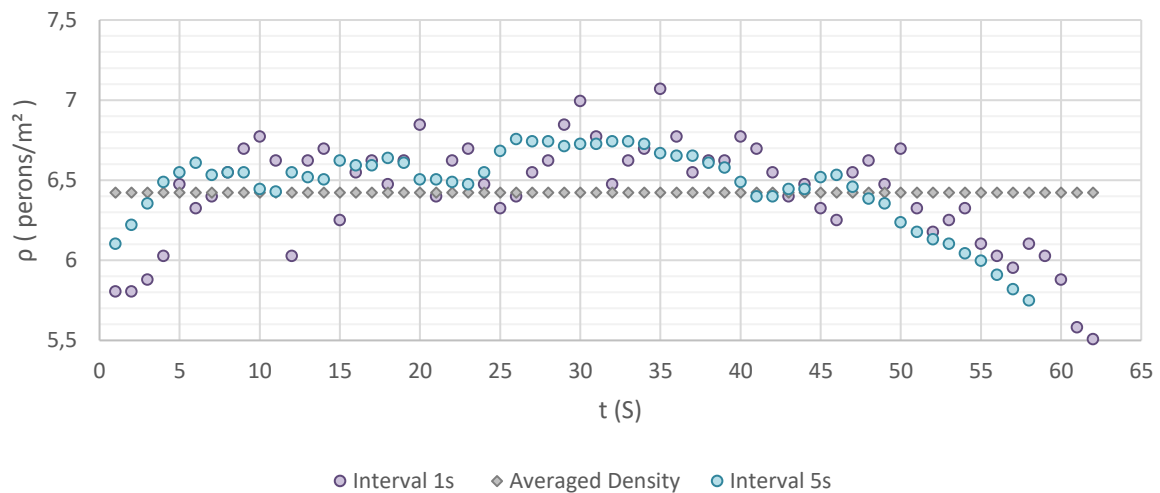
Figure 22. Density diagram at high density scenario from the video analysis

Speed
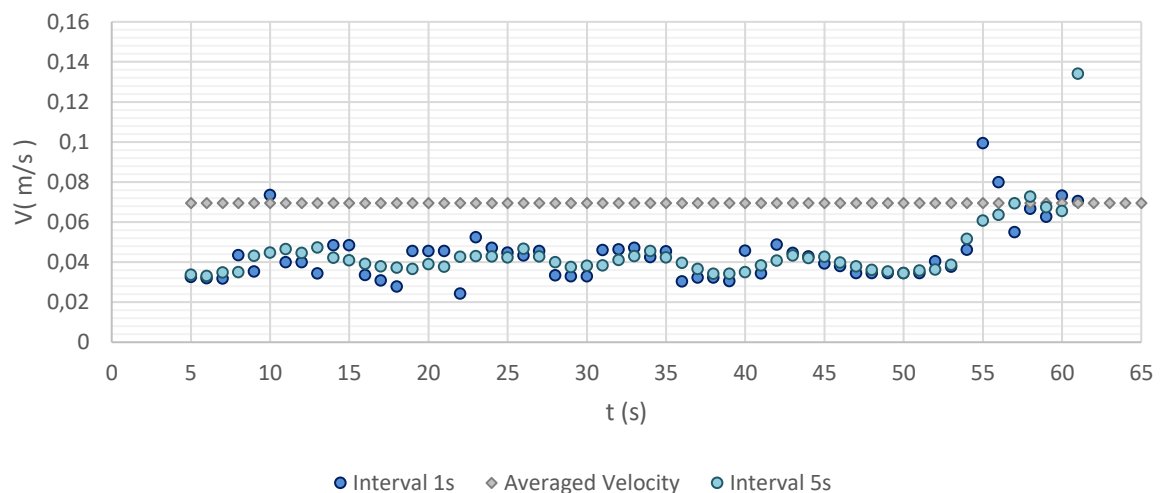
Figure 23. Speed diagram at high density scenario from the video analysis

Fundamental diagrams

As we can see from the graphics below, Figure 24 and Figure 25, it was not possible to build a fundamental diagram collecting these data. Probably this is linked with the choice to develop a detailed analysis in a short time frame.

A trend can be seen in the Speed – Density diagram (see Figure 24). In this case, an R^2 value equal to 0,82 has been obtained using a polynomial curve of the third order. The speed decreases by increasing the density.

The dotted blue line in Figure 24 represents the function R^2, which has been used to determine the trend line. This factor is a statistical measure of how well the data fit the regression line. In a range of [0,1] the higher the R^2, the better the trend line fits the data.
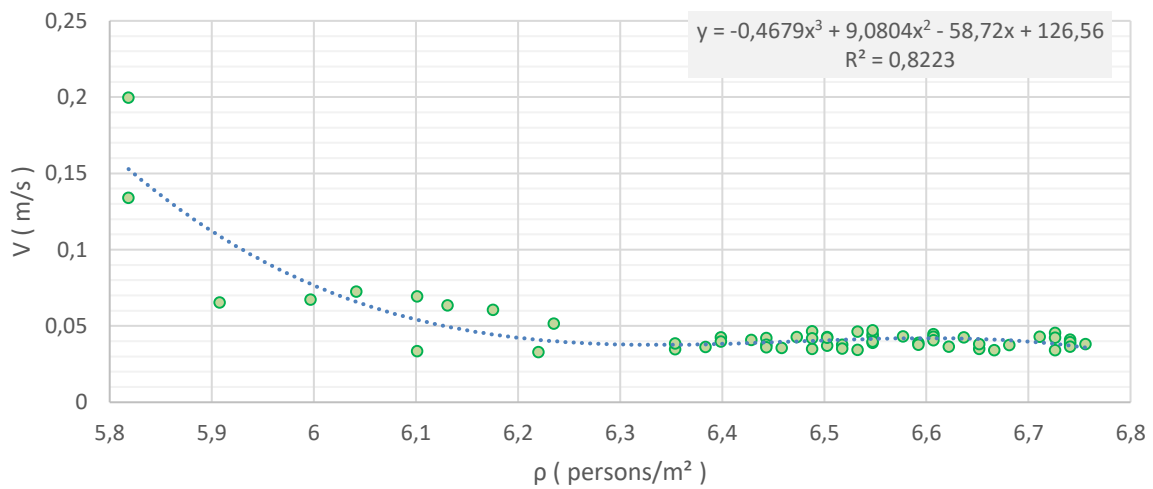
Figure 24. Speed-Density diagram at high density scenario obtained from the video analysis

No clear trend can be identified in the Specific Flow – Density diagram. The average specific flow stands at about 0,21 persons/m*s. The increase in flow according to the increase in density, at steady speed - corresponding to the few spots in Figure 25 - is probably due to the lateral inflow from the arches in a certain period of time, which might cause this jump in the graph.
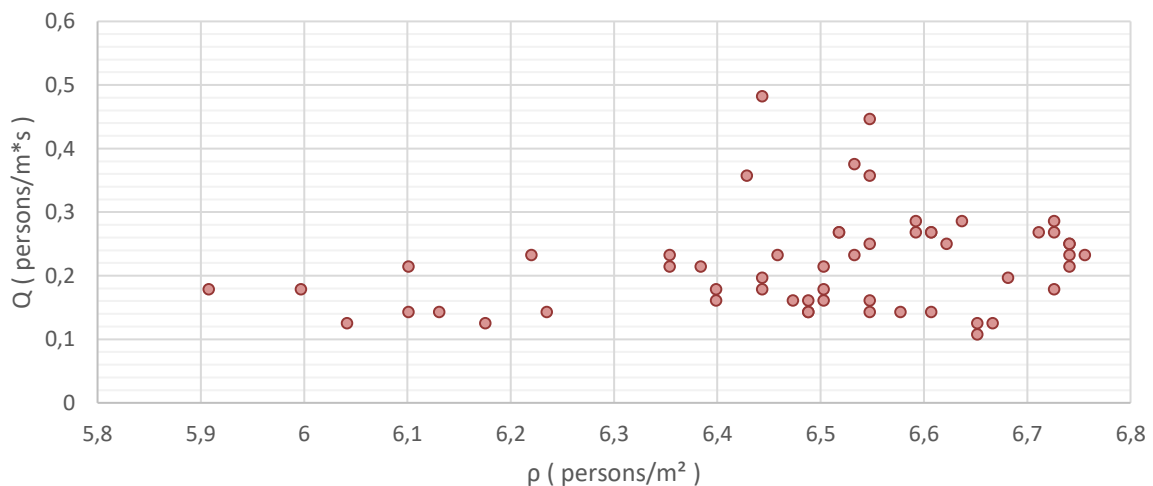
Figure 25. Specific Flow-Density diagram at high density scenario obtained from the video analysis

3.4.2   Modelling results and comparison with the video analysis data

In the series of tests that have been performed, it has been shown that increasing the width of the bottleneck, keeps unchanged the other parameters, while the average speed increase. The results agreed with the values from laboratory experiments [82], but the maximum that

was reached speed shows a fluctuating trend. Until 7m width the maximum speed increases, for 8 m and 9 m width the maximum speed decreases, in 10 m increases and, finally, to reverse once again in 11 m. More details have been shown in Appendix B - Main results obtained in the Tests' Task.

Table 7 from test T6 up to test T12.

The results shown in the graphs below are referring to the more interesting tests carried out, which correspond to the tests T40 and T41 shown in Appendix B - Main results obtained in the Tests' Task.

Both these tests have been set with input parameters corresponding to the analysed data and the real scenario, such as the geometry of the gate, the initial density of the area and the constant averaged speed. The initial density of the area corresponds to ρ = 4persons/m², which have been found from iteration in the previous tests. The constant speed corresponds to the averaged speed v = 0,07 m/s, which has been found from video analysis. The body size of the pedestrians is in the range of 33 cm up to 35,34 cm. All the other values presented in the table are outputs obtained from the simulations. According to the real geometry, where the event took place, in both these tests, the increase of the local density in the bottleneck has increased the distance between the bottleneck and the holding area. This has been possible since this distance affects the density of the inflow to the bottleneck and this effect is similar to the increase of the initial density.

Due to the high densities and the resulted very low speed from the experiment, which is close to zero, and almost unchanged, the related graphs have not been shown. The values are mentioned in Table 7 (Appendix B - Main results obtained in the Tests' Task).

Specific Flow and Flow Rate

In order to measure the flow from the simulation, according to the position, where the flow has been analysed, a *Door* has been located 2m far away from the entrance of the bottleneck. In the schemes, Figure 28 and Figure 33, and in the Table 7 it is shown this section, which corresponds to the *Door 05.*

In the video analysis, it was chosen to analyse the time frame of the maximum density. In light of this choice, the following considerations pay attention to the *"peak"* of the simulations results.

The choice of the time frame in the video to investigate the peak has been confirmed by the results from the simulations. In fact, the averaged specific flow measured in the video analysis corresponds to the averaged peak value obtained from the simulations, which is around 0,2 persons/m*s, see Figure 27. Concerning the Flow Rate, the results are slightly different but in the same order of magnitude, compared with the data from the video analysis, which have been shown in section 3.4.1. In the video analysis, it has been obtained a range of values

between 1,8 up to 4 persons/s, whereas in the simulation the range value is 1,0 up to 3,0 persons/s, see Figure 26. This slight discrepancy seems acceptable, in light of the uncertainties, which affect the type of work, as it has been mentioned previously in Chapter 2. Furthermore, according to the literature, as it as has been shown in laboratory experiment that the calculated flow, by using all data, can be different from the one by using the data solely from steady state exclusively [82]. This difference is present in this work, due to the difference in time frame analysed. Specifically, the video analysis has been performed in a quite steady state condition. By contrast the simulation analysis has been developed for all the period necessary to evacuate the analysed area.
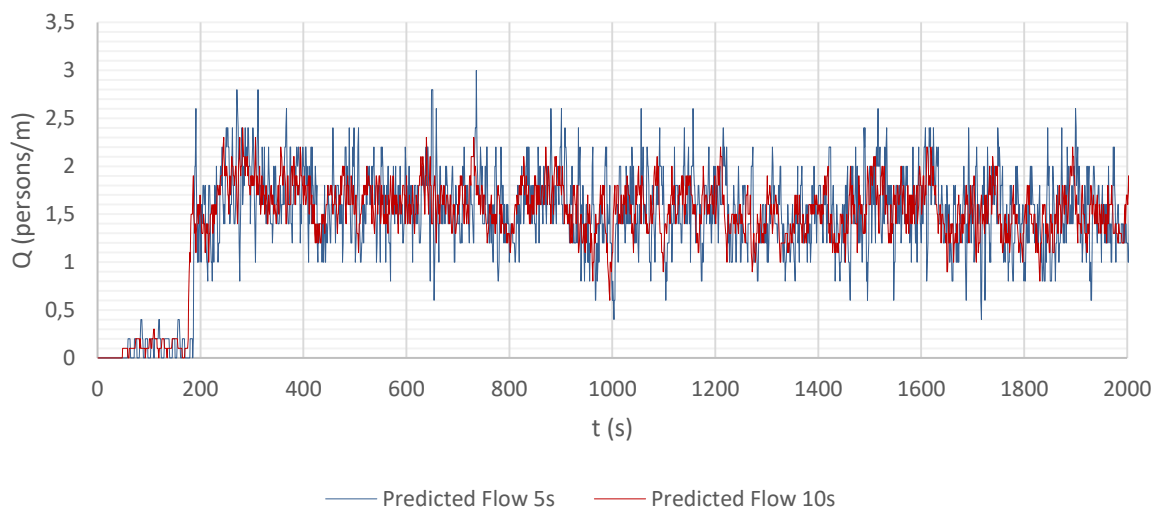
Figure 26. Flow rate for section Door 05
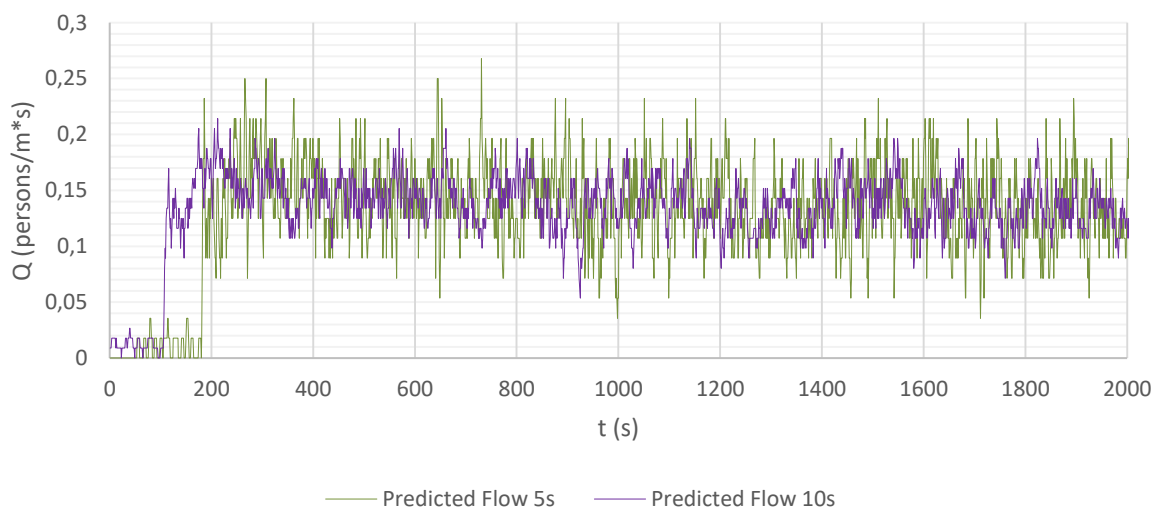
Figure 27. Specific Flow for section Door 05

Density

Referring to the density results, one prefatory remark should be called back from the uncertainties section. The density has been extracted from the simulation introducing a *Measurement Region* in the model, which, in light of the parallelism with the video analysis performed, corresponds to the control area observed in the video analysis. This density output has been measured by the program, by integrating the quantity over the entire region, using an implementation of Steffen and Seyfried's Voronoi diagram-based method [94][96]. For this reason, the model with the same input parameters has been run, introducing a different area subdivision, to obtain more accuracy in the results.

The averaged density measured in the video analysis has been found 6,45 persons/m², with a peak value of 6,8 persons/m². From the simulation run with a raw area, the subdivision with the peak averaged value has been found 5,5 persons/m², see Figure 29. In the more accurate area subdivision of the same region, the peak value of 6,4 persons/m² was found, see Figure 35. Below, it is presented the scheme and the density graphs related to the investigated area concerning the raw data, Figure 28.

The red area corresponds to the interface area between the large area in front of the bottleneck and the bottleneck itself. In Region 02 the density, see Figure 31, is higher, while the speed is lower than the ones in Region 00, see Figure 29, and of course in Region 01, see Figure 30, where the congestion starts decreasing [82].

The yellow area represents properly the bottleneck area, which has been investigated in the video analysis. In this area a peak of 6,6 persons/m² has been recorded. This value has been confirmed also from the video analysis, where a value of 7,06 persons/m² was calculated from the frame, and a value of 6,71 persons/m² calculated as the dynamic density, according to the movement of the pedestrian inside the area and the time frame.

The green area is the area, where the bottleneck has been overcome. It is relevant to point out that, in a so crowded situation also when the bottleneck has been overcome the density recorded is still high, 4,4 persons/m².
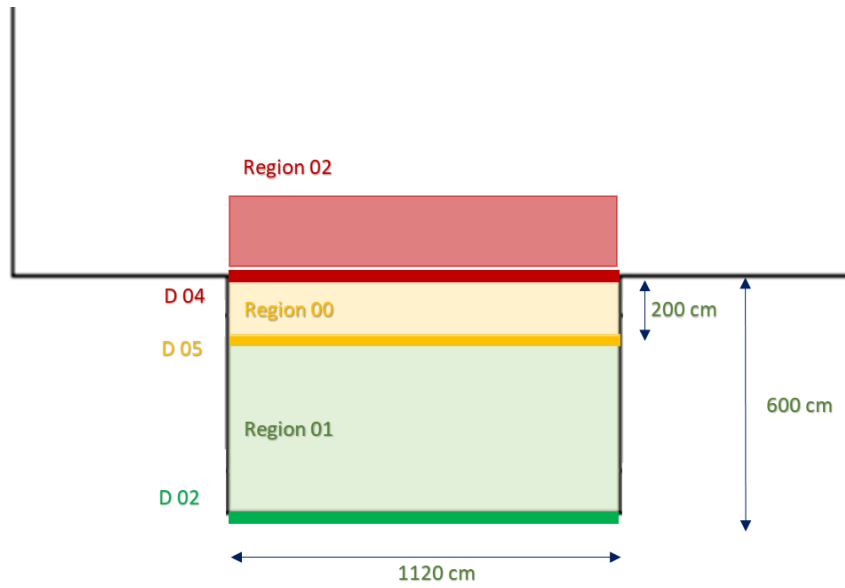
Figure 28. Scheme of the subdivision of the investigated area. In the red regions highest value of density were observed with a maximum value of 5,8 persons/m². In the yellow area, the observed peak values of 5,45 persons/m² was recorded. In the green region the peak value has been observed of 4,2 persons/m².
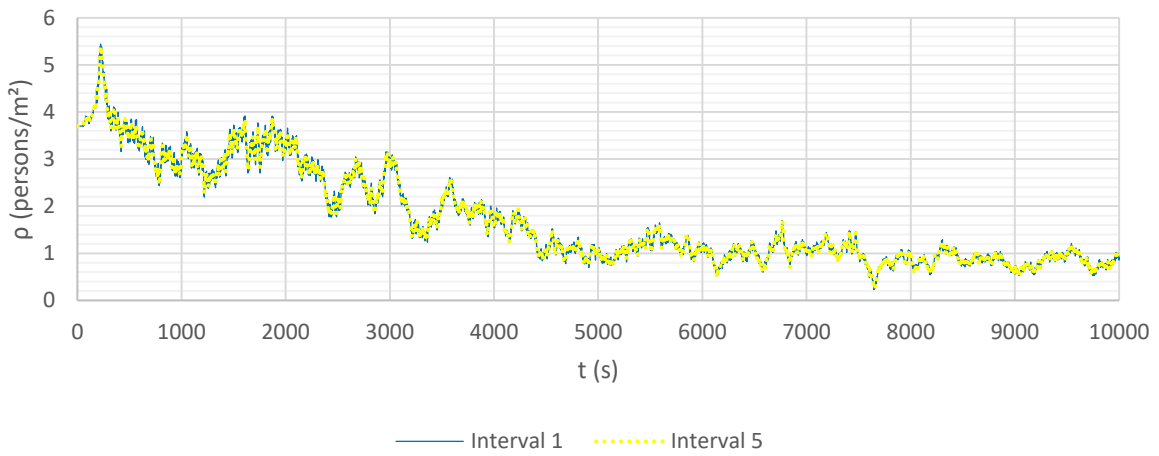
Figure 29. Averaged Density measured in the Bottleneck, Region 00.
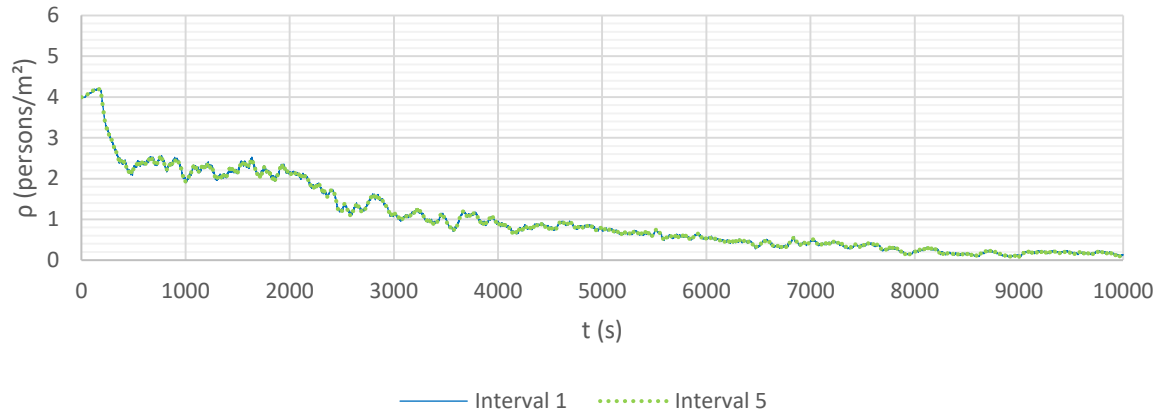
Figure 30. Averaged Density measured in the exit of the Bottleneck, Region 01.
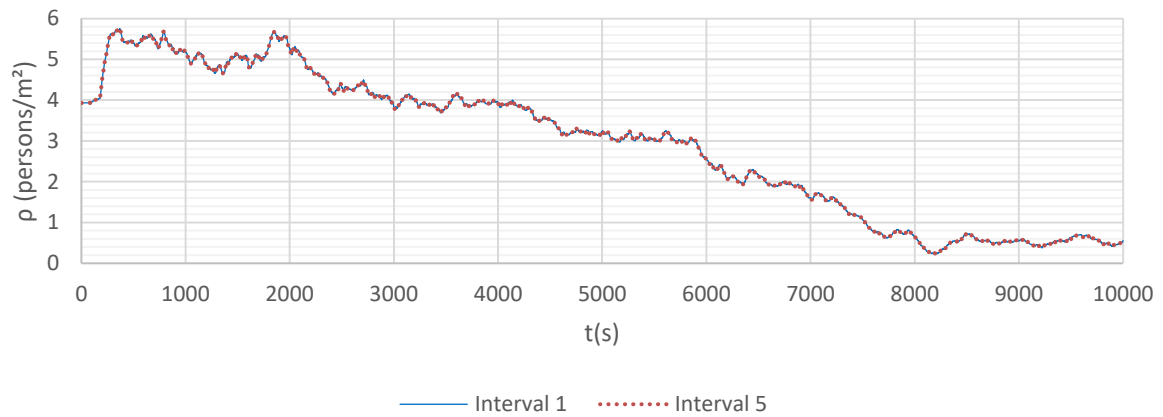
Figure 31. Averaged Density measured in the front of the Bottleneck, Region 02

In the following graph, Figure 32, the densities curves measured in the three different area have been overlapped in order to have a clearer view concerning the density distribution in the different regions.
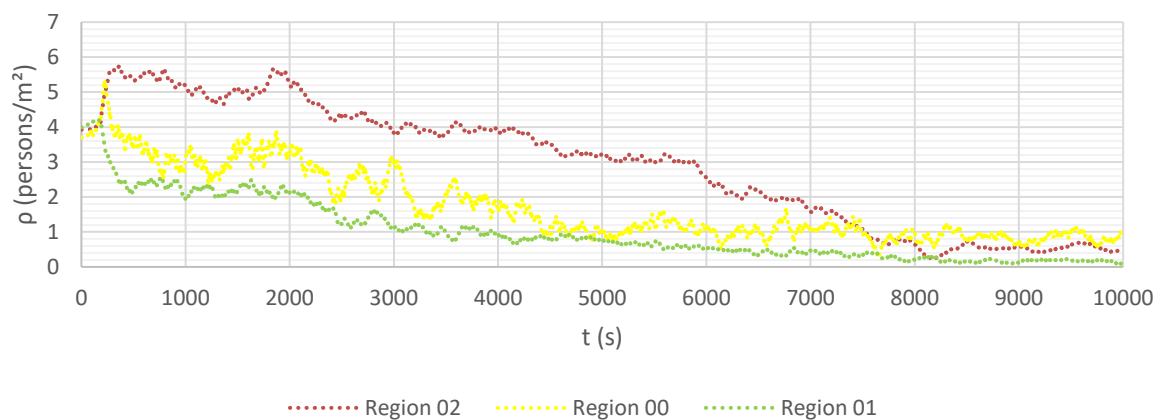
Figure 32. Averaged Density measured in the front of/ in/after the Bottleneck region. The comparison among the three different regions show that the front region is the critical area where a peak value of 5,8 persons/m² was recorded. A similar value, peak of 5,5 persons/m², was recorded in the bottleneck

area, except that suddenly the density dropped below 4 persons/m². In the region after the bottleneck, green region, the bottleneck effect it is over, and the density dropped fast from a peak value of 4 persons/m² to a value of around 2 persons/m².

As we can see from the following graphs, more accuracy has been obtained from a further subdivision of the areas, which is linked to an increase in the recorded local density values. In Figure 33 has been shown the further subdivision of the area, where the different colours point out the difference in recorded densities. From the red regions, square 1 and 6, the highest absolute density has been recorded, at around 8,8 persons/m², see Figure 34. In the yellow regions the highest density has been recorded in the in the squares 7 and 10, with a value of 6,4 persons/m², Figure 35. It is interesting to point out that this value is higher than the peak value reached in the area 2 and 5, which are in the front of the bottleneck. In area 2 and 5 a peak value of 5,4 persons/m² has been recorded, see Figure 36, which remain the peak also in the green zone, squares 3 and 4.
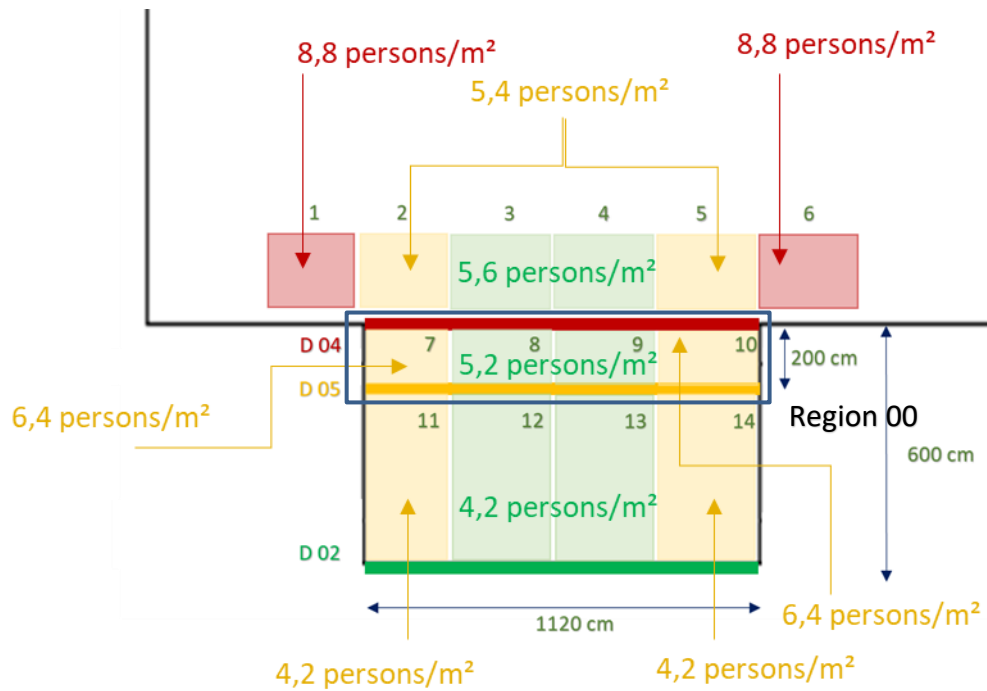
Figure 33. Scheme of the further subdivision of the investigated area and related peak density values. In the red regions highest value of density were observed with a maximum value of 8,8 persons/m². In the yellow area, the peak values have been observed in the square 7 and 10 with a value of 6,4 persons/m². In the squares 3 and 4 in the green region the peak value has been observed of 5,6 persons/m².
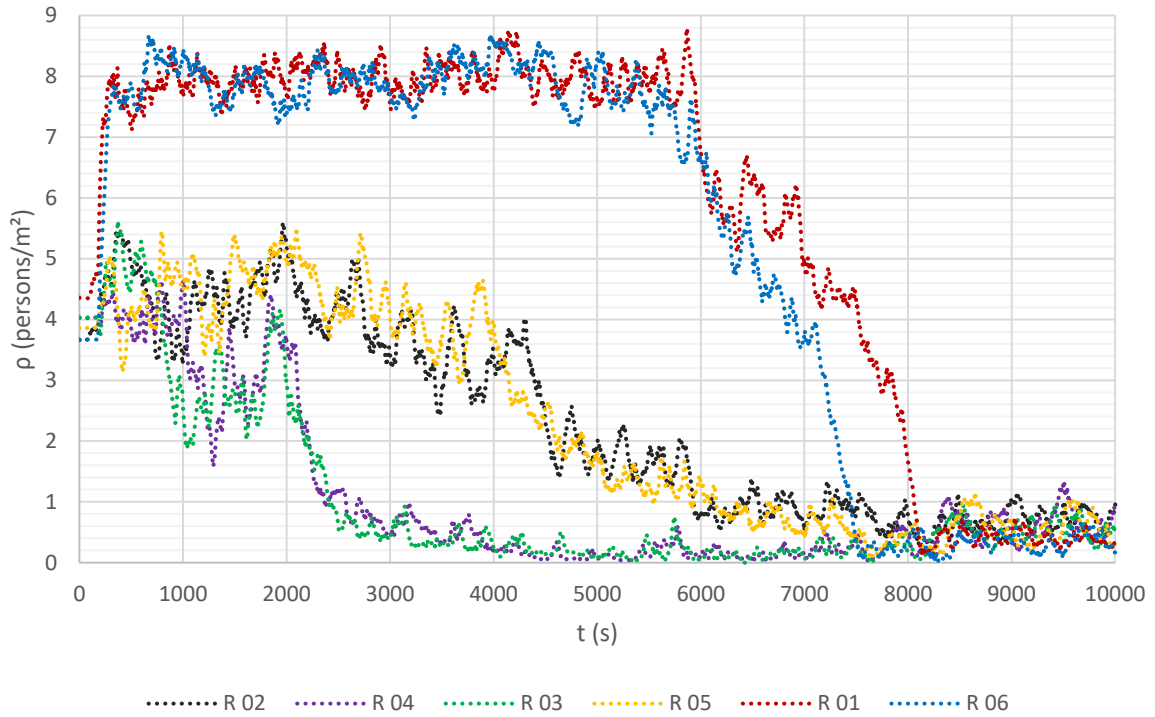
Figure 34. Detailed Averaged Density measured in the front of the Bottleneck region, Region 02. In the red regions highest value of density were observed with a maximum value of 8,8 persons/m², corresponding to the lines R06 and R01. In these areas the wall effect in combination with the merging flow have increased the density, which jumped from a static density value of 4 persons/m² to a value of 8,2 persons/m² in the first 400 seconds (6,66 minutes).
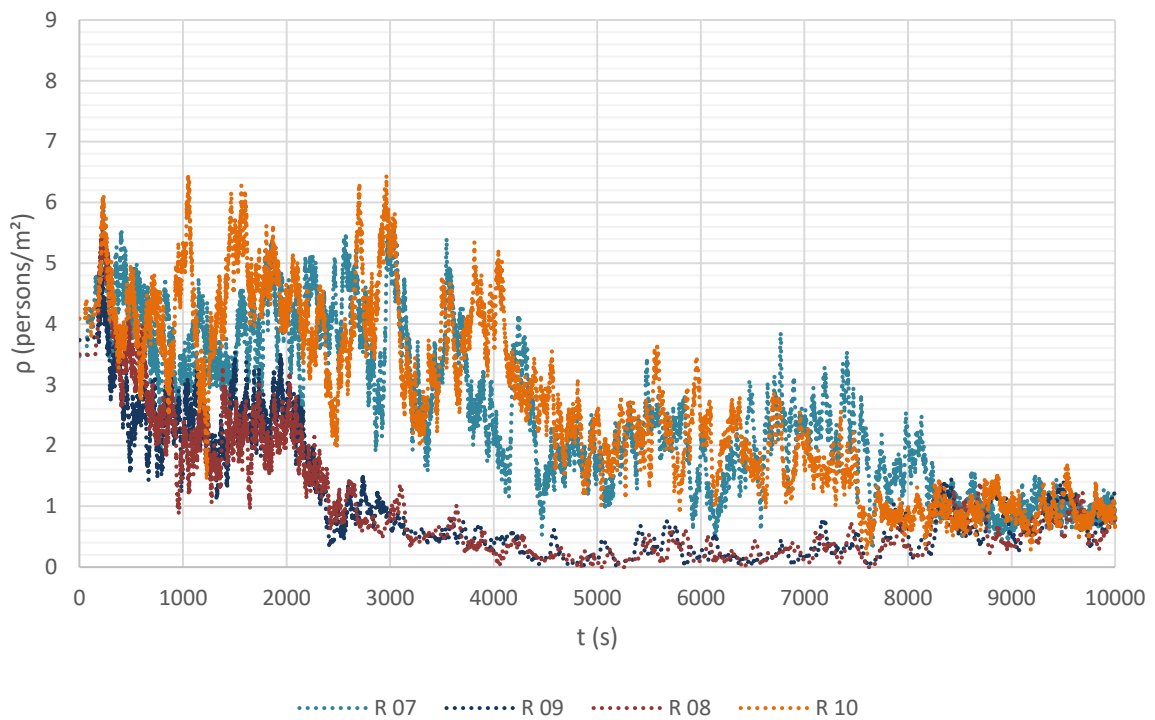
Figure 35. Detailed Averaged Density measured in the Bottleneck region, Region 00. The peak values, 6,2 persons/m², have been recorded in the regions next to the walls, R07 and R10.

47
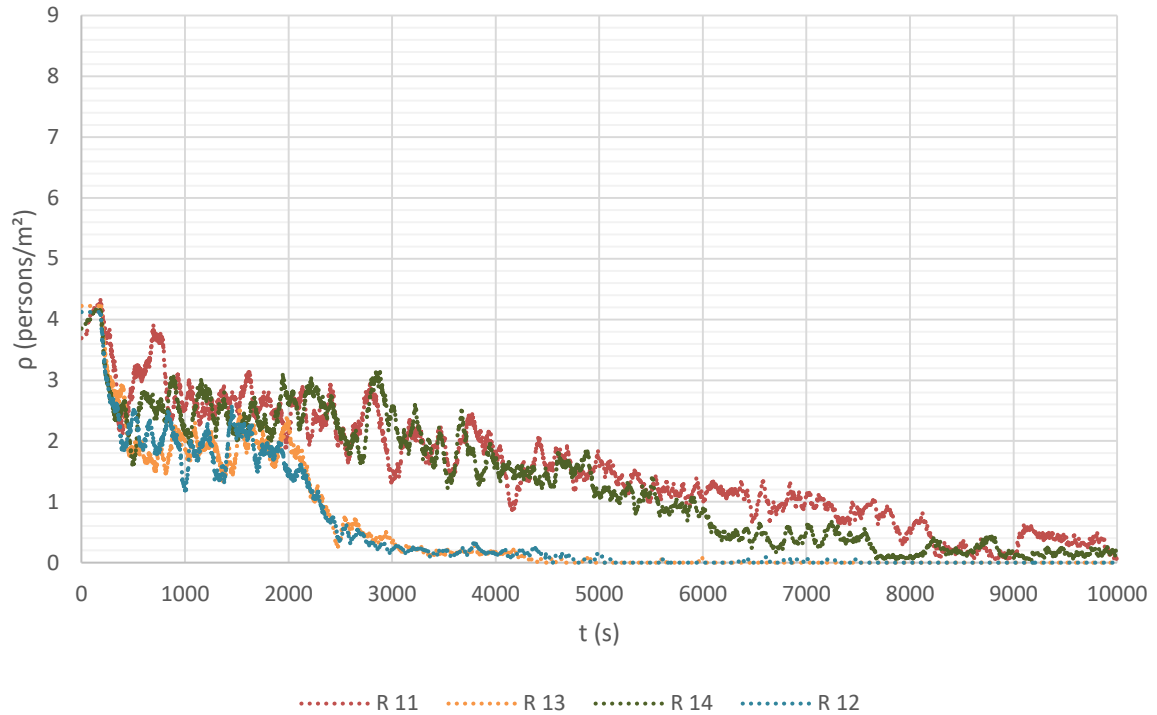
Figure 36. Detailed Averaged Density measured in the exit of the Bottleneck region, Region 01. The peak values, 4,2 persons/m², have been recorded in the regions next to the walls, R11 and R14.

In light of these results, it may be concluded that it is possible to perform a good approximation of the increasing rate of local density, by changing the body size and the comfort distance parameters, and introducing a specific initial density in the area, as well as one of the parameters found in the video analysis, which are either the averaged speed or the averaged flow. As previously mentioned, the comfort distance needs to be set according to the desired density.

Concerning the specific initial local density, it should be noted that this is a value that in public events should be fixed by the emergency and safety management plan, and strictly observed, in order to avoid high density phenomena in the critical points.

4. Interacting forces among pedestrians

The focus of this chapter is the approach at operational level of a force model to represent crowd pressure. This is based on variations of models from physics, due to the similarity of the motion of pedestrian crowd with fluids, flow granular materials or body in static equilibrium [7]. The goal is to develop a model based on existing modelling approaches, which are as simple as possible, but at the same time can reproduce an "approximatively realistic" behaviour, in the sense that the empirical observations can be approximated.

4.1 A simplified model to evaluate the frictional force among pedestrians

The workflow of this model is shown in Figure 37.
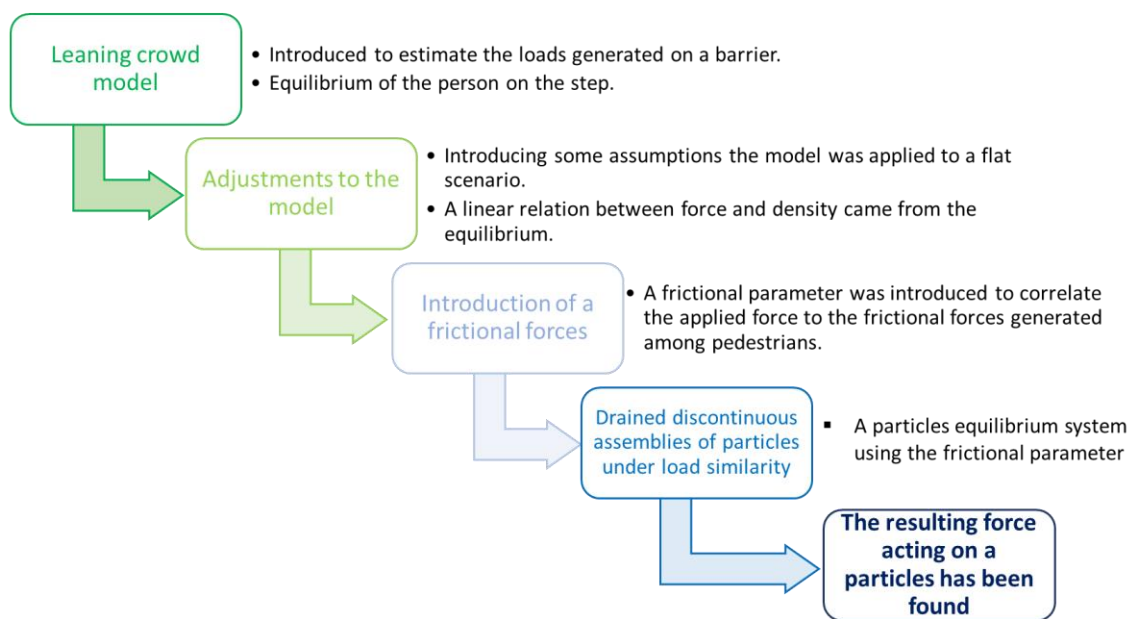
Figure 37. Flow chart related to the model. Starting from the Leaning Crowd model 5 assumptions have been made in order to extend it to a flat scenario. A linear relation among force and density in the area has been made solving the equilibrium. Introducing a frictional parameter, the frictional force has been found in relation to the applied force. From the similarity among crowd in high density and drained discontinuous assemblies of particles a resulting force acting on a pedestrian in the crowd has been found.

The simple model, which has been shown in this section represents an adjustment of a previous model that has been developed from a "leaning crowd" in 1990 to estimate the loads generated on a barrier. Originally, this model has been made in order to investigate the level of comfortable loads for people against crush barriers [97]. Introducing some simplifications, it has been possible to apply the model in a different scenario from the formulated one in the experiment, making possible to apply the same model outside the initial delimitations work.

The equations (4.1) and (4.2) have be taken from a previous work [97]. They have been reported in this section for a better understanding of the model itself and the assumptions made below.

P_n represents the force on the barrier and n represent the number of steps behind the barrier in question, which can be directly formulated:

$$P_n = mg \left(\frac{H}{H'}\right) \tan \theta + P_{n-1} \left(\frac{1+h}{H' \cos \theta}\right);$$

(4.1)

To simplify the writing can be seen the equation as follow:

$$P_n = A \tan \theta + P_{n-1} B;$$

(4.2)

It has been assumed that the pedestrian in the middle of the crowd can be seen behaving as a barrier in order to find the force acting in this point.

Assumptions made in the model:

1. The forces have been assumed acting on the chest;

2. Height of people is given as averaged value calculated among women and men;

3. The push height has been considered as the height of the chest from the ground;

4. In order to make the model working in a flat field the height of the stairs has been assumed equal to 0 and consequently the acting force is horizontal. This assumption simplifies the equilibrium because the term B=1;

5. The flow has been assumed moving in only one direction, which is a strong assumption that has made possible to assume P_{n-1}= 0.

H Centre of mass height

H' Push height

mg Weight of pedestrian

P_n Force on the barrier
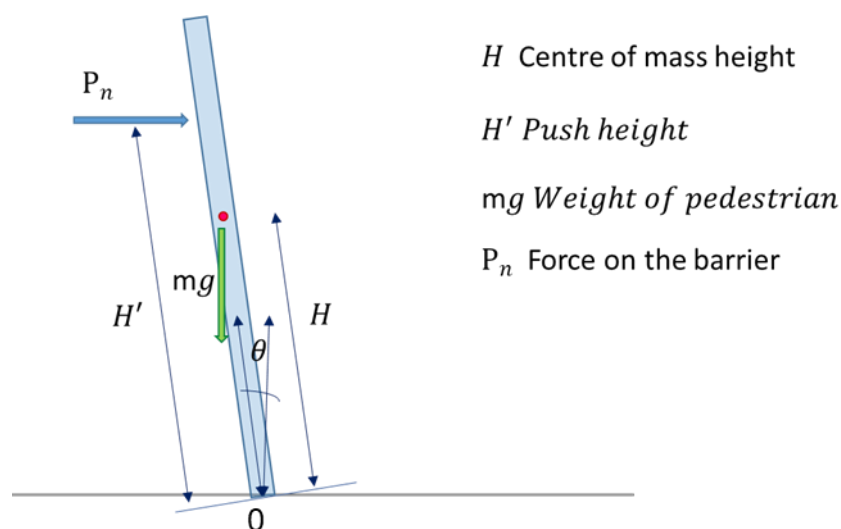
Figure 38. Equilibrium of the person in a row.

Introducing this assumption, a linear relation between force and density coming from the equilibrium of the person has been made, equilibrium moment with respect to 0, see Figure 38.

$$P_n = mg(H/H') \tan\theta ; \qquad (4.3)$$

If the density is linked with the number of people in the area, it would also mean that there is a certain amount of people per unit length. By multiplying the force on the barrier P_n for the number of people, the force per unit length on the barrier has been obtained.

$$N_p = \frac{L}{W}; \; \rho = \frac{N_p}{A}; \; W = \sqrt{1/\rho} ; \qquad (4.4)$$

$$P_n = N_p mg(H/H') \tan\theta ; \qquad (4.5)$$

In this way the force acting in a linear way from the back side to the front has been found. In a highly crowded situation, even if the crowd is acting and behaving as a continuum in terms of motion, frictional forces acting among pedestrians exist.

$F = \mu\, N;$

F frictional force

μ coefficient of friction

N normal force

$P_a = \mu_s P_n;$

P_a frictional force

μ friction parameter

P_n applied force
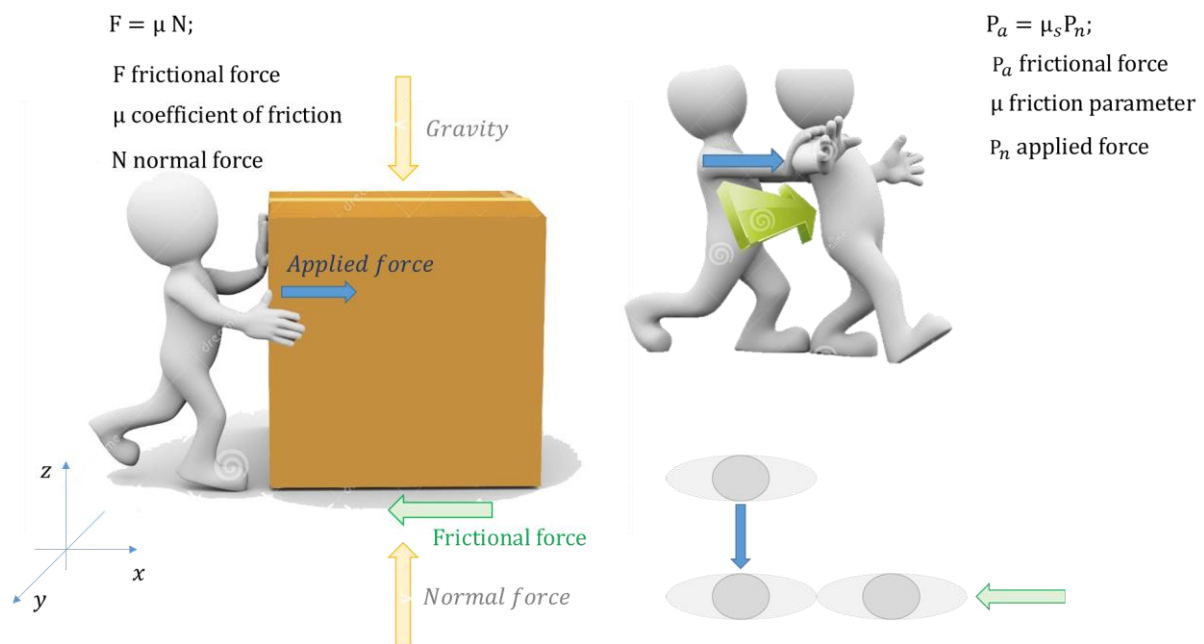
Figure 39. Conceptualization of the forces acting among pedestrian in a row. Scheme of a simple method to represent the frictional force. In the first configuration the frictional force is acting on the ground, plane x-z, due to the creeping of the box. In the second configuration the frictional force acting against the movement is the force in the plane x-y, which is caused by the packing among pedestrians in the crowd.

Then, a simple method to evaluate this frictional force should be introduced for a more precise evaluation of the forces. It can be seen as a proper frictional force acting in the x-y plane rather than x-z, as highlighted in Figure 39. It has been assumed that P_n works as an

applied load [98], which generates the frictional forces P_a, among particles. By referring the correlation between applied force and frictional forces.

$$P_a = \mu_s P_n;\tag{4.6}$$

Where μ_s represents the frictional parameter, which can be interpreted as an internal local pressure between the pedestrians. This becomes really important in regions of high density [99]. In fact, many conflicts occur in this region and the outflow is strongly suppressed for large value of μ_s. This parameter can reach the maximum value of 0,9. In this case the pressure between the pedestrians becomes so strong that any motion is almost impossible [99]. This behaviour has been observed in crowded situations and also in simulations using the *Social Force model* [21].

A granular flow approach has been introduced to find these interacting forces. The stress has been found in response to a localised overload and it is sensitive to the packing arrangement. The similarity with this system of "grains" has been used since the grains reach a mechanical equilibrium after the particles have reached the jammed configurations [98].

More precisely, a drained discontinuous assembly of particles under load is a very similar scenario to the high density packing, due to the configuration itself. In light of this issue, an approximation of the local pressure and stress could be found applying this model to the crowd. Detailed information about the above mentioned model have been provided in "*The stress-dilatancy relation for static equilibrium of an assembly of particles in contact*" [18] and in "*Comportamento meccanico dei terreni non coesivi*" [100]. The main problem is that the parameters used in these models to characterise the triggered stress, such as the true angle of friction, have been found carrying out tests on granular assemblies. This should imply the setting of some parameters, by performing loaded experiment in high density on a crowd. It is easy to imagine that this would imply ethical issues. For this reason, the model has been simplified, by integrated the previous model set up to find the force acting on the crash barrier with a particles equilibrium system using the frictional parameter. In order to set the equilibrium, a lateral force should be found. This lateral force is the P_a previously found. Having P_a and P_n may be conducted the equilibrium. As has been shown in Figure 40.
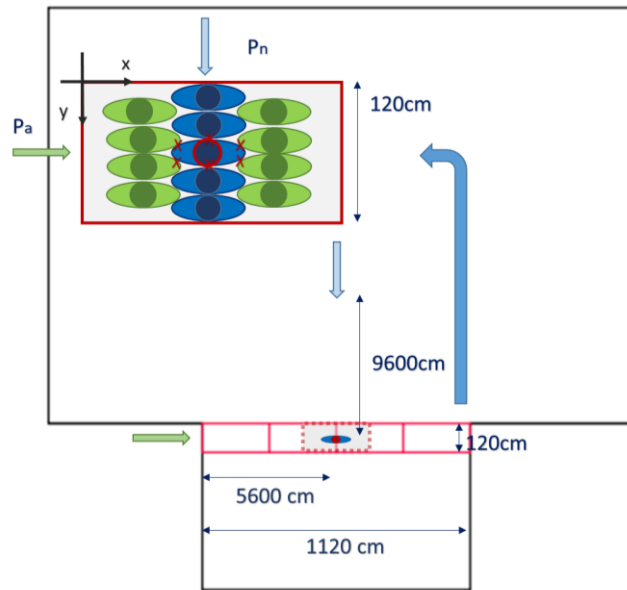
Figure 40. Schemes of investigated force in a crowd scenario. The combination of P_n, applied load, and P_a, frictional force, on the plane x-y generate the resulting force acting on the pedestrian. The red X on the pedestrian investigated are the assumed contact points with the nearby pedestrians.

It has been assumed that each side of a particle has four contact points in direction X and two contact points in direction Y so that the resulting force acting on a particles has been found as follow $R = \sqrt{(P_n/4)^2 + (P_a/2)^2}$.

To sum up, a crowd line acting behind the pedestrian under consideration equal to 9,6m (around 30 people in a line) has been considered. In addition, a frictional crowd line of 5,6m (around 10 people in a line) acting on the same pedestrian is taken into account. The hypothesis of acting force in the thoraces has been made as conservative approach since this is the most sensitive part to the crush force of the body [25]. The found value is around 550N (56kg), which seems a reasonable value, due to the number of interacting particles in the *"cascade effect"*. People feel discomfort when the loadings exceed 400N for more than 30s. When they sustained loadings at an average of about 600N/m, the maximum time people can endure is about 40 min [97]. Experiments to determine concentrated forces on guardrails due to leaning and pushing have shown that force of 30% to 75% of the weight of participants can occur. In a US National Bureau of standard study of guardrails, three persons exerted a leaning force of 792N (80,76kg) and 609 N (62kg) pushing [101]. In a similar Australian Building Technology study centre, three persons in a combined leaning an pushing posture developed a force of 1370 N (139,7 kg) [102]. Studies on the magnitude of loadings that could cause crush asphyxia found that death was estimated to have occurred in 15s or 4-5 minutes after a load of 6227N (635 kg) and 1112N (113,4 kg) was applied respectively [103]. It has been referred values of force and it should be ad that tolerable force is different for each group, i.e. children, female, weak people. In a real scenario, an additional rate of energy due to the rearranging of loose packings should be considered, as well as dealing with the fact that the forces are not uni-directional only.

5. Discussion

Nowadays, there are many events in which a large number of people are gathering in confined areas. Large events related to sports, entertainment, cultural and religious are held all over the world. These events are linked to safety issues for participants and for organizers who must be prepared for "any kind" of emergency and critical situations [7]. Crowd management includes all measures taken in the normal process of facilitating the movement and enjoyment of the people [26][104].

The main objective is the reduction of hazard exposure time, as in risky situations people may need to be guided away as quick as possible. Furthermore, evacuation scenarios may become very complex, due to the space design (e.g., combination of large square and T-junction with the addition of arches merging in the same junction point) and the interactions among pedestrians. It could be stated that the goal of crowd management is the fulfilment of the evacuation time in a challenging scenario.

The *results obtained from the video analysis* performed in this work have been found mostly in accordance to the results obtained from the literature, although universality of the fundamental diagram in high density scenario has been already questioned.

As shown in Figure 41 and Figure 42 the same flow can be found for very different velocities and densities. Following, in the same graphs (Figure 41 and Figure 42) from literature, has been included the averaged value of density, speed and flow found in the video analysis for both low density (LD) and high density (HD). In case of free flow, the average density found has a value of $\rho=0,7$ persons/m^2, in accordance with the graph. By contrast, the averaged value in case of congestion $\rho=6,4$ persons/m^2 is higher than the theoretical literature values.

In Figure 41 and Figure 42 have been referred the fundamental diagrams of pedestrian flow characteristics from literature (Daamen et al.) [105] and (Vanumu et al.) [106] in combination with the averaged value obtained in the analysis of this work.
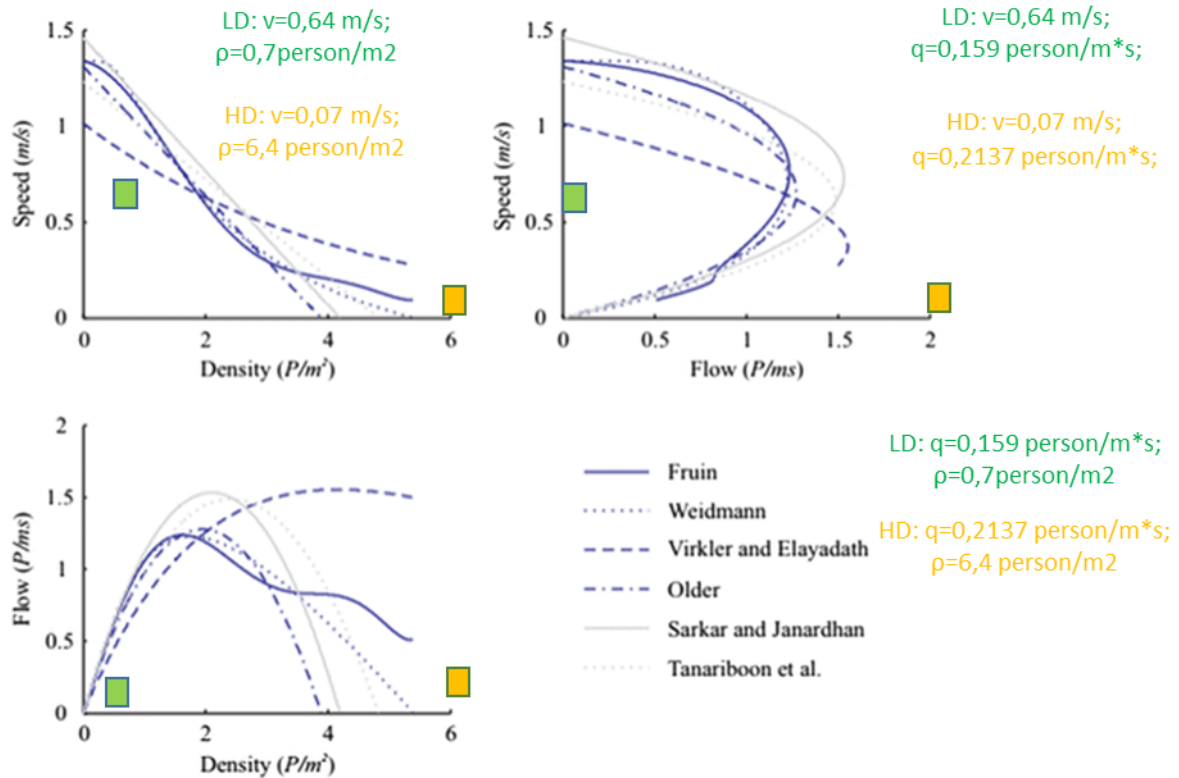
Figure 41. The fundamental diagrams of pedestrian flow characteristics have been taken from literature (Daamen et al.) [105] *and (Vanumu et al.)* [106] *and they have been combined with the averaged value obtained in the analysis of this work. It is present the* comparison with the fundamental diagram from literature, Fruin [6], Weidmann [2], Virkler [107], Older [108], Sarkar [109] and Tanariboon [110].
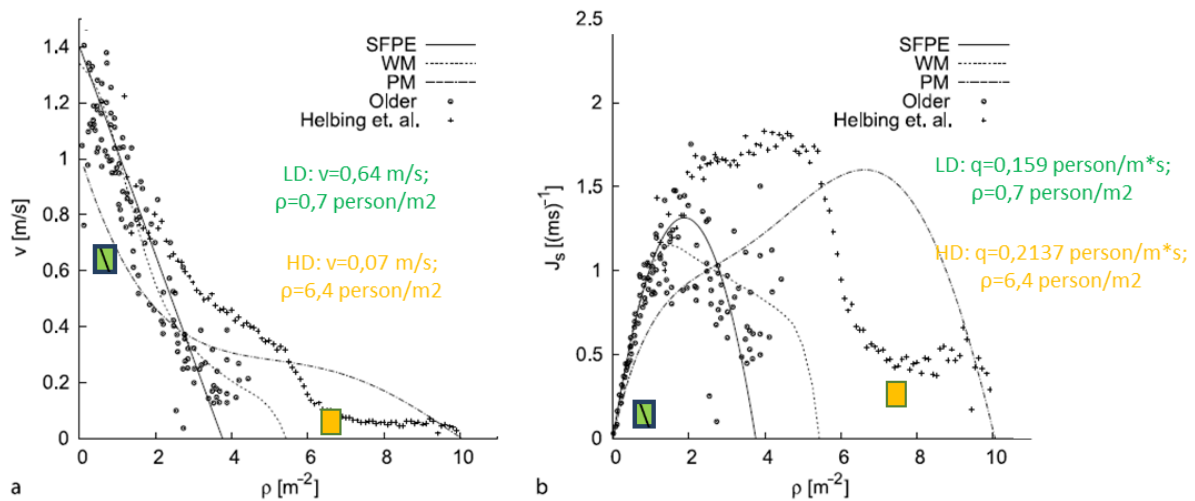
Figure 42. Fundamental diagrams for pedestrian movement in planar facilities taken from (Daamen et al.) [105] *and (Vanumu et al.)* [106]. *The lines refer to the SFPE Handbook [72], Predtechenskii and Milinskii [22], Weidmann [2]. Data points refer to experimental measurements Older [4] and Helbing [24].*

It is interesting to point out that the values observed in high density are close to the experimental measurements found by Helbing at al. [74] for both the speed-density and flow-

density relationships. By contrast, they are far from the values observed in the experimental measurements by Older and from other (in some cases design) curves, i.e., *SFPE Handboo*k [75], *Predtechenskii and Milinskii* [43], *Weidmann* [2].

From Seyfried at al. [82] the density and the speed change with bottleneck width in front of the bottleneck. However, inside the bottleneck area, pedestrians' speed and density are not affected by this width. This parameter influences the dynamic in front of the bottleneck only [82]. Wider bottleneck provides lower density and higher speed. According to the research, jam condition appears in front of the bottleneck, where the pedestrian can only slow down. In this way, the bottleneck limits the inflow, by diminishing the density in the area, so that pedestrians are able, at this point, to move faster, after entering in the bottleneck. It has been found that densities higher than 5 persons/m² appear in front of but not inside the bottleneck, where the recorded density does not exceed the value of 3,5 persons/m². By contrast, in the field observation analysed in this work, the recorded densities are higher and a local density peak of approximately 7persons/m² has been reached inside the bottleneck itself. The data arisen in the simulation task highlighted a difference with the experimental data recorded in the bottleneck investigation [82]. The simulation results, from the further discretized space, shown that the more severe conditions are observed in the corner outside the bottleneck, and in the regions running along the walls, inside the bottleneck. In this real case study the condition is different, due to the presence of arches, which have been used as a further path. All this area become a critical volume, due to the convergence of a further lateral flows. In light of this, even though there is high density in the bottleneck area, the flow has not been increased, due to the further compression from the income lateral flows. By contrast, in the referential laboratory experiment [82] no other restrictions were present and the critical point has been found at the surface of interaction between the area of the bottleneck and the same surface, but located right before the bottleneck region. This transitional area, interface between the bottleneck and in the front of that, according to laboratory experiment [82], represents a critical point. More in detail, these interaction areas have been investigated in the results of the modelling section 3.4.2.

Furthermore, it is interesting to point out the similarity in results according with a further experimental study [111]. It is an experiment, in which a large number of people (270 people) enters a concert hall through two different spatial barrier structures, i.e., a semicircle setup, which is an entry without guiding barriers, and a corridor setup, which is an entry with guiding barriers. The similarity was found with the experiment developed in a corridor set up, where the movement is homogenous, the progress speed does not change in the exanimated time and it is an averaged value of 4,17 m/min, whereas according to the data from literature, which correspond to an averaged value of 4,98 m/min. It might be explained since in the bottleneck region we are already in an almost ordered setup of the crowd. Apparently, this scenario is not exactly the same with the case study of this work, however similarities can be made, due to the homogeneous movement in the area due to the packing effect of the high

density. The high density is a result of the constriction effect, in the moment, when the event ended the subjects moving fast forward, filling up the space, so that no gaps exist anymore.

Comparing the results with previous observed data in high density scenarios, some similarities and differences can be pointed out. Referring the Hajj pilgrimage of 2014 and 2015 to Mecca analysis [23][112], there has been recorded value of density higher than previous analysis carried out. It was observed that at a density of 6 person/m^2 the speed does not vanish, despite the high densities. Even if there was similarity in density with the present study, the difference in speed should be pointed out. This discrepancy may be caused by the difference in flow motions. In the Mecca study pedestrians show an organised-unidirectional flow, on the contrary to the flow conditions considered in the present thesis, which presents a more complex scenario, due to the multidirectional flow, which might be the cause of this observed difference in speed. The universality of the fundamental diagram at high density had been already questioned in the Hajj pilgrimage to Mecca [7].

City evacuation safety may often be based on the respect of given threshold values of design average density levels, while flow and local densities are important factors considering the exit capacity. In this perspective, evacuation models can be used to obtain qualitative and quantitative information on evacuation times and space usage in different scenarios [113].

Based on discussion with festival organisers and according to the regulations, it should be assumed the starting design average density levels of the area, both from a static and dynamic perspectives. It is very important that the allowed maximum density of each area is estimated for the purpose of the evacuation safety [42]. To have a more reliable scenarios, safety designers need to understand how the crowd can plausibly spread on the area according with the type of event, e.g., in case of concerts the indoor stages may be more crowded than the outdoor stages [114]. In case of festivals such as the "San Giovanni", high crowd densities are expected in the areas with greater visibility. To determine the densities and consequently, the number of people, different strategies can be investigated.

Possible scenarios:

1. Initial starting point of the evacuation. This may be related to different initiators, which affect the initial movement of the crowd, i.e. circular wave front if something happens in the heart of the crowd, or linear wave from the front if something happen in the front area.

2. Partial evacuation of the event population. According to the initiator and the related kind of hazard it may be necessary evacuate partially the area.

3. Total evacuation of the entire area at the same time. This should be performed without interfering in exit directions, i.e. dividing the area in subsectors, which of them strictly related to specific exits. This division should be performed according to the availability exits and the characteristic of the main area of the event.

4. Phased evacuation. Referring to the fact that the process is divided into separate phases for different group of the persons within the building or in the same area. This is mainly applied for high rise buildings since the stair capacity is not designed for an immediate and concurrent evacuation [9]. The same issue appears in large outdoor events in historic cities due to the discrepancy between the capacity of the streets and the capacity of the squares. This type of evacuation can be managed by stewarding to provide assistance and guarantee the access in the correct way to the crowd, if one exit has been "drown up" only has an exit cannot be used as an entrance and vice versa.

All these scenarios may be simulated using a multi-agent evacuation model, based on a continuous approach. These models are able to represent, implicitly and explicitly, the behavioural factors that affect people's decision making during a complex evacuation scenarios [42]. As Ronchi at al. suggested, evacuation modelling can be used to identify the critical factors that affect evacuation process under different conditions, to evaluate different evacuation scenarios identifying the impact that different threats may have on it and can also be used to evaluate different evacuation strategies including the simulations of different levels of controls on the process, i.e., spontaneous evacuation up to completely controlled evacuation by the staff [42].

Even if, generally, the focus is to reduce the total evacuation time in the crowd evacuation management [7], the use of an evacuation strategy that reduces the average total evacuation time does not necessarily lead to an increased level of safety [42]. In these scenarios local phenomena should also be taken into account. The increase in local density related to the increasing local pressure represents a serious issue in these events, often related to uneven distribution of people in the area. Different people density is usual in these contexts where there is no assigned location for people.

The high density itself does not cause hazards [23]. The investigation on the pilgrim flows entering the Jamarat Bridge in Mina [23] was performed according to the fluid similarity and taking into consideration the density parameter. Further to that, the turbulent waves can be observed in several public events. The analysis of all these cases showed that the average density rarely exceeds 6 person/m2 [43], in contrast to the local density that can be twice as larger [23][1]. In practice, this phenomenon has been observed in several tests, e.g., the BaSiGo tests [115], which have been developed in 2013 in Düsseldorf, Germany. These experiments focused on the entrances to music events where pushing by highly motivated fans can lead to dangerous situations. More than 2000 test subjects were performed in all the exhibition site. Those tests showed that starting from an initial density of 3,8 person/m2, it is possible to suddenly reach the value of 8person/m2 during the first 10 seconds, as soon as the gate had been opened. It has been found, however, that even evaluating the local densities is not enough to identify the critical time and locations of the potential hazard [5][115]. The key quantity seems to be rather the "crowd pressure", the density multiplied

with the variance of speeds, which represent the density change in time in the moving system. This quantity is important because it may allow to identify critical locations and times [23].

Furthermore, calculating the entry capacity of the Wembley Stadium (Old) following the Green Guide, allowed the packing density of the area above the limit of 4 persons/m2 [1][116]. The entry capacity is the number of people who can pass through all the turnstiles or entry points serving the whole ground of one section, within a period of one hour [116]. Once again the average density did not exceeded the value of 6 persons/m2 and the local density can reach higher peaks but no one of them caused injuries in itself. The exposure time to a certain level of density is often the cause of pedestrian safety issues. How long high density can be sustained is related to the sustainable pressure acting on the chest cavity where breathing is restricted. From the Green Guide [116], as already mentioned, there is the limit of 4 persons/m2 set as a safe density for a moving crowd, which may be exceeded during ingress and egress phase. The exposure time defines the hazard. This is the time that an individual would take to navigate a high density area. A reasonable time exposure to high density is around 6 minutes. A higher threshold value would lead to a safety alert [1]. In the San Giovanni case study the time exposure to a local density, in the range of 5,51 persons/m2 up to 7 persons/m2, is around 6 minutes. In this time no injuries have been shown but warning signs of critical crowd conditions have been observed. In this specific case the transition from laminar flow to stop-and-go waves has been evident. This transition is related to the drop of the flow which may cause a further compression of the crowd exceeding the limit exposure time.

The relation of the crowd pressure with warning signs of a critical crowd conditions is important from a crowd control perspective. This could be evaluated on-line by a video analysis system, allowing to gain time for corrective measures like flow control, pressure relief strategies or the separation of a crowd into blocks to stop the propagation of the shockwaves, increasing the level of safety during mass events [23]. The warning signal [46] consists on the breakdown of the pedestrian flows under congested conditions, which causes stop and go waves and a further compression of the crowd. Another very serious indicator of criticality is the occurrence of high values of the pressure, which relate to the occurrence of turbulent crowd motion [74].

In case of exposure for longer time to high density, this may lead to over critical compression [46]. The issue related to overpressure in high density scenario point out the necessity of evaluating the contact force among pedestrians. Due to the occurrence of people crush, mostly related to local increase in pressure, it becomes essential to investigate and evaluate the forces reached in a scenario. Until now, no contact force modelling have been developed, despite the prominence of this factor in safety evacuation and in order to provide an invaluable support in the crowd management decision.

In light of this complexity, it has been observed the necessity of carefully calibrating inputs. This can be done based on video observation of similar events in a similar context. This is

needed, as models employed with their default values may not be able to reproduce high local densities observed from the video recordings or in laboratory experiments.

Running a model before an event can be important to better understanding the magnitude of the critical points, with the aim of taking appropriate safety measures. It can improve successful safe egress, by informing event management and allowing the estimation of the impact of the staff actions or inactions on successful safe egress [42].

6. Conclusion

Understanding the crowd dynamics in high density scenarios is essential to design crowd safety [1]. The validity of a physical model of crowd movement, in case of high densities, seems to be strictly related to the information needed by the safety designer.

The use of a hydraulic modelling approach may not be valid, if the objective is to consider high density scenarios, where the interacting physical forces among pedestrians can play a significant role. In this case a particle model that considers contact interactions becomes necessary. The combination of the *"leaning crowd",* based on the equilibrium of the human body, i.e., moment around the contact point with the ground, with the *granular flow* approach, made it possible to come up with a simple model to evaluate the interacting forces among pedestrians. In this context, a simplification, which introduces the frictional parameter, is necessary, so that to find the frictional force. It would be interesting, in future, to develop a more detailed model along the line of discontinuous assemblies of particles under load, in order to properly calculate the shear force among pedestrians. The main issue is the empirical aim of these correlations in the granular flow. For this reason, it would be necessary to perform tests to obtain empirical values, e.g., the frictional angle among pedestrians, like for the geotechnical model. In a more ethical way, it would be advisable the development of programs that can record the interacting pressure among agents to avoid tests on pedestrians.

Concerning the data and because of the limit of benchmark data in extreme high density scenarios, i.e., $\rho > 6$person/m^2, further studies and field observations are necessary, in order to reach a wide data set to perform better simulations. More reliable previsions can be obtained performing more consistent assumptions in the analysed model. This is a key issue in public event safety in large areas, as generally the management safety plans are focussed on the maximum capacity of a place on exits looking at these issues as a static problem. However, in this way the issues of the local high density connected with the mass dynamics have been neglected. Oftentimes this is the cause of injury in many crowded scenarios. The high density can be investigated using a continuous model, (e.g., Pathfinder has been used in this work), and useful output can be obtained if calibration allows to reach high densities. In the present case study, it has been possible to achieve at the same time the observed flow and the local high density, by imposing the speed, the agent's body size, the comfort distance and the initial density. Finding a good approximation of the output values, without running several simulations, even though the input values are based on distributions, could make the stochastic approach more affordable from a practitioner perspective.

References

[1]   G. Keith Still, "Crowd Dynamics - PhD Thesis," University of Warwick, 2000.

[2]   U. Weidmann, *Transporttechnik der Fussgänger*, vol. 90. Zurich: Institut für Verkehrsplanung, Transporttechnik, Strassen - und Eisenbahnbau (IVT), ETH Zürich, 1993.

[3]   B. D. Hankin and R. A. Wright, "Passenger Flow in Subways," *Oper. Res. Soc.*, vol. 9, no. 2, pp. 81–88, 1958.

[4]   S.J.Older, *Movement of pedestrians on footways in shopping streets*, vol. 10, no. 4. 1968.

[5]   D. Helbing and A. Johansson, "Pedestrian, Crowd, and Evacuation Dynamics," in *Encyclopedia of Complexity and Systems Science*, R. A. Meyers, Ed. New York: Springer, 2009, pp. 6476–6495.

[6]   J. J. Fruin, "Designing for Pedestrians : A Level-Of-Service Concept," in *50th Annual Meeting of the Highway Research Board*, 1971, no. 355, pp. 1–15.

[7]   S. A. Schadschneider A., Klingsch W., Klüpfel H., Kretz T., Rogsch C., "Evacuation Dynamics : Empirical Results , Modeling and Applications," in *Extreme Environmental Events*, Robert A. Meyers, Ed. New York, NY: Springer, 2011, pp. 517–550.

[8]   X. Chen, M. Treiber, V. Kanagaraj, and H. Li, "Social force models for pedestrian traffic – state of the art," *Transp. Rev.*, vol. 38, no. 5, pp. 625–653, 2018.

[9]   H. Klüpfel, "Crowd Dynamics Phenomena , Methodology , and Simulation," in *Pedestrian Behaviour*, H. Timmermans, Ed. Emerald Group Publishing, 2009, pp. 213–243.

[10]   R. L. Hughes, "A continuum theory for the flow of pedestrians," *Transp. Res. Part B Methodol.*, vol. 36, no. 6, pp. 507–535, 2002.

[11]   A. S. Andreas Schadschneider, Hubert Klüpfel, Tobias Kretz, Christian Rogsch, "Fundamentals of Pedestrian and Evacuation Dynamics," in *Multi-Agent Systems for Traffic and Transportation Engineering.*, A. Bazzan and F. Klügl, Eds. IGI Global, 2009, pp. 124–154.

[12]   D. Helbing, *Stochastische Methoden, nichtlineare Dynamik und quantitative Modelle sozialer Prozesse Literaturverz*, 2nd ed. Stuttgart: Shaker Verlag GmbH, 1992.

[13]   L. P. Kadanoff, "Simulating Hydrodynamics : a Pedestrian Model," *J. Stat. Phys.*, vol. 39, no. 3/4, pp. 267–283, 1985.

[14]   D. Helbing, P. Molnar, I. J. Farkas, and K. Bolay, "Self-organizing pedestrian movement," in *TRAFFIC AND GRANULAR FLOW '03*, S. P. Hoogendoorn, S. Luding, P. H. L. Bovy, M. Schreckenberg, and D. E. Wolf, Eds. Springer, 2005, pp. 361–383.

[15]   H.-H. Stølum, "River Meandering as a Self-Organization Process," *Am. Assoc. Adv. Sci. Stable*, vol. 271, no. 5256, pp. 1710–1713, 1996.

[16] X. Shi, Z. Ye, N. Shiwakoti, and O. Grembek, "A State-of-the-Art Review on Empirical Data Collection for External Governed Pedestrians Complex Movement," *J. Adv. Transp.*, vol. 2018, p. 42, 2018.

[17] D. HELBING and A. JOHANSSON, "Pedestrian, Crowd and Evacuation Dynamics," in *Encyclopedia of Complexity and Systems Science*, R. A. Meyers, Ed. New York, NY: Springer, 2009, pp. 6476–6495.

[18] P. W. Rowe, "The stress-dilatancy relation for static equilibrium of an assembly of particles in contact," vol. 269, no. 1339, pp. 500–527, 1962.

[19] S. Bandini, S. Manzoni, and G. Vizzari, "Situated Cellular Agents : a Model to Simulate Crowding Dynamics," *IEICE Trans. Inf. Syst.*, vol. E85–A, no. 1, pp. 1–8, 2002.

[20] R. Kukla, A. Willis, and J. Kerridge, "Application of context-mediated behavior to a multi-agent pedestrian flow model (PEDFLOW)," Edinburgh, 2003.

[21] Â. Farkas, D. Helbing, and T. Vicsek, "Simulating dynamical features of escape panic," *Nature, Int. J. Sci.*, vol. 407, pp. 487–490, 2000.

[22] F. Farina, D. Fontanelli, A. Garulli, A. Giannitrapani, and D. Prattichizzo, "When Helbing Meets Laumond : The Headed Social Force Model," in *2016 IEEE 55th Conference on Decision and Control (CDC)*, 2016, pp. 3548–3553.

[23] A. Johansson and D. Helbing, "From Crowd Dynamics to Crowd Safety : A Video-Based Analysis," *Adv. Complex Syst.*, vol. 11, no. 04, pp. 497–527, 2008.

[24] M. Hou, W. Chen, T. Zhang, and K. Lu, "Global Nature of Dilute-to-Dense Transition of Granular Flows in a 2D Channel," *Phys. Rev. Lett.*, vol. 91, no. 20, pp. 1–4, 2003.

[25] W. Zhen, L. Mao, and Z. Yuan, "Analysis of trample disaster and a case study – Mihong bridge fatality in China in 2004," *Saf. Sci.*, vol. 46, pp. 1255–1270, 2008.

[26] J. J. Fruin, "The causes and prevention of crowd disasters," in *International conference, Engineering for crowd safety*, 1993, pp. 99–108.

[27] D. Dieckmann, "Die Feuersicherheit in Theatern, Dissertation/thesis at Technische Hochschule Hannover," P.L. Jung, Hannover, 1911.

[28] T. H. Kean (Chair) *et al.*, "The 9/11 Commission Report: Final Report of the National Commission on Terrorist Attacks Upon the United States (9/11 Report)," 2004.

[29] J. D. Averill *et al.*, *World Trade Center Disaster Occupant Behavior , Egress , and Emergency Communications*. Washington: NIST NCSTAR 1-7 U.S., Government printing office, 2005.

[30] S. Consortium, "Final Report - Research Study on the Sinking Sequence of MV Estonia," Goteborg, 2008.

[31] N. Waldau, "Massenpanik in Gebauden," Dissertation/Thesis at Technische Universitat Wien, Wien, 2002.

[32] Europol, "European Union Terrorism Situation and Trend Report," The Hague, 2017.

[33] "More than 1,500 Juventus fans injured in stampede in Turin," *The Telegraph, online article*. News Agency Reuters, Associated Press, London, 2017.

[34] A. Custodero, "Panico in discoteca a Corinaldo per spray urticante: 6 morti nella calca al concerto del rapper Sfera Ebbasta," *Republica, online article*. Roma, 2018.

[35] "Italy nightclub stampede leaves six dead and dozens injured," *The Telegraph, online article*. London, 2018.

[36] D. Helbing and P. Mukerji, "Crowd Disasters as Systemic Failures: Analysis of the Love Parade Disaster," *EPJ Data Sci.*, vol. 1, no. 1, pp. 1–7, 2012.

[37] M. Novak, "Liquid architectures," in *Cyberspace. Primi passi nella realtà virtuale*, M. Benedikt, Ed. Padova: Muzzio, 1993, pp. 233–265.

[38] S. Colonna, "La dialettica classico/anticlassico tra Argan, Zevi e Novak per un definizione critico-estetica di 'Architettura Liquida,'" *BTA - Boll. Telemat. dell'Arte*, no. 715, 2014.

[39] Z. Bauman, *Liquid Modernity*. Oxford,Cambridge, 2000.

[40] Z. Bauman, *Liquid Life*. Oxford,Cambridge, 2005.

[41] R. Scozzari, M. Fronterré, and G. G. Amaro, "Modeling Crowd Movement in large scale events, the case of Storco Carnevale di Ivrea," in *PROOCEDINGS, Fire and Evacuation Modeling Technical Conference (FEMTC)*, 2018.

[42] X. Criel, E. Ronchi, F. N. Uriz, X. Criel, and P. Reilly, *Modelling large-scale evacuation of music festivals*, vol. 5. Elsevier Ltd, 2015, pp. 11–19.

[43] V. M. Predtechenskiĭ and A. I. Milinskii, *Planning for foot traffic flow in buildings*. New Deli: Amerind, 1978.

[44] R. Lohner, B. Muhamad, P. Dambalmath, and E. Haug, *Fundamental Diagrams for Specific Very High Density Crowds*, vol. 2. 2017, pp. 1–15.

[45] N. Shiwakoti, X. Shi, Y. Zhirui, and W. Wang, "Empirical study on pedestrian crowd behaviour in right angled junction," in *37th Australasian Transport Research Forum (ATRF 2015) - Pedestrian traffic and interaction characteristics under complex environment*, 2015, pp. 1–13.

[46] D. Helbing, A. Johansson, and H. Z. Al-Abideen, "Dynamics of crowd disasters : An empirical study," *Phys. Rev.*, vol. E 75, no. 046109, pp. 1–7, 2007.

[47] D. Erica, A. Paul, D. Richard, and D. Nilsson, *The Process of Verification and Validation of Building Fire Evacuation Models*, vol. 1822. National Institute of Standards and Technology, 2013.

[48] J. Zhang, W. Klingsch, A. Schadschneider, and A. Seyfried, "Transitions in pedestrian fundamental diagrams of straight corridors and T-junctions," *J. Stat. Mech. Theory Exp.*

P06004, pp. 1–18, 2011.

[49]   E. Ronchi and D. Nilsson, "Modelling total evacuation strategies for high-rise buildings," *Build. Simul.*, vol. 7, no. 1, pp. 73–87, 2014.

[50]   H. Yin, D. Li, and X. Zheng, "An energy based method to measure the crowd safety," *Transp. Res. Procedia*, vol. 2, pp. 691–696, 2014.

[51]   E. Ronchi, D. Nilsson, E. D. Kuligowski, R. D. Peacock, and P. A. Reneke, "Assessing the Verification and Validation of Building Fire Evacuation Models," *Fire Technol.*, vol. 52, no. 1, pp. 197–219, 2016.

[52]   E. Ronchi, P. A. Reneke, and R. D. Peacock, "A Method for the Analysis of Behavioural Uncertainty in Evacuation Modelling," in *Fire Technology*, vol. 50, no. 6, Springer, 2014, pp. 1545–1571.

[53]   Kardi Teknomo, "Microscopic Pedestrian Flow Characteristics : Development of an Image Processing Data Collection and Simulation Model - Ph.D. Dissertation," Tohoku University Japan, 2002.

[54]   J. L. Pauls, J. J. Fruin, and J. M. Zupan, "Minimum Stair Width for Evacuation, Overtaking Movement and Counterflow — Technical Bases and Suggestions for the Past, Present and Future," in *Pedestrian and Evacuation Dynamics*, N. Waldau, P. Gattermann, H. Knoflacher, and M. Schreckenberg, Eds. Berlin, Heidelberg: Springer, 2005, pp. 57–69.

[55]   R.Wiseman, "R. Pace of Life." http://www.paceoflife.co.uk/2008.

[56]   X. Shi, Z. Ye, N. Shiwakoti, D. Tang, C. Wang, and W. Wang, "Empirical investigation on safety constraints of merging pedestrian crowd through macroscopic and microscopic analysis," *Accid. Anal. Prev.*, vol. 95, pp. 405–416, 2016.

[57]   D. C. Duives, W. Daamen, and S. P. Hoogendoorn, "State-of-the-art crowd motion simulation models," *Transp. Res. Part C*, vol. 37, pp. 193–209, 2013.

[58]   D. Helbing, A. Johansson, and H. H. Z. Al-Abideen, "Crowd turbulence : the physics of crowd disasters," in *The Fifth International Conference on Nonlinear Mechanics (ICNM-V)*, 2007, pp. 967–969.

[59]   V. J. Kok, M. K. Lim, and C. S. Chan, "Crowd Behavior Analysis : A Review where Physics meets Biology," *Neurocomputing*, vol. 177, pp. 342–362, 2016.

[60]   P. A. Thompson, "Developing new techniques for modelling crowd movement - PhD Thesis," University of Edinburgh, 1994.

[61]   B. D. Hankin and R. A. Wright, "Passenger Flows in Subways," *J. Oper. Res. Soc.*, vol. 9, no. 2, pp. 81–88, 1958.

[62]   W. Daamen and S. P. Hoogendoorn, "Self-Organization in walker experimentis," in *TRAFFIC AND GRANULAR FLOW '03*, S. P. Hoogendoorn, S. Luding, P. H. L. Bovy, M. Schreckenberg, and D. E. Wolf, Eds. Springer, 2005, pp. 373–382.

[63]   J. K. K. Yuen and E. W. M. Lee, "The effect of overtaking behavior on unidirectional

pedestrian flow," *Saf. Sci.*, vol. 50, no. 8, pp. 1704–1714, 2012.

[64]   X. Jia, H. Yue, X. Tian, and H. Yin, "Simulation of pedestrian flow with evading and surpassing behavior in a walking passageway," *Simulation*, vol. 93, no. 12, pp. 1013–1035, 2017.

[65]   M. Haghani and M. Sarvi, "Following the crowd or avoiding it? Empirical investigation of imitative behaviour in emergency escape of human crowds," *Anim. Behav.*, vol. 124, pp. 47–56, 2017.

[66]   Y. Zhao, T. Lu, M. Li, and L. Tian, "The self-slowing behavioral mechanism of pedestrians under normal and emergency conditions," *Phys. Lett. Sect. A Gen. At. Solid State Phys.*, vol. 381, no. 37, pp. 3149–3160, 2017.

[67]   A. U. K. Wagoum, A. Tordeux, and W. Liao, "Understanding human queuing behaviour at exits : an empirical study," *R. Soc. Open Sci.*, vol. 4, no. 1, p. (1)160896-(13)160896, 2017.

[68]   A. Gorrini, L. Crociani, C. Feliciani, and P. Zhao, "Social Groups and Pedestrian Crowds : Experiment on Dyads in a Counter Flow Scenario," in *8th International Conference on Pedestrian and Evacuation Dynamics (PED2016)*, 2016, p. 7.

[69]   M. Kremer and L. Debo, "Herding in a Queue : A Laboratory Experiment," pp. 1–33, 2012.

[70]   S. P. Hoogendoorn and W. Daamen, "Pedestrian Behavior at Bottlenecks," *Transp. Sci.*, vol. 39, no. 2, pp. 147–288, 2005.

[71]   D. Helbing, L. Buzna, A. Johansson, and T. Werner, "Self-Organized Pedestrian Crowd Dynamics : Experiments , Simulations , and Design Solutions," *Transp. Sci.*, vol. 39, no. 1, pp. 1–24, 2005.

[72]   D. Helbing, I. Farkas, and T. Vicsek, "Freezing by Heating in a Driven Mesoscopic System," 1999.

[73]   D. Helbing, "Traffic and Related Self-Driven Many-Particle Systems," *Rev. Mod. Phys.*, vol. 73, no. 4, pp. 1067–1141, 2000.

[74]   D. Helbing, A. Johansson, and H. Z. Al-Abideen, "Dynamics of crowd disasters : An empirical study," *Phys. Rev. E 75 046109*, pp. 1–7, 2007.

[75]   R. W. Bukowski and J. S. Tubbs, "Egress Concepts and Design Approaches," in *SFPE Handbook of Fire Protection Engineering*, 5th ed., M. J. Hurley, Ed. New York: Springer, 2016, pp. 2012–2046.

[76]   J. J. Fruin, *Pedestrian Planning and Design - Ph.D Thesis*. New York: Metropolitan Association of Urban Designers and Environmental Planners, 1971.

[77]   W. H. K. Lam, J. Y. S. Lee, K. S. Chan, and P. K. Goh, "A generalised function for modeling bi-directional flow effects on indoor walkways in Hong Kong," *Transp. Res. Part A*, vol. 37, pp. 789–810, 2003.

[78]   V. M. Predtechenskiĭ and A. I. Milinskii, "Planning for foot traffic flow in buildings," in *translation of: Proekttirovanie Zhdaniis Uchetom Organizatsii Dvizheniya Lyuddskikh Potokov, Stroiizdat Publishers, Moscow, 1969*, 1978.

[79]   J. J. Fruin, "Design for pedestrian: a Level of Service concept," in *50th Annual Meeting of the Highway Research Board*, 1971, pp. 1–15.

[80]   X. Shan, J. Ye, and X. Chen, "Proposing a Revised Pedestrian Walkway Level of Service Based on Characteristics of Pedestrian Interactive Behaviours in China," *Promet - Traffic&Transportation*, vol. 28, no. 6, pp. 583–591, 2016.

[81]   K. Kitazawa and T. Fujiyama, "Pedestrian Vision and Collision Avoidance Behavior: Investigation of the Information Process Space of Pedestrians Using an Eye Tracker," in *Pedestrian and Evacuation Dynamics*, W. W. F. Klingsch, C. Rogsch, A. Schadschneider, and M. Schreckenberg, Eds. London: Springer, 2008, pp. 95–108.

[82]   W. Liao, A. Seyfried, J. Zhang, M. Boltes, and X. Zheng, "Experimental Study on Pedestrian Flow through Wide Bottleneck," *Transp. Res. Procedia*, vol. 2, pp. 26–33, 2014.

[83]   E. Ronchi and M. Kinsey, "Evacuation models of the future : insights from an online survey of user ' s experiences and needs," in *Proceedings of the Advanced Research Workshop: "Evacuation and Human Behaviour in Emergency Situations,"* 2011, pp. 145–155.

[84]   R. Enrico and N. Daniel, "Basic Concepts and Modelling Methods," in *Evacuation Modeling Trends*, A. Cuesta, O. Abreu, and D. Alvear, Eds. New York: Springer, 2016, pp. 1–23.

[85]   R. Peacock, "A Review of Building Evacuation Models, 2nd Edition," in *Technical Note 1680*, no. 1680, 2010, pp. 1–36.

[86]   E. Ronchi, S. Safety, P. A. Reneke, and R. D. Peacock, "A Method for the Analysis of Behavioural Uncertainty in Evacuation Modelling," in *Fire Technology*, vol. 50, no. 6, Springer, 2014, pp. 1545–1571.

[87]   U. S. Nuclear Regulatory Commission, "Verification and Validation of Selected Fire Models for Nuclear Power Plant Applications - NUREG-1824," in *Nuclear News*, vol. 58, no. 3, Washington, 2015, p. 104.

[88]   J. D. Averill, "Five Grand Challenges in Pedestrian and Evacuation Dynamics," in *Pedestrian and Evacuation Dynamics*, R. Peacock, E. Kuligowski, and J. Averill, Eds. Boston: Springer, 2011.

[89]   OECD Publications Centre, *Data and Metadata Reporting and Presentation Handbook*. Paris, 2007.

[90]   R. Quintero, I. Parra, D. F. Llorca, and M. A. Sotelo, "Pedestrian Path Prediction based on Body Language and Action," in *17th International IEEE Conference on Intelligent Transportation Systems (ITSC)*, 2014, pp. 679–684.

[91] Thunderhead Engineering, *Verification and Validation*, 2nd ed. Manhattan, 2015.

[92] K. E. Boyce, T. J. Shields, and G. W. H. Silcock, "Toward the Characterization of Building Occu ancies for Fire Safety Engineering : Capabilities of Disabled People Moving Horizontally and on an Incline," in *Fire Technology*, vol. 35, no. 1, Boston: Springer US, 1999, pp. 51–67.

[93] E. Ronchi, "Testing the predictive capabilities of evacuation models for tunnel fire safety analysis," *Saf. Sci.*, vol. 59, pp. 141–153, 2013.

[94] Thunderhead Engineering, *Pathfinder User Manual*. Manhattan, 2018.

[95] T. Korhonen and S. Hostikka, "Fire Dynamics Simulator with Evacuation : FDS + Evac," in *Technical Reference and User ' s Guide*, VTT Technical Research Centre of Finland, 2009, pp. 1–91.

[96] Thunderhead Engineering, *Pathfinder Technical Reference*. Manhattan, 2017.

[97] R. A. Smith and L. B. Lim, "Experiments to investigate the level of ' comfortable ' loads for people against crush barriers," *Saf. Sci.*, vol. 18, no. 4, pp. 329–335, 1995.

[98] A. P. F. Atman and P. Claudin, "Numerical Stress Response Functions of Static Granular Layers," in *TRAFFIC AND GRANULAR FLOW '03*, S. P. Hoogendoorn, S. Luding, P. H. L. Bovy, M. Schreckenberg, and D. E. Wolf, Eds. Springer, 2003, pp. 531–536.

[99] A. Kirchner, K. Nishinari, and A. Schadschneider, "Friction effects and clogging in a cellular automaton model for pedestrian dynamics," *Phys. Rev.*, vol. E 67, no. 056122, pp. 1–10, 2003.

[100] R. Lancellotta, *GEOTECNICA*, 4th ed. Roma: Zanichelli, 2012.

[101] S. G. Fattal and L. E. Cattaneo, "Investigation of Guardrails for the Protection of Employees from Occupational Hazards," Washington, 1976.

[102] R. J. Dayeh, "Horizontal loading on handrails," National Building Technology Centre, Chatswood, N.S.W, 1985.

[103] R. A. Smith and J. F. Dickie, "Crowd Pressure Monitoring," in *International Conference on Engineering for Crowd Safety*, 1993.

[104] A. E. Berlonghi, "Understanding and planning for different spectator crowds," *Saf. Sci.*, vol. 18, no. 4, pp. 239–247, 1995.

[105] W. Daamen, S. Hoogendoorn, and P. H. L. Bovy, "First-Order Pedestrian Traffic Flow Theory First-order Pedestrian Traffic Flow Theory," *Transp. Res. Rec. J.*, vol. 1934, no. 1, pp. 1–14, 2005.

[106] L. D. Vanumu, K. R. Rao, and G. Tiwari, "Fundamental diagrams of pedestrian flow characteristics : A review," in *European Transport Research Review*, vol. 9, no. 4, European Transport Research Review, 2017, pp. 1–13.

[107] M. R. Virkler and S. Elayadath, "Pedestrian Speed-Flow-Density Relationships.," in

Transportation Research Record Journal of the Transportation Research Board, no. 1438, Washington: Transportation Research Board, 1994, pp. 51–58.

[108] S.J.Older, *Movement of pedestrians on footways in shopping streets*, vol. 10, no. 4. Traffic engineering & control, 1968.

[109] S. S. E. Rabbi and Q. S. Hossain, "A Study on pedestrian flow characteristics for selected walkways in Khulna Metropolitan Area, Bangladesh," in *4th International Conference on Civil Engineering for Sustainable Development (ICCESD)*, 2018, pp. 1–12.

[110] Y. Tanariboon, S. S. Hwa, and C. H. Chor, "Pedestrian Characteristics Study in Singapore," *J. Transp. Eng.*, vol. 112, no. 3, 1986.

[111] A. Sieben, J. Schumann, and A. Seyfried, "Collective phenomena in crowds — Where pedestrian dynamics need social psychology," *PLoS One*, vol. 12, no. 6, pp. 1–19, 2017.

[112] R. Lohner, B. Muhamad, P. Dambalmath, and E. Haug, *Fundamental Diagrams for Specific Very High Density Crowds*, vol. 2. 2017, pp. 1–15.

[113] S. Gwynne, E. R. Galea, M. Owen, and P. J. Lawrence, "A review of the methodologies used in the computer simulation of evacuation from the built environment," *Build. Environ.*, vol. 34, no. 6, pp. 741–749, 1999.

[114] X. Criel, E. Ronchi, F. N. Uriz, X. Criel, and P. Reilly, "Modelling large-scale evacuation of music festivals Case Studies in Fire Safety Modelling large-scale evacuation of music festivals," no. January 2016, pp. 10–19, 2015.

[115] A. Sieben, J. Schumann, and A. Seyfried, "Collective phenomena in crowds — Where pedestrian dynamics need social psychology," *PLoS One*, vol. 12, no. 6, pp. 1–19, 2017.

[116] *Guide to Safety at Sports Grounds*, 5th ed. Sports Grounds Safety Authority, 2008.

Appendix A - Uncertainty

In this section he method used to evaluate the uncertainty in high density and low density scenarios is whom.

The averaged recorded speed is given by:

$$v_{(av)} = \frac{L}{t};$$
(a.1)

where L represent the length of the grid cell, as shown in Figure 12 and Figure 13, and t represent the transient time.

The path length has been calculated using a CAD tool. It is necessary to point out that trajectories were very irregular. Paths outside a single cell for high density scenario, and outside two cells for low density scenario have not been taken into consideration.

The error in the *transient time* measurement has been found calculating the difference in transient time, which is given from the difference between the two different measurement $\Delta(\Delta\tau)$ and the averaged measurements in transient time $\Delta_{(av)}(\Delta\tau)$, as follow:

$$\varepsilon_{t\,(\%)} = \frac{\Delta(\Delta\tau)}{\Delta_{(av)}(\Delta\tau)};$$
(a.2)

The error in the *speed* measurement has been found in the same way has shown above. Calculating the difference in speed, which is given from the difference between the two different speed measurement $\Delta(\Delta v)$ and the averaged measurements $\Delta_{(av)}(\Delta V)$, as follow:

$$\varepsilon_{v\,(\%)} = \frac{\Delta(\Delta v)}{\Delta_{(av)}(V)};$$
(a.3)

The error in the *density* measurement has been found according to the previous one, as follow:

$$\varepsilon_{\rho\,(\%)} = \frac{\Delta N_p}{\Delta_{(av)}\,N_p};$$
(a.4)

Where N_p is the number of pedestrians in the region and ΔN_p is the difference between the two different measurement and $\Delta_{(av)}\,N_p$ is the averaged measurements.

As shown in Appendix A for both low density and high density scenarios the error is above the 5%, which is the general criteria accepted in the evaluation of the discrepancy of results obtained in well controlled laboratory experiment. In this context, due to the field

experiment and the several uncertainties which should be taken in to account, it is not unexpected that the error is higher. It is relevant to point out that the highest error has been recorded in the speed found in high density scenario.

LOW DENSITY

$\Delta(\Delta T)$	$\Delta_{(av)}(\Delta\tau)$	$\varepsilon_{t\,(\%)}$	$\varepsilon_{t(av)\,(\%)}$	$\Delta(\Delta v)$	$\Delta_{(av)}(V)$	$\varepsilon_{v\,(\%)}$	$\varepsilon_{v(av)\,(\%)}$
TRANSIENT TIME AND SPEED ERROR IN A RANGE OF 0,61<P<0,73
3,88	10,94	35,47	21,19	0,05	0,14	35,47	21,19
2,58	10,25	25,17		0,04	0,15	25,17	
0,94	10,93	8,60		0,01	0,14	8,60	
1,15	10,58	10,87		0,02	0,14	10,87	
0,23	11,29	2,04		0,00	0,13	2,04	
0,90	11,85	7,59		0,01	0,13	7,59	
0,64	3,74	17,11		0,07	0,41	17,11	
3,40	12,44	27,33		0,03	0,12	27,33	
2,16	10,20	21,18		0,03	0,15	21,18	
2,56	9,72	26,34		0,04	0,16	26,34	
3,75	5,42	69,25		0,22	0,32	69,25	
1,58	14,21	11,12		0,01	0,11	11,12	
0,16	12,40	1,29		0,00	0,12	1,29	
3,84	11,56	33,22		0,04	0,14	33,22	
1,52	7,16	21,23		0,05	0,21	21,23	

Table 3. Transient Time and Speed error in Low Density scenario

HIGH DENSITY

$\Delta(\Delta T)$	$\Delta_{(av)}(\Delta\tau)$	$\varepsilon_{t\,(\%)}$	$\varepsilon_{t(av)\,(\%)}$	$\Delta(\Delta v)$	$\Delta_{(av)}(V)$	$\varepsilon_{v\,(\%)}$	$\varepsilon_{v(av)\,(\%)}$
TRANSIENT TIME AND SPEED ERROR IN A RANGE OF 5,5<P<6,92
13,38	40,73	32,85	40,33	0,05	0,14	32,85	40,33
24,28	28,48	85,25		0,21	0,24	85,25	
4,50	27,83	16,17		0,03	0,21	16,17	
2,04	31,10	6,56		0,01	0,18	6,56	
15,54	42,81	36,30		0,05	0,14	36,30	
22,37	36,04	62,08		0,11	0,17	62,08	
48,77	49,22	99,10		0,15	0,15	99,10	
12,00	41,84	28,68		0,04	0,14	28,68	
0,37	39,18	0,94		0,00	0,15	0,94	
24,49	31,12	78,71		0,17	0,22	78,71	
9,77	21,57	45,30		0,13	0,28	45,30	
1,83	27,33	6,70		0,01	0,21	6,70	
12,34	32,57	37,89		0,07	0,18	37,89	
15,22	41,87	36,35		0,05	0,14	36,35	
8,78	27,33	32,13		0,07	0,21	32,13	

Table 4. Transient Time and Speed error in High Density scenario

<div align="center">

LOW DENSITY

</div>

DENSITY ERROR IN A RANGE OF 0,61<P< 0,73			
$\Delta \mathbf{N}_p$	$\Delta_{(av)} \mathrm{N}_p$	$\varepsilon_{\rho\,(\%)}$	$\varepsilon_{\rho(av)\,(\%)}$
2	35	5,71	7,44
4	34	11,76	
2	35	5,71	
2	34	5,88	
2	36	5,56	
1	39,5	2,53	
2	37	5,41	
4	38	10,53	
5	38,5	12,99	
5	38,5	12,99	
1	36,5	2,74	

Table 5. Density error in Low Density scenario

<div align="center">

HIGH DENSITY

</div>

DENSITY ERROR IN A RANGE OF 5,5 <P<6,92			
$\Delta \mathbf{N}_p$	$\Delta_{(av)} \mathrm{N}_p$	$\varepsilon_{\rho\,(\%)}$	$\varepsilon_{\rho(av)\,(\%)}$
13	82,5	15,76	13,28
8	86	9,30	
3	85,5	3,51	
4	83	4,82	
8	82	9,76	
9	83,5	10,78	
15	81,5	18,40	
22	81	27,16	
20	83	24,10	
12	85	14,12	
7	83,5	8,38	

Table 6. Density error in High Density scenario

Appendix B - Main results obtained in the Tests' Task

N°	Geometry gate	n° of Agents	Shoulder Width	Averaged Density in the Area	Maximum Local Density in the Gate	Comfort Distance	Measured averaged flow D02	Measured averaged flow D04	Measured averaged flow D05	Imposed Flow	Maximum Speed	Averaged Speed	Imposed Speed
1	6,2*6	835	45,58	1,79	2,46	0,080	4,304	x	x	x	0,347	0,348	unif. 0,4-1,2
2	6,2*6	835	45,58	1,79	2,12	0,347	4,217	x	x	x	0,379	0,380	unif. 0,4-1,2
3	6,2*6	835	45,58	1,79	2,28	0,347	4,196	4,1514	x	x	0,378	0,379	unif. 0,4-1,2
4	6,2*6	835	45,58	1,79	2,54	0,080	4,446	4,3390	x	x	0,342	0,342	unif. 0,4-1,2
5	6,2*6	835	45,58	1,79	2,63	0,080	4,282	4,2905	4,2757	x	0,470	0,348	unif. 0,4-1,2
6	6,2*6	835	45,58	1,79	2,31	0,347	4,181	4,1739	4,1852	x	0,520	0,384	unif. 0,4-1,2
6P	6,2*6	835	45,58	1,79	2,34	0,347	4,245	4,1739	4,1852	x	0,590	0,389	unif. 0,4-1,2
7	7*6	845	45,58	1,79	2,28	0,347	4,817	4,7407	4,7545	x	0,660	0,386	unif. 0,4-1,2
8	8*6	855	45,58	1,79	2,18	0,347	5,439	5,3706	5,4082	x	0,570	0,387	unif. 0,4-1,2
9	9*6	866	45,58	1,79	2,16	0,347	5,966	5,9077	5,9259	x	0,415	0,402	unif. 0,4-1,2
10	10*6	876	45,58	1,79	2,15	0,347	6,380	6,2951	6,3307	x	0,880	0,415	unif. 0,4-1,2
11	11*6	887	45,58	1,79	2,13	0,347	7,072	6,8571	6,9569	x	0,700	0,422	unif. 0,4-1,2
12	11,2*6	890	45,58	1,79	2,19	0,347	8,000	12,0000	7,0000	x	0,660	0,427	unif. 0,4-1,2
13	11,2*6	1490	45,58	3,00	3,04	0,164	7,805	7,3543	7,5278	x	0,640	0,330	unif. 0,4-1,2

14	11,2*6	1490	45,58	3,00	3,15	0,080	7,724	7,2303	7,4044	x	0,600	0,363	unif. 0,4-1,2
15	11,2*6	1985	45,58	4,00	4,01	0,081	8,036	7,2669	7,5208	x	0,620	0,348	unif. 0,4-1,2
16	11,2*6	2468	45,58	5,00	4,27	0,024	7,987	x	7,4702	x	0,820	0,357	unif. 0,4-1,2
17	11,2*6	2468	45,58	5,00	4,82	0,080	7,835	x	7,2984	x	0,690	0,346	unif. 0,4-1,2
18	11,2*6	2639	45,58	6,00	5,06	0,001	7,925	x	7,4677	x	0,690	0,355	unif. 0,4-1,2
19	11,2*6	1985	33,00 - 35,34	4,00	4,08	0,080	7,576	x	7,0784	x	0,830	0,403	unif. 0,4-1,2
20	11,2*6	1985	33,00 - 35,34	4,00	4,05	0,0527-0,076	7,548	x	7,1344	x	0,740	0,401	unif. 0,4-1,2
21	11,2*6	1985	33,00 - 35,34	4,00	4,06	0,0527-0,076	7,462	x	6,7857	x	0,810	0,412	unif. 0,4-1,2
22	11,2*6	1985	33,00 - 35,34	4,00	4,06	0,0527-0,076	6,965	x	6,3333	x	0,970	0,403	unif. 0,4-1,2
23	11,2*6	2480	33,00 - 35,34	5,00	4,06	0,0527-0,076	7,337	x	6,6746	x	0,970	0,403	unif. 0,4-1,2
24	11,2*6	1985	33,00 - 35,34	4,00	4,03	0,0527-0,076	0,493	x	0,4536	x	0,040	0,017	unif. 0,4-1,2
25	11,2*6	1985	33,00 - 35,34	4,00	4,03	0,0527-0,076	0,852	x	0,7938	x	0,070	0,068	const. 0,07
26	11,2*6	2480	33,00 - 35,34	5,00	4,05	0,0527-0,076	0,890	x	x	x	0,070	0,068	const. 0,07
27	11,2*6	0	33,00 - 35,34	5,00	7,66	0,0527-0,076	0,212	x	0,2248	0,2137	0,030	0,003	const. 0,07
28	11,2*6	2480	33,00 - 35,34	5,00	7,37	0,0527-0,076	0,214	x	0,2269	0,2137	0,030	0,002	const. 0,07
29	11,2*6	2001	33,00 - 35,34	4,00	7,39	0,0527-0,076	0,214	x	0,2196	0,2137	0,040	0,012	const. 0,07
30	11,2*6	1489	33,00 - 35,34	3,00	7,46	0,0527-0,076	0,214	x	0,2269	0,2137	0,060	0,013	const. 0,07
31	11,2*6	1894	33,00 - 35,34	3,79	4,13	0,0527-0,076	0,309	x	0,2483	x	0,070	0,053	const. 0,07

32	11,2*6	1984	33,00 - 35,34	3,79	4,06	0,0527-0,076	0,774	x	0,7098	x	0,040	0,031	unif.0,05-0,08
33	11,2*6	1984	33,00 - 35,34	3,79	4,06	0,0527-0,076	0,774	x	0,7098	x	0,040	0,030	const. 0,045
34	11,2*6	2481	33,00 - 35,34	5,00	5,38	0,0527-0,076	0,688	x	0,6075	x	0,070	0,046	const. 0,07
35	11,2*6	2480	33,00 - 35,34	5,00	5,31	0,0527-0,076	0,642	x	x	x	0,070	0,056	const. 0,07
36	11,2*6	1984	33,00 - 35,34	4,00	4,03	0,0527-0,076	0,291	x	0,2882	x	0,080	0,068	const. 0,08
37	11,2*6	1984	33,00 - 35,34	4,00	4,07	0,0527-0,076	0,283	x	0,2773	x	0,050	0,042	const. 0,055
38	11,2*6	1984	33,00 - 35,34	4,00	4,02	0,080	0,291	x	0,2901	x	0,070	0,048	const. 0,07
39	11,2*6	3650	33,00 - 35,34	4,00	6,03	0,0527-0,076	0,612	x	0,4916	x	0,070	0,047	const. 0,07
40	11,2*6	5315	33,00 - 35,34	4,00	8,79	0,0527-0,076	0,696	x	0,6183	x	0,070	0,047	const. 0,07
41	11,2*6	5315	33,00 - 35,34	4,00	5,74	0,0527-0,076	0,5351	x	0,6189	x	0,070	0,046	const. 0,07

Table 7. Main results obtained from the Tests